A sweet and sour relationship:
Algal-bacterial interactions and the interplay of carbohydrate accumulation and fermentation on biohydrogen production

Ph.D. dissertation
Prateek Shetty

Supervisor:
Gergely Maróti
Institute of Plant Biology
Biological Research Center

Doctoral School of Biology

2022
University of Szeged

Table of contents

Abbreviations

FDX – Ferredoxin
FNR – ferredoxin/NAD(P)H oxidoreductase
PFL – Pyruvate formate lyase
BOD – Biological oxygen demand
CCM – CO_2 concentrating mechanism
HydA – Hydrogenase gene
ATP – Adenosine triphosphate
TCA – Tricarboxylic acid cycle
ADH – Alcohol dehydrogenase
ALD–DH – Aldehyde dehydrogenase
PTA–ACK – Phosphotransacetylase–acetate kinase
PQ – Plastoquinone
POX – Pyruvate oxidase
NPQR – NAD(P)H–plastoquinone oxidoreductase
PFR1 – Pyruvate ferredoxin oxidoreductase
TAP – Tris-acetate phosphate
PCA – Plate count agar
SWW – Synthetic wastewater
MACC – Mosonmagyaróvár Algal Culture Collection
SPV – Sulfo–phosphovanillin
MAPK – Mitogen-activated protein kinases
EFF – Dark fermentation effluent
RIW – Raw initial wastewater
EMI – Enriched microbial inoculum
EFF+A – Dark fermentation effluent without enriched microbial inoculum and with 10% *Micractinium* inoculum
S–EFF+A – Filter–sterilized dark fermentation effluent with 10% *Micractinium* inoculum
EFF+M+A – Dark fermentation effluent with added 5% microbial and 10% *Micractinium* inoculum
EFF+M – Dark fermentation effluent with added 5% microbial inoculum without green algae

1. Introduction

Green algae are photosynthetic organisms with a polyphyletic origin. They are ubiquitously found across different ecosystems as primary producers and account for approximately 40% of global photosynthesis. Consequently, they display a substantial diversity in shape, size, life history, environmental ranges (salinity, pH, and temperature gradients), and functional potential. Green algae can absorb nutrients at a faster rate compared to terrestrial plants or macroalgae due to their comparatively small size and high affinity to nitrogen and phosphorus compounds in the growth media [Hein et al., 1995]. They also show high carbon capturing efficiency through the CO_2 concentrating mechanism (CCM) and can be grown and harvested throughout the year. These advantages, coupled with the immense diversity, make these organisms the ideal candidates for industrial cultivation to produce algal-based biomass, bioproducts, and bioenergy. This thesis will focus on the influence of bacterial partners on the biohydrogen production, algal biomass generation, and nutrient uptake potential of green algae growing in complex wastewater media.

1.1 Bioenergy and green algae

It is widely acknowledged that major adjustments to fossil fuel policies are necessary to prevent unchecked rises in average global temperature, which could result in accelerated rates of extreme weather patterns and rising sea levels [IPCC 2013]. To avoid such scenarios, the development and implementation of novel renewable energy technologies coupled with carbon capture and storage/usage systems are required [Subramanian et al., 2013]. Among the various strategies put forth, the bioenergy industry could be instrumental in defining the future of energy because it can profitably utilize a wide range of organic substrates, such as waste products and wastewater while producing a variety of useful metabolites and energy-carrying molecules. Over the past decade, there has been a shift in focus away from existing anaerobic technologies and toward creating photosynthesis-based systems to transform organic waste into biohydrogen and other useful by-products [Wirth et al., 2018; Boboescu et al., 2014; Prabakar et al. 2018]. The renewable, affordable, and environmentally friendly aspect of biohydrogen production makes it a promising strategy.

1.2 Brief history of biohydrogen production from green algae

Multiple species of eukaryotic green algae have been studied for their biohydrogen production potential including *Chlamydomonas reinhardtii*, *Chlorella vulgaris*, [Rashid et al., 2011], and *Scenedesmus obliquus* [Ruiz-Marin et al., 2020], etc.

In 1942 Gaffron and Rubin reported hydrogen production was observed by anaerobically incubated *Scenedesmus obliquus* [Gaffron and Rubin 1942]. Klein and Betz studied the anaerobic metabolism

of *Chlamydomonas moewusii* under light and dark conditions. During anaerobic state, starch decomposes into glycerol, acetate, ethanol, carbon dioxide, and hydrogen. The release of hydrogen and carbon dioxide comes to an end when the starch pool is depleted. There were also only slight differences in the ratio of end-products of fermentation during light and dark metabolism. Light metabolism leads to enhanced hydrogen evolution and reduced glycerol production [Klein and Betz 1978]. Erbes et al. first reported the irreversible inactivation of hydrogenases upon O_2 exposure. Removal of O_2 or treatment with strong reducing agents did not restore hydrogenase activity [Erbes et al., 1979]. Further studies focused on purifying and characterizing the algal hydrogenase. In 1993, Happe and Naber identified and completely purified the hydrogenase gene (*hydA1*) from *Chlamydomonas reinhardtii*. HydA1 is a 49 kDa protein with a total of 497 amino acids [Happe & Naber 1993]. Shortly after, a novel protocol for the sustained photobiological production of biohydrogen was described [Melis et al., 2000]. Under sulfur deprivation, PSII and oxygen evolution are reversibly inactivated, leading to anaerobiosis in the culture and eventually hydrogen evolution. A second [FeFe]-hydrogenase HydA2 protein was isolated and identified from *C. reinhardtii.* HydA2 is a 49 kDa protein containing 505 amino acids and shares 73% identity with HydA1. Both *hydA1* and *hydA2* transcripts are expressed immediately after anaerobiosis [Forestier et al., 2003]. A later study examining enzyme activities after gene silencing revealed that HydA1 catalyzes the majority of hydrogen production and showed no sizeable contribution of HydA2 protein in algal hydrogen production [Meuser et al., 2012]. In 2004, *hydEF*, an accessory gene required for the maturation of HydA1 protein was identified adjacent to the *hydG* gene. HydEF protein contains two unique domains; shows high homology to 2 distinct prokaryotic proteins called HydE and HydF. These two proteins are exclusively found in organisms with [FeFe]-hydrogenase. Mutant *C. reinhardtii* with disrupted *hydEF* gene showed no hydrogen evolution despite the accumulation of full-length hydrogenase protein. Further, heterologous expression of active *C. reinhardtii* HydA1 protein in *E. coli* was only possible under the co-expression of both HydEF and HydG, indicating that both proteins are essential and played an active role in hydrogenase maturation [Posewitz et al., 2004] and the genetic sequences and location of hydrogenase maturation factors were confirmed after the whole nuclear genome sequence of *Chlamydomonas* available [Merchant et al., 2007].

Figure 1: Brief history of all the important events in algal biohydrogen production.

1896 - First observation of algal bloom evolving hydrogen

1942 - First scientific investigation in Scenedesmus

1972 - Multiple green algae investigated for biohydrogen production

1978 - Fermentive metabolism contributes to biohydrogen production

1979 - Study showing oxygen inactivation of Hydrogenases

1984 - Iron supply integral for hydrogen production

1993 - HydA1 completely purified for the first time

2000 - Sulfur deficiency leads to intense, continuous hydrogen production

2004 - Study showing oxygen inactivation of Hydrogenases

2004 - Discovery of hydrogenase maturation proteins

2007 - Metabolite and microarray profiling of pathways under hydrogen production

2009 - Improved understanding of the role of maturation proteins

2014 - Hydrogen production using CO_2 as sole carbon source

2014 - First report of bacterial cocultivation improving biohydrogen production across several miroalgae

1.3 Diversity, structure, and role of Hydrogenases

The hydrogenase family comprises of numerous enzymes catalyzing the reversible oxidation of molecular hydrogen.

$$2H^+ + 2e^- \rightleftarrows H_2$$
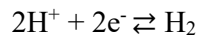
Hydrogenases are extensively distributed across all domains of life in nature [Stripp and Happe 2009]. Hydrogenases are differentiated into three types based on their active site metal cluster: a) [FeFe]-hydrogenase, b) [NiFe]-hydrogenase, c) [Fe]-hydrogenase.

All three hydrogenases are phylogenetically distinct. [FeFe]-hydrogenases can be found in green algae of the division Chlorophyta and some bacteria. Most [FeFe]-hydrogenases are also reversible and will catalyze either H_2 production or oxidation, depending on the redox partner. In contrast, [NiFe]-hydrogenases are predominantly found in bacteria, including cyanobacteria and archaea. Importantly, no [NiFe]-hydrogenase has yet been found in eukaryotes. [Fe]-hydrogenase is a homodimer found only in some methanogenic archaea.

Algal [FeFe]-hydrogenases are monomeric enzymes with a molecular weight of around 45-65 kDa. They are characterized by the presence of a unique prosthetic group referred to as the "H-cluster" at their catalytic centers. Prokaryotic [FeFe]-hydrogenases normally show a high degree of variation in their structure and contain additional N- and C-terminal iron-sulfur (FeS) cluster-binding domains (F-cluster domains). Most algal hydrogenases on the other hand characteristically lack additional FeS clusters and consist of only the active site domain (H-cluster domain). Enzyme activity of [FeFe] hydrogenases is easily inactivated in the presence of O_2.

Despite the independent evolutionary history of the hydrogenase families, the complex metal centers of both [NiFe]-hydrogenase and the [FeFe]-hydrogenase share many traits, indicating convergent evolution. The active sites of [FeFe] and [NiFe] hydrogenases share the same bimetallic framework and the presence of CO and CN^- as iron ligands and are bridged by sulfur atoms. These similarities appear to be required for the functioning of the catalytic activity. Other [FeFe] hydrogenases found in older algal lineages and bacteria have an additional [Fe-S] cluster [Boyd et al., 2011]. Studies have shown that [FeFe] hydrogenases have high turnover rates, and the highest turnover rates are found in bacterial [FeFe] hydrogenases like CpI, DdH and HydA of *Megasphaera elsdenii* (5000-8000 µmol H_2 min^{-1} mg^{-1}).

The hydrogenase family of enzymes plays a vital role in the fermentative metabolism of green algae. Green algae switch into fermentative metabolism under anaerobiosis. In natural ecosystems, green algae can face such conditions during low water flow or high biological oxygen demand (BOD) environment. It is also important to remember that fermentative pathways are significantly different

between light and dark (Table 1). During light fermentation, the photosynthetically produced O_2 permits oxidative pyruvate degradation and respiratory ATP generation (adenosine triphosphate). The photosynthetically produced O_2 permits oxidative pyruvate degradation and respiratory ATP generation, leading to increased CO_2 evolution and decreased amounts of pyruvate formate lyase (PFL) products. However, the partially active respiratory chain isn't sufficient as an electron sink. Also, under anaerobiosis, the electron-consuming Calvin cycle fails to function as an electron sink. By utilizing the excess photosynthetically generated electrons, the production of hydrogen can be considered a survival mechanism.

Table 1: Comparison of pathways active during light and dark in *C. reinhardtii*

	Light	Dark
First steps of glucose breakdown	Glycolysis	Glycolysis
Conversion of pyruvate	PFL, tricarboxylic acid cycle (TCA)	PFL
Main step of reoxidation	Hydrogenase, respiratory chain, reductase	Alcohol dehydrogenase (ADH), Aldehyde dehydrogenase (ALD-DH)
Steps of energy supply	Photophosphorylation, oxidative phosphorylation	Phosphotransacetylase-acetate kinase (PTA-ACK), Glycolysis

1.4 Pathways for hydrogen production in green algae

Biohydrogen production in green algae is linked to the conversion of solar radiation to chemical energy following the Z-scheme [Ghirardi et al., 2009]. Briefly, light absorbed by PSII induces a charge-separated state involving P_{680}^+ and Pheophytin, oxidizing two water molecules and leading to the release of O_2 and protons into the lumenal side of the thylakoid membrane. Simultaneously, light absorbed by PSII generates a strong oxidant P_{700}^+ that oxidizes intermediate electron carriers like plastocyanin. The released electrons in turn are transferred to the electron acceptor ferredoxin (FDX), reducing it. Ferredoxin acts as a carrier of reductant to a number of different acceptors, such as the algal [FeFe]-hydrogenase and the ferredoxin/NAD(P)H oxidoreductase (FNR). Transfer of electrons to FNR leads to the reduction of $NADP^+$ to NADPH which is utilized in CO_2 fixation to sugars. It is across these reactions that electrons generated can be used for biohydrogen production, mediated by hydrogenase. Below the three main pathways for biohydrogen production are discussed in detail (Figure 2).

1) Direct photolysis

$$2H_2O + \text{solar energy} \rightarrow 2H_2 + O_2$$
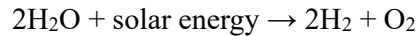
Green algae use their photosynthetic systems (PSII and PSI) to carry out oxygenic photosynthesis. Upon light exposure, PSII absorbs photons with a wavelength shorter than 680 nm, generating a strong oxidant with the capacity to split water into protons, electrons, and O_2. The electrons are then transferred through a series of electron carriers to PS1. PS1 in turn, absorbs photons with a wavelength shorter than 700 nm, raising the energy of the electrons and reducing ferredoxin (Fd) and $NADP^+$. The proton gradient thus formed across the thylakoid membrane drives ATP production via ATP synthase. Both, ATP and NADPH can then be used to reduce CO_2 through the Pentose Phosphate pathway or the Calvin cycle, increasing cell growth and excess reduced CO_2 is stored as biomolecules like carbohydrates or lipids.

The reduced ferredoxin can alternatively act as an electron donor, giving rise to molecular hydrogen from protons. The ferredoxin enzyme FDX1 or PETF is the only natural electron donor for algal hydrogenases. The reaction is catalyzed by the hydrogenase enzyme. This pathway is extremely attractive as it makes use of readily available sunlight, CO_2, and water. Unfortunately, hydrogen production from this pathway is not continuous as the enzyme is highly sensitive to O_2 and is inactivated shortly after illumination.

2) Indirect photolysis

In indirect biophotolysis non-photochemical reduction of plastoquinone (PQ) by NAD(P)H occurs due to electrons released by glycolytic degradation of starch. The electrons are shuffled into the Plastoquinone pool from NADPH, completely bypassing PSII. The concomitant O_2 depletion creates an anaerobic environment in the culture and activates the O_2-sensitive hydrogenase, which in turn produces hydrogen. The electrons are transported through PSI, FDX1, and finally hydrogenase (Show et al., 2012). This pathway makes use of NAD(P)H-plastoquinone oxidoreductase (NPQR) activity and is independent of PSII.

3) Dark fermentation pathway

During dark fermentation, hydrogen is produced in the absence of light and O_2 and is independent of both PSII and PSI. In this process, pyruvate oxidation is coupled with the reduction of FDX and is catalyzed by pyruvate ferredoxin oxidoreductase (PFR1). The reduced FDX then transfers electrons to the hydrogenase to reduce protons to form hydrogen.

Figure 2: **The three pathways for hydrogen production in green algae.** A) schematic figure depicting PSII-dependent hydrogen production. B) schematic figure depicting indirect photolysis C) schematic figure depicting dark fermentation [Wang et al., 2020]
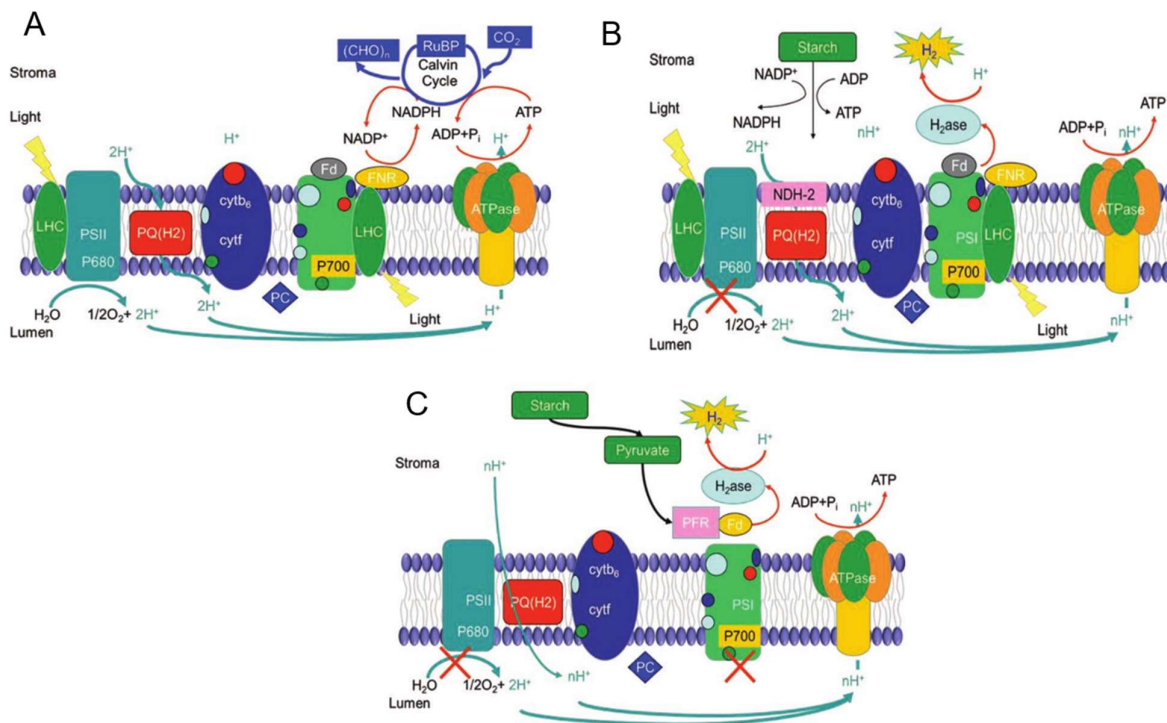
1.5 Efforts to improve algal biohydrogen production

a) Nutrient deprivation

Nutrient deprivation to produce biohydrogen is an extensively studied process. The absence of elements such as sulfur, nitrogen magnesium, or phosphate in the culture medium directly impacts the normal cellular metabolism of green algae and attenuates photosynthesis. The D1 protein of The PSII reaction center rapidly degrades in the absence of sulfur and directly impeding PSII activity. The mitochondrial respiration on the other hand remains unperturbed and continues to consume the ambient O_2 until complete anaerobiosis is achieved. Nitrogen deprivation and Sulfur deprivation exhibit similar responses from green algae; such as starch accumulation. However, in nitrogen deprivation the aerobic period lasts longer, leading to delayed hydrogen production [Philipps et al., 2012].

There are multiple drawbacks to this strategy. Hydrogen production through nutrient deprivation is conventionally a two-step process. The first step is to culture green algae under optimal conditions to achieve high density, followed by placing the freshly cultured green algae under nutrient deprivation. This separation of growth and culture media can have a detrimental impact on not only the total

production cost but also on the algal biomass. It's also crucial to remember that prolonged sulfur deficiency results in the death of algal cells, making this approach unattractive on an industrial scale.

b) Mutants/ Transgenic green algae

The numerous obstacles to continuous hydrogen production have been effectively addressed by utilizing naturally occurring mutants and genetic engineering techniques. A common strategy is to target the O_2 sensitivity of Hydrogenase. Random mutagenesis of *C. reinhardtii in vivo* [Ghirardi et al., 1997] and *in vitro* [Stapleton and Swartz 2010] has led to the development of O_2-tolerant Hydrogenase. However, these studies only show a small improvement in O_2 tolerance. An alternative approach involves targeting the proteins involved in photosystems. Krishna et al. achieved sustained hydrogen production by using a *C. reinhardtii* mutant with a lower ratio of PSI/PSII (0.35 in the mutant vs 0.85 in the wild type). This prevents the inhibition of hydrogenase enzyme by O_2 produced by PSII and leads to the continuous production of hydrogen for 42 days [Krishna et al. 2019]. Other studies have used fusion proteins to achieve lower O_2 evolution. Wu et al., transferred the ferrochelatase gene (*hemH*) from *Bradyrhizobium japonium* and the leghemoglobin, *lba*, a gene from *Glycine max* into *C. reinhardtii* chloroplast [Wu et al., 2010]. Leghemoglobin is essential to prevent the inactivation of nitrogenase gene in soybean. It was hypothesized that transgenic green algae expressing active leghemoglobin could play a similar role in maintaining Hydrogenase activity even under aerobic conditions. Results showed that it was indeed the case, and the headspace of transgenic algal cultures had reduced O_2 content and increased hydrogen production. Codon optimization of *hemH* gene led to a 22% increase in hydrogen yield compared to wilt-type *C. reinhardtii* cultures [Wu et al., 2011]. Apart from using O_2 sequestering enzymes like leghemoglobin, it is also possible to remove O_2 from the headspace by introducing new pathways utilizing oxygen. Xu et al., used pyruvate oxidase (POX) enzyme responsible for catalyzing the decarboxylation of pyruvate to acetyl-phosphate and CO_2 in the presence of O_2 [Xu et al., 2011]. Transgenic green algae expressing *E. coli* POX enzyme showed low O_2 evolution and twice as much H_2 evolution compared to wild-type.

Carbon fixation through by Calvin cycle is a major pathway competing for photosynthetic reducing power required by hydrogenase. Manipulating the enzymes involved in CO_2 fixation can theoretically lead to improve biohydrogen production. One of the steps in the process involves carboxylation of ribulose bis-phosphate by the enzyme Rubisco. Strains lacking the large subunit of Rubisco showed a higher rate of H_2 production compared to wild type under sulfur deprivation [Hemschemeier et al., 2007]. Pinto et al. engineered a *C. reinhardtii* mutant with reduced Rubisco activity and stability to improve biohydrogen production in TAP (Tris-acetate phosphate) media [Pinto et al., 2013]. Apart from preventing active CO2 fixation, it is also possible to increase reductant flux for hydrogen production. Doebbe et al. introduced a HUP1 (hexose uptake protein) hexose symporter protein from

Chlorella kessleri into *Chlamydomonas* stm6 mutant strain [Doebbe et al., 2007]. Upon exogeneous addition of hexose into the medium, the transgenic Chlamydomonas could use the hexose as a respiratory substrate. Table 2 lists all major advancements in using transgenic green algae for biohydrogen production.

Finally, transcriptomic studies can provide additional genes of interest to be used for transformation studies. Shu et al. studied microRNA transcriptomes of *C. reinhardtii* under sulfur-replete and sulfur-depleted conditions and identified a total of 47 miRNAs that were upregulated under sulfur-depleted conditions [Shu et al. 2012]. Wang et al. used 3 miRNAs from the previous studies and transformed *C. reinhardtii* cells with a heat-inducible vector [Wang et al., 2018]. Of the 3 different miRNAs, miR1166.1 greatly enhanced hydrogen production under sulfur replete conditions. Overexpression of mi1166.1 led to a downregulation of the Phosphatidylglycerophosphate synthase gene. This was the first study showing modulating miRNA expression can improve biohydrogen production.

Table 2: Major advancements in using transgenic green algae for biohydrogen production.

Barrier	Algal species	Modification/ Target protein	Genetic engineering technique	Results	References
Oxygen sensitivity	*C. reinhardtii*	D1 protein	Site-directed mutagenesis	increased photosynthetic capacity, respiration rate, and quantum yield of photosynthesis	Torzillo et al.,2009
	Chlorella sp. DT	PsbO	RNA interference	Silencing led to a 10-fold increase in photobiological hydrogen production compared to wild type	Lin et al., 2013
	C. reinhardtii	PSII	Homologous recombination	PsbD gene is silenced, leading to lower oxygen evolution and sustained hydrogenase activity	Surzycki et al., 2007
	C. reinhardtii	Attenuated photosynthesis to respiration capacity ratio	DNA insertional mutagenesis coupled with glycolaldehyde treatment	The resulting transformants had a higher respiration rate and low photosynthetic rate, leading to anaerobiosis even under illumination. Calvin cycle is inactivated upon Glycoaldehyde leading to hydrogen production.	Rühle et al., 2008
	C. reinhardtii	Addition of ferrochelatase gene and leghemoglobin gene into chloroplast	Genetic transformation with fusion protein	Decreased Oxygen content and improved hydrogen production	Wu et al., 2008
	C. reinhardtii	Sulfate permease	RNA interference	Transformants had limited supply of sulfates to the chloroplast, down-regulating oxygen evolution and leading to sustained hydrogen production	Chen et al., 2005
Proton gradient	*C. reinhardtii*	PGRL1	DNA insertional mutagenesis	Mutant had an impaired cyclic electron flow around PSI, leading to enhanced hydrogen production under sulfur deficiency	Tolleter et al., 2011
	C. reinhardtii	PGRL1 and PGRL5	Deletion	The PGRL mutants showed prolonged PSII activity and increased oxygen consumption capacity under sulfur deprivation	Steinbeck et al., 2015
Photosynthetic efficiency	*C. reinhardtii*	Truncated light-harvesting chlorophyll antenna size	DNA insertional mutagenesis	Mutant showed lower amount of light-harvesting proteins than the wild type and had lower steady-state levels of Lhcb mRNA	Polle et al., 2003
	C. reinhardtii	LHCBM1, 2 and 3	RNA interference	Resulting triple knockout mutant exhibited reduced expression of all 3 light-harvesting complexes and improved hydrogen and biomass production. Improvement in hydrogen production is attributed to reduced inhibition, reduction in loss of energy by non-photothemical quenching and increased light distribution to cells within the reactor.	Oey et al., 2013

Competition for electrons	*C. reinhardtii*	Large subunit of Rubisco	DNA insertional muta-genesis	Lack of starch accumulation leads to hydrogenase taking up excess electrons instead of the Calvin cycle.	Hemschemeier et al., 2008
	C. reinhardtii	Small subunit of Rubisco	Site-directed mutagene-sis	Mutants displayed attenuated Calvin' cycle, increasing the amount of reducing power available for hydrogenases.	Pinto et al., 2013
	C. reinhardtii	Hydrogenase-Superoxide dismutase fusion protein	Insertion and expression of fusion protein	Promotes hydrogen production even in the presence of active Calvin cycle. Energy for Hydrogen production putatively comes from Linear electron flow and starch degradation. Transformants also show re-duced growth rate compared to wild type.	Ben-Zvi et al., 2019
Small RNA expression	*C. reinhardtii*	miRNA1166.1	Overexpression of miRNA	Enhanced biohydrogen production	Wang et al., 2018

c) Bacterial co-cultures

Several studies in the recent past have focused on using algal-bacterial co-cultures for biohydrogen production. Co-cultures provide several advantages over monocultures, primarily in an ecological context. In natural ecosystems, green algae live in association with a multitude of different organisms including bacteria, fungi, viruses, and cyanobacteria; collectively termed the microbiome. The associated microbiome is generally found surrounding or attached to the algal host in a region called the phycosphere. Algal hosts release dissolved organic matter or signaling molecules to promote certain bacterial communities in the phycosphere. The bacterial partners, in turn, improve the growth of algal hosts by providing additional major essential nutrients (N, P) [Reshef et al., 2006], vitamins [Croft et al., 2005], phytohormones, and siderophores. Bacterial reparation can also mitigate problems arising from the high dissolved oxygen concentrations and prevent algal photo-oxidative culture death. Consumption of O_2 by bacterial respiration raises photosynthetic efficiency by allowing Rubisco to preferentially bind CO_2 rather than O_2.

Pairwise co-cultivation of *C. reinhardtii* with bacterial partners such as *Pseudomonas sp.* and *Bradyrhizobium japonium* has shown to improve hydrogen production rate, total yield, and duration in TAP medium devoid of sulfur. It is important to note that members of neither the *Pseudomonas* genus nor the *Bradyrhizobium* genus are known to be hydrogen producers and most of the biohydrogen produced is still generated due to the physiological condition impressed by sulfur deprivation. Wu et al., co-cultivated wild-type *C. reinhardtii* cc849 and its transgenic strain *lba* expressing leghemoglobin with *B. japonicum* in TAP medium deficient for sulfur [Wu et al., 2012]. Transgenic *lba* strain showed a 15-fold enhancement in H_2 production and improved growth under co-cultivation. Both strains also showed higher chlorophyll content under bacterial association compared to monoculture. Ban et al., used a consortium of bacteria from a contaminated algal culture as inoculum to improve hydrogen production. Further investigation revealed that *Pseudomonas sp.* Strain D was the most effective partner and improved algal biohydrogen production, chlorophyll, protein, and starch content of algal cells. In this study, both direct and indirect pathways were essential for overall hydrogen production, with the direct pathway playing a bigger role in H_2 production after 7 days of co-cultivation [Ban et al., 2018]. Lakatos et al., used *E. coli* JW5433 (Δ*hypF*) with 3 different green algae to identify high hydrogen producers, and associated conditions. *Micractinium* co-cultivated with *E. coli* JW5433 (Δ*hypF*) was found to be the highest producer of hydrogen (~88.98 ml/L) [Lakatos et al., 2017]. Sulfur deprivation was not necessary for hydrogen production in this study. Fakhimi et al., explored the use of co-cultures with exogenous addition of glucose. Hydrogen production in co-cultures increased dramatically with the exogenous addition of Glucose. The increase in hydrogen production was attributed to the ability of *C. reinhardtii* to take up acetic acid produced by the bacterial partners. Both *P. putida* and *E. coli* were able to take up glucose and secrete

acetic acid increasing algal hydrogen production in the absence of sulfur deplete conditions (Fakhimi et al., 2019). **Table 3** details a comprehensive list of studies using bacterial co-cultivation for hydrogen production.

Table 3: List of bacterial co-cultivation studies. (µmol to ml conversions were carried out using Avogadro' law: 1 mole H$_2$ gas equals 22.41 liters of H$_2$)

Algal strain	Bacteria strain	Medium	Light intensity	Reported Hydrogen production in monoculture	Estimated H$_2$ in ml/L	Reported Hydrogen production in co-cultures	Estimated H$_2$ in ml/L	Total cultivation duration
Transgenic *C. reinhardtii lba* (based on cc849)	*Bradyrhizobium japonicum*	TAP-S	60	20.02 (µmol/40 mL)	≈11.22	298.54 (µmol/40 mL)	≈167.25	21
C. reinhardtii cc849	*Bradyrhizobium japonicum*	TAP-S	60	15.08 (µmol/40 mL)	≈8.44	82.95 (µmol/40 mL)	≈46.47	21
C. reinhardtii FACHB-265	contaminated culture	TAP-S	50	6 ml/L		154 ml/L		18
C. reinhardtii FACHB-265	*Pseudomonas sp.* Strain D	TAP-S	50	10 ml/L		120 ml/L		15
C. reinhardtii FACHB-265	*Pseudomonas sp.* Strain C	TAP-S	50	10 ml/L		63 ml/L		15
C. reinhardtii FACHB-265	*Herbaspirillum sp.* Strain F	TAP-S	50	10 ml/L		40 ml/L		15
C. reinhardtii FACHB-265	*Pseudomonas sp.* Strain D + *E.coli*	TAP-S	50	20 ml/L		124.29 ml/L		17
C. reinhardtii FACHB-265	*Pseudomonas sp.* Strain D + *B. subtilus*	TAP-S	50	20 ml/L		111.74 ml/L		17
C. reinhardtii cc124	*E. coli* (Δhyp F)	TAP-S	50	25.02 ml/L		47.24 ml/L		10
Micractinium MACC 360	*E. coli* (Δhyp F)	TAP	50	Not reported		~88.98 ml/L		1
C. reinhardtii cc124	*E. coli* (Δhyp F)	TAP	50	Not reported		~18.67 ml/L		1
C. reinhardtii cc124	*Pseudomonas putida*	TAP + glucose	50	~17 ml/L		40.8 ml/L		4
C. reinhardtii cc124	*E. coli* (Δhyp F)	TAP + glucose	50	~17 ml/L		35.1ml.L		4
C. reinhardtii cc124	*Rhizobium etli*	TAP+mannitol	50	~17 ml/L		16.1ml/L		4
Chlamydomonas sp. & Scenedesmus sp.	*E. coli* (Δhyp F)	TAP	50	0		1.5 ml/L		24
Chlamydomonas sp. & Scenedesmus sp.	Mixed bacterial community	TAP	50	0		1.1 ml/L		24
Chlamydomonas cc849	*Azotobacter chroococcum*	TAP-S	30	19 (µmol/mg chl)		56 (µmol/mg chl)		15

Chlamydomonas cc849	*Azotobacter chroococcum*	TAP-S	100	22 (µmol/mg chl)	74 (µmol/mg chl)		15
Chlamydomonas cc849	*Azotobacter chroococcum*	TAP-S	200	16 (µmol/mg chl)	255 (µmol/mg chl)		15

1.6 Drawback to conventional hydrogen production strategies

Conventional studies on biohydrogen production have been mainly carried out under two standard conditions: Sulfur/ Nutrient depleted TAP media and using *C. reinhardtii* as the focal green algae. These techniques have been essential in elucidating the mechanisms for biohydrogen production. However, the conditions are not representative of industrial requirements. Utilizing TAP media for biohydrogen production is cost prohibitive. Furthermore, *C. reinhardtii* isn't a prime candidate for biohydrogen production.

Recent studies have considered these limitations and sought to overcome them through alternative strategies. Studies utilizing effluents from food industries have shown that there is no significant change in algal bioproducts obtained from algae cultivated in food industry wastewater compared to that obtained from cultivation in a standard growth medium [Nwoba et al., 2019]. Utilizing wastewater effluents is a great strategy to combat the high media costs frequently associated with algal cultivation and has been used successfully for the large-scale production of algal biofuels. Unfortunately, the dearth of information on how microbial partners interact with algae is tempering further progress in the field; specifically, which microbes, genes, and pathways are involved. Large-scale algal cultivation typically focuses on improving the yield at the algal species level and completely ignores natural interactions with microbial partners. The first comprehensive microbiome study was carried out a couple of years ago [Krohn-Molt et al., 2017] and showed that algal species associate in a species-specific manner with bacterial partners. This is a pattern also found in animal and plant microbiomes.

These knowledge gaps can be filled by adopting methods used to investigate the plant rhizosphere or human and mouse gut microbiomes, i.e., by viewing the algal host as a superorganism whose function depends not only on the DNA and environment of the host but also on the associated microbiome. There is immense empirical evidence that an imbalance in the gut microbiome can lead to poor health in hosts. Plant microbiome studies have reproducibly modulated host traits such as biomass, flowering time [Panke-Buisse et al., 2015], and reduced pathogen incidence [Duran et al., 2019]. Other microbiome studies have shown that modulation of host traits depends on their associated microbiome in a phylogenetic manner; i.e bacterial species from the same genera can result in similar host responses [Martiny et al., 2015]. Furthermore, soil microbiomes can be selected to enrich the abundance of pathogen-preventing microbes, which has been successfully done in plant microbiome studies [Siegel-Hertz et al., 2018]. Data from large-scale microbiome experiments coupled with in vitro studies have been used to design artificial consortia capable of reproducing some specific function carried out by the entire microbiome. Similarly, it is hypothetically possible to identify bacterial genera and species that can selectively improve algal hydrogen and biomass production.

This thesis aims to address some of these knowledge gaps. The thesis is divided into two parts. Part A focuses on the use of pairwise co-cultivation of green algae with different bacterial species to identify bacterial species that can improve biohydrogen production and algal growth. It would be important to explore if phylogenetically similar bacterial members can promote algal biohydrogen production. Studies have revealed that despite the functional flexibility offered by horizontal gene transfer, closely related bacterial taxa share more similar traits than expected if the traits were randomly distributed across the phylogenetic tree [Losos 2008]. However, it is important to remember that phylogenetically conserved traits should be empirically examined and the extent to which it exists must be carefully uncovered. We are particularly curious to know if microorganisms that boost hydrogen generation in one species of green algae may similarly improve biohydrogen production in other species of green algae. Results from these studies will inform the mechanistic nature of algal biohydrogen production: general mechanism (if biohydrogen is improved across different species of green algae with the same bacteria) or species-specific mechanism (if biohydrogen is improved only in one species of green algae).

Part B of the thesis focuses on using effluents from a brewery under different conditions to identify key properties leading to improved biohydrogen production under co-cultivation of green algae with wastewater native microbes. We test the importance of three parameters: Effluent concentration, effluent pretreatment, and filter sterilization to reduce bacterial presence. Despite the dissimilar approaches, Part A and Part B of the thesis aim to study the impact of bacterial association in conditions more reminiscent of commercial algae cultivation.

2. AIMS AND OBJECTIVES

2.1 Part A - High-throughput co-culture assays to investigate algal-bacterial interactions

1) Presence of phylogenetically conserved traits in algal biohydrogen and biomass production

   a) Do members of the same bacterial genus increase algal biohydrogen production?

   b) Do members of the same bacterial genus increase algal biomass?

2) Mechanistic nature of improvement in biohydrogen production

   a) Do members of the same bacterial genus increase algal biohydrogen production across different species of algae?

3) Impact of algal-bacterial co-cultivation on algal biomolecule concentration

   a) Does bacterial co-cultivation change algal chlorophyll a/b ratio?

   b) Does bacterial co-cultivation change accumulated algal lipid and carbohydrate content?

4) Deeper understanding of expressed genes under algal-bacterial co-cultivation

   a) Do members of the same genus show similar gene expression patterns?

   b) Is there clear evidence of which pathways lead to improved biohydrogen production?

2.2 Part B - Algal-Bacterial Consortia in Combined Biohydrogen Generation and Wastewater Treatment

1) Impact of wastewater concentration

   a) Does wastewater concentration linearly improve algal growth?

   b) Does wastewater concentration linearly improve hydrogen production?

2) Impact of pretreatment of wastewater

   a) Does pretreatment (Filter-sterilization and heat treatment) of wastewater have an impact on algal biohydrogen production?

3) Metagenome studies

   a) Is there evidence for algal selection on wastewater microbiomes?

   b) What bacterial members are enriched in wastewater effluent samples?

3. MATERIALS AND METHODOLOGY

3.1 Part A - High-throughput co-culture assays to investigate algal-bacterial interactions

3.1.1 Preparation of pairwise co-cultures

3.1.1a Media formulations used

Two different media types were utilized. TAP media with PCA media added in an 85:15 ratio make up the mixed media (MM) employed in this study. Mixed media was used to culture both algal and bacterial cells to keep culture conditions the same. Previous studies in the lab and preliminary studies in this project confirmed that most bacteria did not grow in only TAP. This was overcome by a small amendment of PCA media components to TAP media.

We also used synthetic wastewater media to mimic the formulation of domestic wastewater. A 25x concentration of synthetic wastewater (SWW) media based on OECD formulation was freshly prepared prior to Hypo-vial experiments to measure hydrogen.

Formulations for Mixed media and Synthetic wastewater media are mentioned below. Both algal and bacterial strains were maintained on mixed media plates for short-term storage.

Mixed media formulation

Ingredients (in 800ml RO water, pH 7)	
Glucose	0.12g
Tryptone	0.6g
Yeast	0.3g
Tris base	1.646g
TAP salt	17ml
Phosphate buffer	0.68ml
Hutners trace elements	0.68ml
Glacial acetic acid	0.68ml
Agar (if needed)	11.28g

25x Synthetic wastewater media

Ingredients (in 800ml RO water, pH 7)	
Peptone	6.4g
Meat extract	4.4g
Urea	1.2g
NaCl	0.28g
$CaCl_2.2H_2O$	0.16g
$MgSO_4.7H_2O$	0.08g
K_2HPO_4	1.112g

3.1.1b Isolation and identification of bacterial strains

A total of twenty-eight bacterial strains were used; 1) five strains from contaminated algal cultures, 2) six strains from biogas samples 3) one strain from an environmental samples and 4) six strains from a commercially available biostimulant inoculum (link). We also obtained ten additional bacterial strains from frozen stock (Figure 3).

Bacterial isolation from contaminated algal cultures, biogas samples, and biostimulant inoculum was carried out based on the following protocol. The initial inoculum was serially diluted up to 10^7 dilution factor in sterile MQ water. 100µl of sample from 10^{-5} to 10^{-7} dilution factor was spread plated on mixed media plates. Individual strains were picked and streaked on mixed media plates to confirm the presence of a single isolated strain. Identification of bacterial isolates was carried out using 16S rDNA-based PCR amplified sequences. Universal 16S rDNA oligonucleotides were used for the amplification (f27 5′-AGAGTTTGATCCTGGCTCAG-3′ and r1492 5′-ACGGCTACCTTGTTACGACTT-3′). The PCR products were isolated from agarose gel and sequenced using Sanger sequencing. Homology matches against the NR/NT database using BLASTN (http://blast.ncbi.nlm.nih.gov/) were used for taxonomic identification of bacterial isolate.

3.1.1.c Culture conditions for bacterial growth rate measurements

The bacterial growth rate in synthetic wastewater was measured in 48 well microplates. Bacterial strains, cultured in mixed media were used as starting inoculum. Each well received 450 µl of Synthetic wastewater media and 50 µl of bacterial inoculum standardized to 10^5 cells ml^{-1}. Each strain was grown in 4 replicates. The plates were continuously measured every 20 minutes at 600nm on the

Hidex Sense instrument. The growth rate was calculated using a Rscript with a rolling regression model to estimate the maximum slope.

<u>3.1.1d Description of algal strains used in this study</u>

Three different algal strains are used in this study. All pairwise combinations were screened using *C. reinhardtii* cc124 strain (henceforth referred to as *C. reinhardtii*). 2 other strains: *Micractinium* MACC-360 (henceforth referred to as *Micractinium*) and *Parachlorella* MACC38 (henceforth referred to as *Parachlorella*) were used for additional tests against select bacterial strains. All algal strains were obtained from Mosonmagyaróvár Algal Culture Collection (MACC; Institute of Plant Biology, University of West-Hungary, Hungary) and maintained on mixed media plates.

<u>3.1.1.e Preparation of Hypo-vials for hydrogen measurements</u>

Algae used for hydrogen measurements are first grown in mixed media and incubated at 25ºC under 50 μmol m^{-2}s^{-1}. The algal culture was grown for 4 days with continuous stirring at 180 rpm. Algae were then harvested on the 4th day and algal stock inoculum was prepared by standardizing counts at 1x10^7 cells ml^{-1}. Bacteria strains used for pairwise co-cultivation were cultured overnight in mixed media at 30ºC. Bacterial stock inoculum was prepared by standardizing cell counts of overnight cultures to 1x10^5 cells ml^{-1}.

All samples were cultured in 40ml sterile glass Hypo-vials. Hypo-vials are small, clear glass vials with a narrow neck and gas-tightly capped with a rubber septum to prevent gas from escaping. Hypo-vials were prepared with 19ml 25x synthetic wastewater media, 0.5ml count standardized algal inoculum and 50 μl count standardized bacterial inoculum. Axenic algal Hypo-vials were prepared using 50 μl of mixed media instead of bacterial inoculum. All combinations were grown in 2 replicates. Hypo-vials were incubated at 25ºC under 50 μmol m^{-2}s^{-1} and cultivated for 3 days. Hydrogen concentration in the headspace of Hypo-vial bottles was measured using gas chromatography.

3.1.2 Analytical methods

<u>3.1.2a Cell counts</u>

Both the algal and bacterial cells were counted using automated cell counters. The LUNA-FL dual fluorescence cell counter was used with the red fluorescence channel. When chlorophyll molecules are excited, they emit red fluorescence. This can be used as a proxy for automated counted of live algal cells.

Bacterial cells were enumerated using the QUANTOM Tx microbial cell counter using live cell staining. 20 µl sample from overnight cultures was mixed with 4 µl of live cell staining dye and incubated at 37ºC for 40 minutes. The cell loading buffer was added to the incubated samples and 7µl was loaded into the counting slide. All the counting slides were centrifuged for 10 minutes at 300 RCF (relative centrifugal force). Finally, all slides were measured on the microbial counter with the following parameters:

Minimum fluorescent object size	0.3um
Maximum fluorescent object size	50um
Roundness (0-100%)	30
Declustering (0-10)	7

3.1.2c Hydrogen measurements

Hydrogen was directly measured by gas chromatography using an Agilent Technologies 7890A GC system equipped with a thermal conductivity detector and argon as a carrier gas. The temperatures of the injector, detector, and column were kept at 30, 200, and 230°C, respectively. An HP MolSieve column was used (Agilent). Total accumulated hydrogen production was measured everyday by injecting 100 µl of headspace sample using a gas tight syringe.

3.1.2b Chlorophyll measurements

1 ml of each sample was collected from Hypo-vial and dissolved in 1ml of 100% methanol. The samples were incubated for 30 minutes at 45ºC, followed by centrifugation at 8000 rpm for 10 minutes to collect the cell debris. Absorbance was calculated at 665, 653, and 470 nm. Chlorophyll a and b concentrations were calculated according to the following equations:

$$C_a = 15.65A_{666} - 7.3A_{653}$$
$$C_b = 27.05A_{653} - 11.21A_{666}$$

3.1.2c Total carbohydrate measurement

Samples from three days old cultured were collected after hydrogen and cell count measurements. 10 ml of sample standardized to 10^7 cell ml^{-1} was centrifuged at 4000 rpm for 10 minutes, and the supernatant was discarded. 5 ml of methanol was added to the pellet and mixed with pipetting. The samples were then incubated in dark at 45°C for 30 minutes. The sample was then centrifuged at 8000 rpm for 10 minutes and the supernatant was removed. The pellets left behind were used for total

carbohydrate measurement. First, the pellets were washed with Milli-Q water and mixed in 1 ml of Milli-Q water. 100 µl volume from each sample was taken in a fresh glass tube and mixed with 0.5 ml of freshly prepared anthrone reagent. Anthrone reagent was prepared by dissolving 0.5 g of anthrone in 250 mL of concentrated sulfuric acid. During the addition of anthrone reagent, tubes were cooled down in an ice bath and then incubated at 90°C for 17 minutes in the water bath. After incubation, tubes were cooled down again at room temperature and the absorbance was taken at 620 nm in the Hidex microplate reader.

3.1.2d Lipid estimation and visualization under a confocal microscope

Sulfo-phosphovanillin (SPV) method was used to estimate lipid concentration. Briefly, phosphovanillin reagent was prepared by dissolving 0.15 g vanillin in 2.5 ml absolute ethanol and 22.5 ml DI water and stirred continuously. Subsequently, 100 ml of concentrated phosphoric acid was added to the mixture. The resulting reagent was stored in dark until further use. To ensure high activity, fresh phosphor-vanillin reagent was prepared shortly before every analysis.

A known quantity of 3-day old algal biomass was collected by centrifugation and re-suspended in 100 µl of RO water. 2ml of concentrated (98%) sulfuric acid was added to the sample and heated for 10mins at 100ºC and was cooled for 5 minutes in an ice bath. 5 ml of freshly prepared phosphor-vanillin reagent was then added, and the sample was incubated for 15mins at 37ºC while shaking at 200 rpm. Absorbance of the sample was measured at 530 nm to quantify the lipid within the sample. The standard lipid stocks were prepared using commercial canola oil at 5 mg in 10ml chloroform (final concentration 0.5 mg/ml). Different amounts of lipid concentration were obtained by serially diluting lipid stock using chloroform in empty glass tubes. The tubes were kept at 60ºC for 10 mins to ensure chloroform evaporates. 100µl of RO water was added to the lipid standard.

A 4 mM solution for BODIPY was prepared by dissolving 1g of BODIPY dye in 1ml of absolute methanol. Samples from 3-day old culture were collected and 1 µl of 4 mM BODIPY dye was added to 100 µl of the respective sample. Samples were observed under Olympus Fluoview FV1000 confocal laser scanning microscope. The emission range was fixed between 500 nm to 515 nm to visualize BODIPY fluorescence. Images were taken under 60X oil immersion objective at 6X zoom.

3.1.3 Transcriptome analysis

2-day old samples cultivated in the same manner as in hydrogen production studies were used to extract total RNA. Briefly, 40 ml Hypo-vial bottles, filled with 19 ml 25x SWW and inoculated with 0.5 ml *C. reinhardtii* (cell concentration - 10^7 cell ml^{-1}) and 50µl of bacteria (cell concentration - 10^5 cell ml^{-1}) were cultivated for 48 hours. Four different conditions were used: Axenic, *Bacillus cereus*,

Bacillus thuringiensis, and *Methylobacterium* sp., with 3 replicates per condition. The Hypo-vials were opened 48 hours post inoculation and the entire culture was centrifuged. RNA was extracted by adding 500 µL TriReagent (Sigma). After 5 minutes of incubation at room temperature, 100 µl of saturated Phenol/chloroform/ isoamyl alcohol (25:24:1) was added and manually shaken for 15 seconds and incubated at room temperature for 3 min. The samples were then centrifuged at 17,000g for 15 minutes at 4°C, and the upper aqueous phase (about 300 µL) was loaded into a new Eppendorf tube. An equal volume of isopropyl alcohol was added to the sample and incubated for 10 min at room temperature. The mixture was centrifuged again at 17,000g for 10 minutes at 4°C. The supernatant layer was discarded, and the pellet was washed with 500 µL of 70% ethanol. The pellet was dissolved with RNase-free water and the purified RNA sample was treated with 5 units of DNase according to the manufacturers' instructions (Fermentas). The quality of extracted RNA was assessed using an RNA ScreenTape on a TapeStation 4150 (Agilent Technologies) and the quantity of extracted RNA was determined with Qubit RNA Assay and sequenced on an Illumina NextSeq550 NGS platform to generate 150nt of poly-A selected, paired end reads. This ensured that only algal transcripts were sequenced in axenic and bacterial co-cultivated samples.

3.1.4 Differential expression analysis

Sequenced reads were first processed using rcorrector (link), which is a kmer-based error correction method for RNAseq data. The error-corrected reads were then trimmed using Trimmomatic v0.39 (link) with adapter sequences and keeping a quality score of 25 over a 5bp sliding window. Reads shorter than 50bp were discarded from further analysis. The trimmed reads were then mapped to reference *C. reinhardtii* transcripts v5.6 downloaded from phytozyme (link) using Kallisto v0.46.1 (link). Differential analysis on Kallisto quantified transcripts were carried out on R v4,1 using Deseq2 v1.34.0 (link). Read abundances were then quantified at the gene level using a transcript id to gene id map, also downloaded from phytozyme. Functional annotation was also used from the same version of phytozyme.

3.2 Part B - Algal-Bacterial Consortia in Combined Biohydrogen Generation and Wastewater Treatment

3.2.1 Preparation of Microbial Inoculum

Samples were collected from a full-scale methane bioreactor using sludge generated by the wastewater pre-treatment process of a beer brewing factory. Once collected, the samples were incubated for 24 hours at 32°C. The samples were then incubated at 70°C for 1 hour to selectively reduce the abundance of potential hydrogen-consuming microorganisms, primarily methanogenic

Archaea. This community (mostly consisting of bacteria) was applied as enriched microbial inoculum (EMI) used in a 5% volume for photo-fermentation experiments.

3.2.2 Green algae Inoculum

For the photoheterotrophic degradation experiments axenic green algae *Micractinium* MACC-360 (henceforth referred to as *Micractinium*) was added to the dark fermentation effluents. Freshly grown algae (OD_{750}: 0.7 equal to $2.77 * 10^8$ algae cell ml^{-1}) were added to the dark fermentation effluent in a 10% volume (2 ml in 20 ml). The green algae strain was obtained from the Mosonmagyaróvár Algal Culture Collection (MACC; Institute of Plant Biology, University of West-Hungary, Hungary) and grown on TAP medium as described in our previous work [Lakatos et al., 2017]. The algae liquid cultures and plates were continuously incubated under 50 µmol $m^{-2}s^{-1}$ light intensity at 25°C.

3.2.3 Photoheterotrophic Bioreactor Operation

The green algae-driven photoheterotrophic degradation of the dark fermentation effluent (EFF) was conducted under several different experimental conditions (Table 5, Figure 15). EFF was the result of microbial dark fermentation of a brewery's raw initial wastewater (RIW) [Boboescu et al., 2014]. The batch-mode experiments were conducted in 40 mL serum vials with 20 ml of dark fermentation effluent (either 3x diluted or non-diluted effluents), inoculated with 2 mL freshly grown *Micractinium* green algae ($5.54 * 10^8$ algae cell). For certain samples, 1 ml (5 %) of enriched microbial inoculum (EMI) was added. Photoheterotrophic fermentation was performed at 24°C in batch mode for a period of 72 hours under continuous illumination with 50 µmol $m^{-2}s^{-1}$ light intensity, the vials were shaken at 120 rpm. Samples were taken at 72 hours for the determination of substrate degradation rates and microbial community composition. All experiments were performed in triplicate.

3.2.4 Analytical Methods

Biomass in each culture was estimated by daily measurement of optical density (OD_{600}) with a Jenway 6320D Spectrophotometer. The algae cell numbers were counted on Tris-Phosphate solid media using serial dilutions. All experiments were repeated three times.

Hydrogen was directly measured by gas chromatography using an Agilent Technologies 7890A GC system equipped with a thermal conductivity detector and argon as a carrier gas. The temperatures of the injector, detector, and column were kept at 30, 200, and 230°C, respectively. An HP MolSieve column was used (Agilent). Since a concentration gradient of H_2 gas can form in the vial headspace, gas samples (0.5 ml) were taken out after mixing the headspace gas by sparging several times with a gas-tight syringe. Both daily (by sparging the headspace with nitrogen every 24 hours after the

measurement) and total accumulated (without headspace sparging) hydrogen production were measured.

Wastewater degradation efficiency was monitored as a result of BOD analysis (Biological Oxygen Demand) as well as total N and total P measurements. BOD measurements were performed according to the instructions of Hach-Lange Cuvette Test LCK555 at the start of the photo-fermentation experiment and 72 hours. Total nitrogen and total phosphorous were measured according to the instructions of Hach-Lange Cuvette Tests LCK138 and LCK349, respectively, at the start of the photo-fermentation experiment and 72 hours.

3.2.5 Total DNA Extraction from Samples

DNA from complex samples was extracted and purified according to described methods with some modifications (Sharma et al., 2007). Samples (0.5 g) were extracted with 1.3 ml extraction buffer (100 mM Tris-Cl pH 8.0, 100 mM EDTA pH 8.0, 1.5 M NaCl, 100 mM sodium phosphate pH 8.0, 1% CTAB). After thorough mixing, 7 μl of proteinase K (20.2 mg ml^{-1}) was added. After incubation for 45 min, 160 μl of 20% SDS was added and mixed by inversion several times with further incubation at 60°C for 1 h with intermittent shaking every 15 min. Samples were centrifuged at 13,000 rpm for 5 min and the supernatant was transferred into new Eppendorf tubes. The remaining pellets were treated three times with 400 μl extraction buffer and 60 μl SDS (20%) and kept at 60°C for 15 min with intermittent shaking every 5 min. Supernatants collected from all four extractions were mixed with an equal quantity of chloroform and isoamyl alcohol (25:24:1). The aqueous layer was separated and precipitated with 0.7 volume isopropanol. After centrifugation at 13,000 rpm for 15 min, the brown pellet was washed with 70% ethanol, dried at room temperature, and dissolved in TE (10 mM Tris-Cl, 1 mM EDTA, pH 8.0).

3.2.6 Metagenomic Characterization of Microbial Communities

Total DNA from selected samples was prepared for high-throughput next-generation sequencing analysis performed on the Ion Torrent PGM platform (Life Technologies). To estimate coverage in sequenced metagenomes we used Nonpareil [Rodriguez-R and Konstantinidis, 2014].

Taxonomic profiling and assessment of metabolic potential were conducted using the public MG-RAST software package, which is a modified version of RAST (Rapid Annotations based on Subsystem Technology) [Meyer et al., 2008]. The sequence data were compared to M5NR database using a maximum e-value of 1×10^{-5}, a minimum identity of 95%, and a minimum alignment length of 15, measured in amino acids for protein and base pairs for RNA databases.

All results for taxonomy and functional assignment were downloaded from MG-RAST and visualized in R (Version 3.5.1) using Vegan [Oksanen et al., 2016] and ggplot2 [Wickham, 2016]. This also allowed us to filter assignments with read counts lower than five reads per taxonomy unit and incorrectly assigned reads.

3.2.7 Metagenome Assembly, Genome Binning, and Annotation

All reads were then trimmed to increase quality and remove contaminants using bbduk (http://jgi.doe.gov/data-and-tools/bb-tools/). Reads matching algal genomes were identified and separated. Multiple draft algal genomes were downloaded from NCBI and were used as reference to identify algal-specific reads using bbduk. This allowed for the assembly of the prokaryotic microbiome and eukaryotic algal reads individually.

The microbiome and algal reads were assembled using Megahit [Li et al., 2015]. This is one of the few programs that can assemble single-end metagenome reads. We then used MetaWrap to bin the bacterial contigs into species-specific bins [Uritskiy et al., 2018]. MetaWrap accepts bacterial assembled contigs and extracts individual draft genomes by using multiple binning software (metaBAT2, MaxBin2, and CONCOCT) and identifying those bins with the highest evidence across all three binning tools. The extracted bins were uploaded to the RAST server to annotate draft bacterial bins.

The three bacterial bins were also subsequently annotated using Prokka [Seemann, 2014]. Annotated protein sequences were then uploaded to KEGG database and BlastKoala [Kanehisa et al., 2016] was used to identify specific genes involved in biosynthesis pathways such as cobalamin, biotin, and thiamine biosynthesis.

All raw fastq files were uploaded to NCBI with SRA accession number PRJNA521112.

4. RESULTS

4.1 Part A – High-throughput co-culture assays to investigate algal-bacterial interactions

4.1.1 Impact of algal-bacterial co-cultivation on *C. reinhardtii* biohydrogen and biomass production.

A total of twenty-eight bacterial strains were used for pairwise co-cultivation studies with *C. reinhardtii*, ten isolates selected from frozen stock, five isolates from contaminated cultures, six isolates from biogas sludge samples, six isolates from a commercially available bacterial biostimulant product, and one isolate coming from an environmental sample (Figure 3).

The accumulated biohydrogen production from algal-bacterial co-cultivation samples varied from 0 ml L^{-1} culture medium to 14.18 ml L^{-1} culture medium on day 3 post-inoculation. It was interesting to identify some cultures producing no biohydrogen even when the oxygen concentration in the headspace was very low due to bacterial respiration. It is currently unclear if the absence of hydrogen production was due to the uptake of hydrogen by the bacterial partner or other circumstances. This data demonstrates the importance of choosing bacterial partners, to guarantee high biohydrogen generation.

All co-cultivations, except one, led to an improvement in algal biomass. Increase in algal biomass was calculated in the following manner:

$$\text{Percentage increase} = \frac{(\text{Counts under co} - \text{cultivation}) - (\text{Counts under Axenic condition})}{\text{Counts under Axenic condition}} * 100$$

Linear regression models were used to identify bacterial genera that consistently improved biohydrogen. Biohydrogen production was statistically significant for *Bacillus* (p-value=0.00123) and *Rummeliibacillus* (p-value = 0.02) (Figure 3). Another important finding was the extremely low values of biohydrogen observed under co-cultivation with members of the family *Methylobacteriaceae*. So, we did indeed find an interaction between closely related bacterial species and trait improvement in algal biohydrogen production. Interestingly, there seems to be no detectable relationship between bacterial phylogeny and percentage increase in algal biomass (Figure 4).

We also explored the importance of bacterial growth characteristics on biohydrogen production and biomass. A fairly obvious but weak signal was identified with percentage increase in algal biomass being negatively correlated with bacterial inflection point (Supplementary figure 2). The inflection point is described as the time required to reach half the carrying capacity. Carrying capacity is the maximum population density in a particular habitat or medium. Thus, percentage increase in algal counts was reduced if the bacterial partner did not have vigorous growth in the medium.

Figure 3: Amount of accumulated hydrogen under pairwise co-cultivation with different bacterial species. The length of bar at the end of each branch indicates the amount of biohydrogen (ml L^{-1}) and colors indicate the source of bacterial strain.
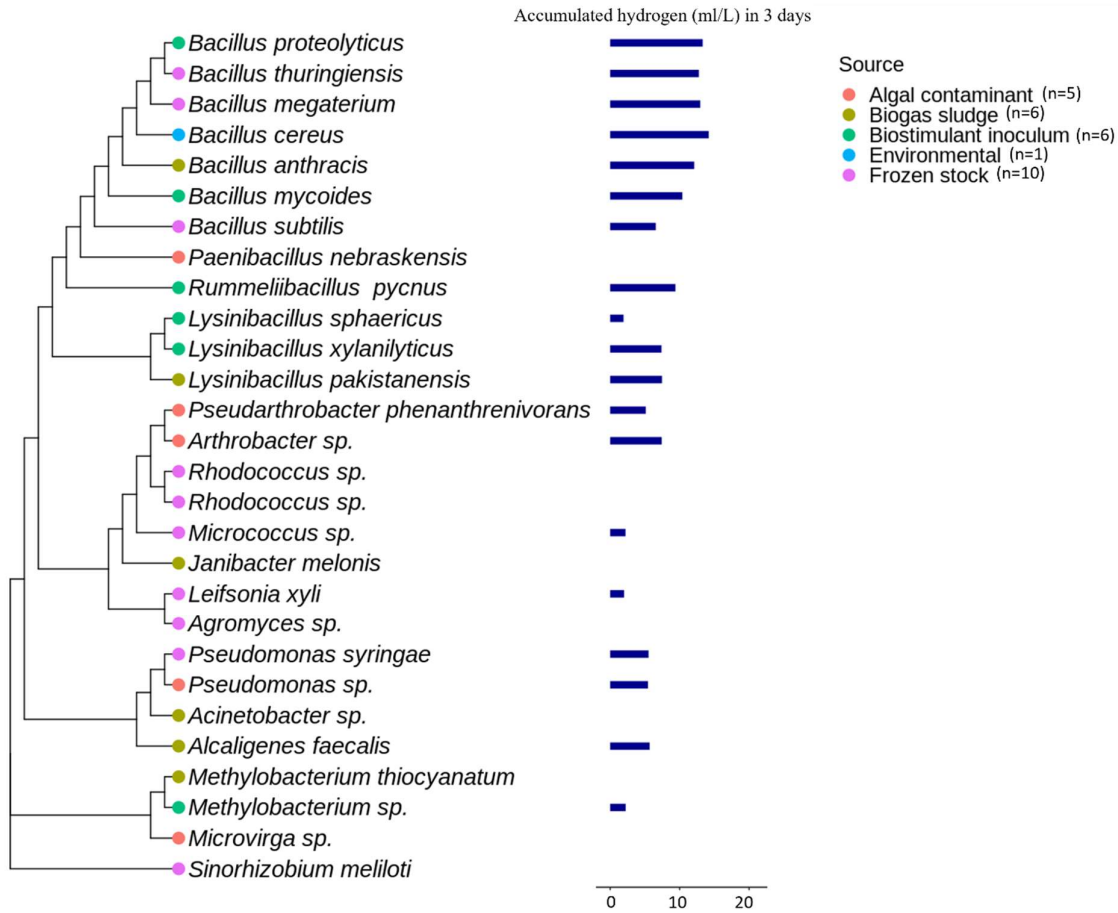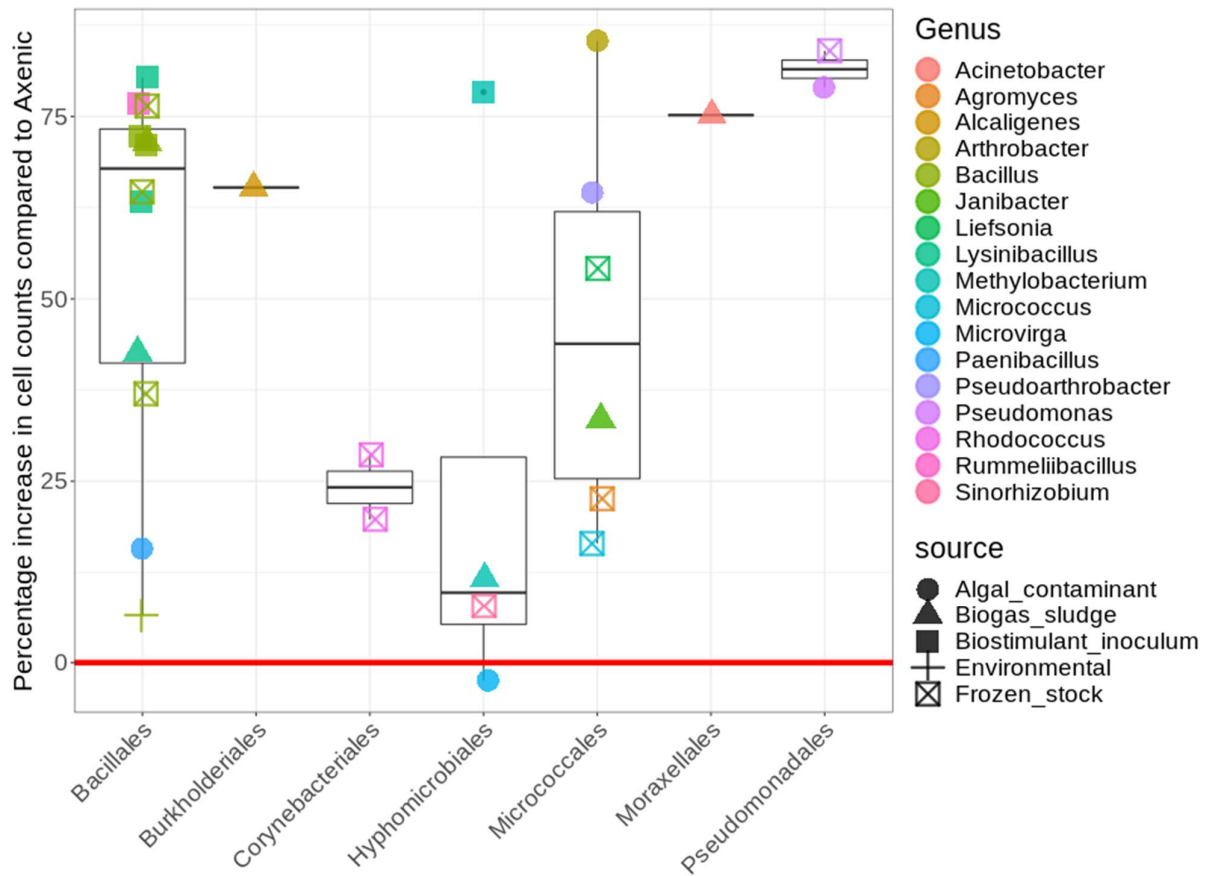
Figure 4: Percentage increase in algal cell counts under bacterial co-cultivation. No significant relationship was identified between high algal cell counts and accumulated biohydrogen production

4.1.2 Impact of algal-bacterial co-cultivation across different algal species.

The second objective was to study if the bacterial species improving algal biohydrogen production was conserved across different algal species. We shortlisted four bacterial species, three from the *Bacillus* genus (*Bacillus megaterium, Bacillus thuringiensis,* and *Bacillus cereus*); that greatly improve biohydrogen production and one that moderately improves biohydrogen production (*Methylobacterium* sp.) as observed from the previous experiment. We compared the biohydrogen production and cell counts under axenic conditions and bacterial association across 3 different green algae; *C. reinhardtii* (model green algae), *Micractinium* (high biohydrogen producer), and *Parachlorella* (high biohydrogen producer). A cross-species comparison across different algal species and the same bacterial combinations allowed us to identify if the relationship between bacterial strains and high biohydrogen production in green algae was conserved.

Members of the *Bacillus* genus consistently improved biohydrogen production when co-cultivated with different alga, while hydrogen production using *Methylobacterium* sp. as bacterial partner stayed around 5ml L^{-1} culture medium regardless of the algal host. *Parachlorella* produced about 50.87±2.4

ml L^{-1} culture of biohydrogen under co-cultivation with *Bacillus thuringiensis* and *Micractinium* produced about 42.51±1.2 ml L^{-1} culture of biohydrogen on day 3 post-inoculation (Figure 5).

All bacterial species increased algal growth to different percentages, depending on the algal host. *Parachlorella* had the lowest improvement in algal cell counts under bacterial cultivation (~10% increase) relative to axenic cultivation while *Micractinium* had the highest (~200% increase) (Figure 6).

Figure 5: Accumulated biohydrogen across different algal species, when co-cultivated with bacterial partners.
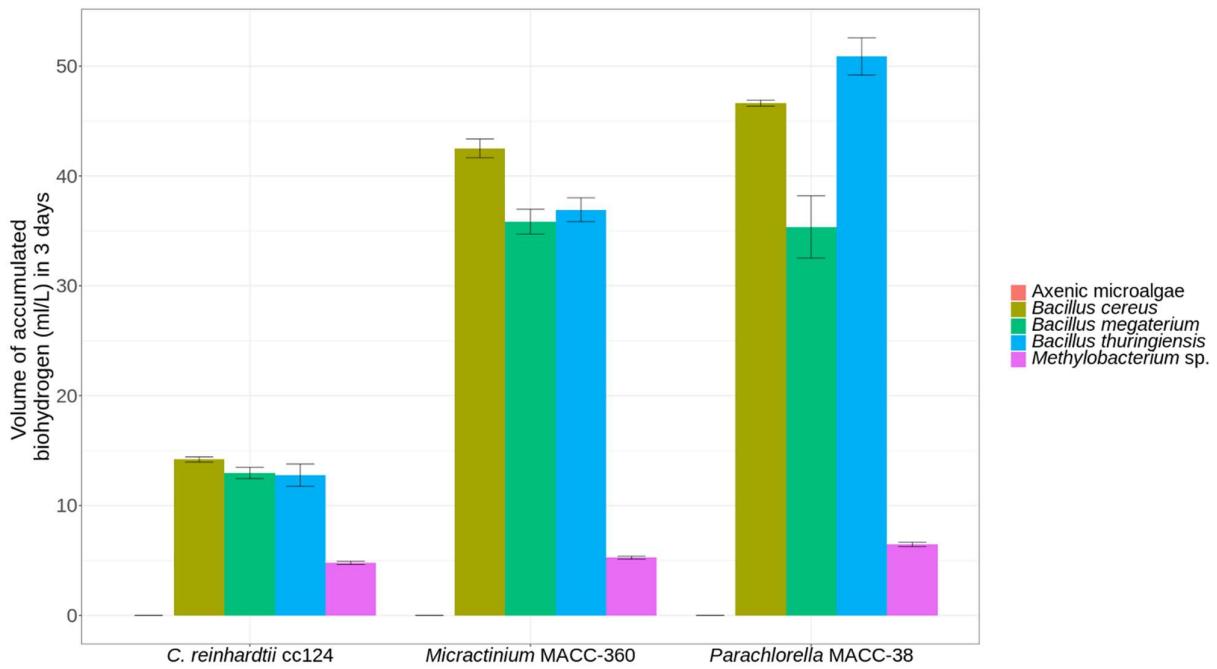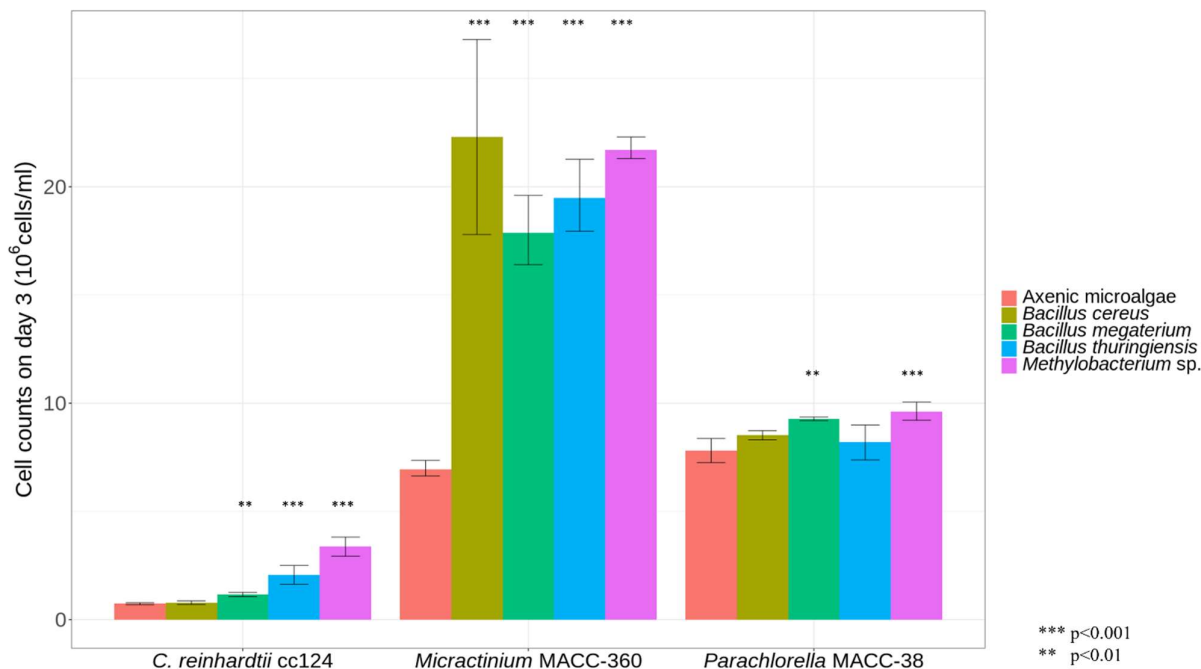
Figure 6: Percentage increase in cell counts under bacterial co-cultivation relative to axenic cultivation across different algal species.

4.1.3 Impact of algal-bacterial co-cultivation on algal biomolecule concentration

We explored the impact of bacterial co-cultivation on 3 different biomolecules: Chlorophyll a/b ratio, Carbohydrates, and Lipids.

Bacterial co-cultivation led to an increase in the Chlorophyll a/b ratio across all bacterial cultivation, with *Bacillus* co-cultivation showing the highest ratio of ~2 and co-cultivation with *Methylobacterium* sp. showing a ratio of ~1.9 on day 3 post-inoculation. This is roughly a 33% increase in chlorophyll a/b ratio compared to axenic cultivation (Figure 7A). Only in axenic cultures we observe a steady reduction in the chlorophyll content over the course of the 3 days of cultivation, suggesting that *C. reinhardtii* may be nutrient limited in axenic circumstances (Figure 7B).

Carbohydrate concentration measurement was done with 2 biological replicates and 4 technical replicates. Results indicated a significant improvement in carbohydrate concentration under all bacterial cultivation, with *Methylobacterium* sp. showing the highest amount of accumulated carbohydrate on day 3 post-inoculation (Figure 8).

Finally, we also observed a significantly high lipid accumulation under bacterial co-cultivation. Under axenic conditions total accumulated lipids were estimated to be 2.13 ± 0.262 µg mg^{-1} of biomass. However, under bacterial co-cultivation total accumulated lipids was always greater than 7 µg mg^{-1} of biomass (Figure 9A). There is always the possibility that the increased total lipid was coming from the associated bacterial partners. Thus, we used confocal microscopy to visualize the lipid vesicles.

Confocal microscopy corroborated the increased lipid accumulation finding with almost no lipid vesicles being identified under axenic condition and huge lipid droplets visualized under *Bacillus* co-cultivation (Figure 9B).

Figure 7A: Chlorophyll a/b ratio of *C. reinhardtii* under axenic and co-cultivation on day 3 post-inoculation
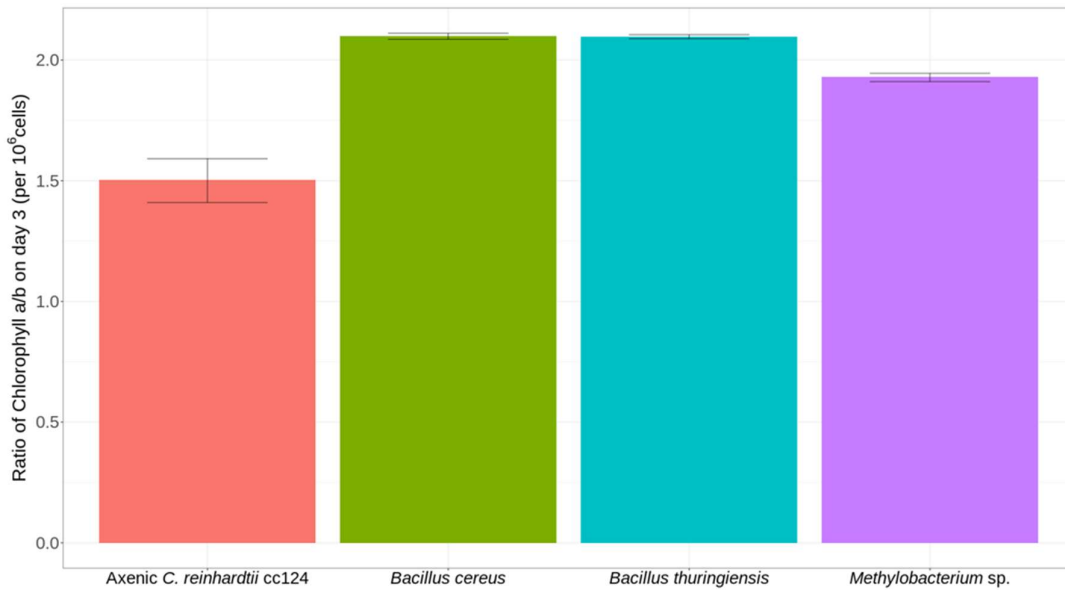
Figure 7B: Chlorophyll A and chlorophyll B content measured across three days. Chlorophyll content shows a steady reduction only in axenic cultures.
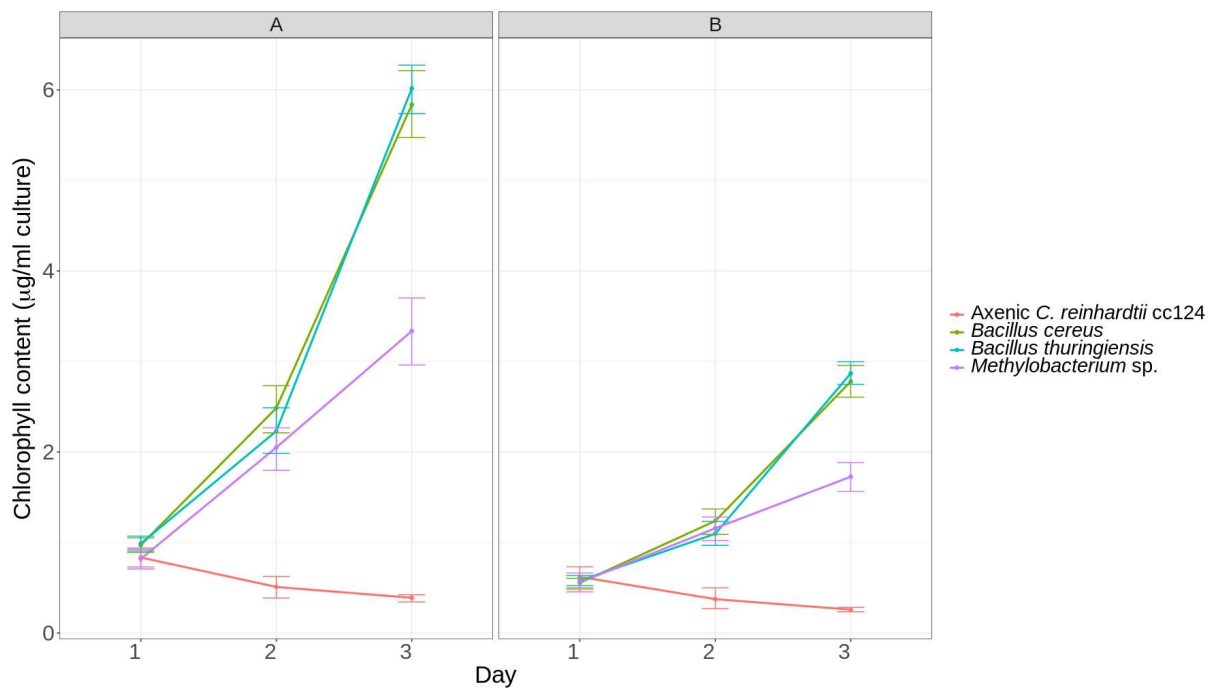
Figure 8: Total accumulated carbohydrate by *C. reinhardtii* on day 3 post-inoculation
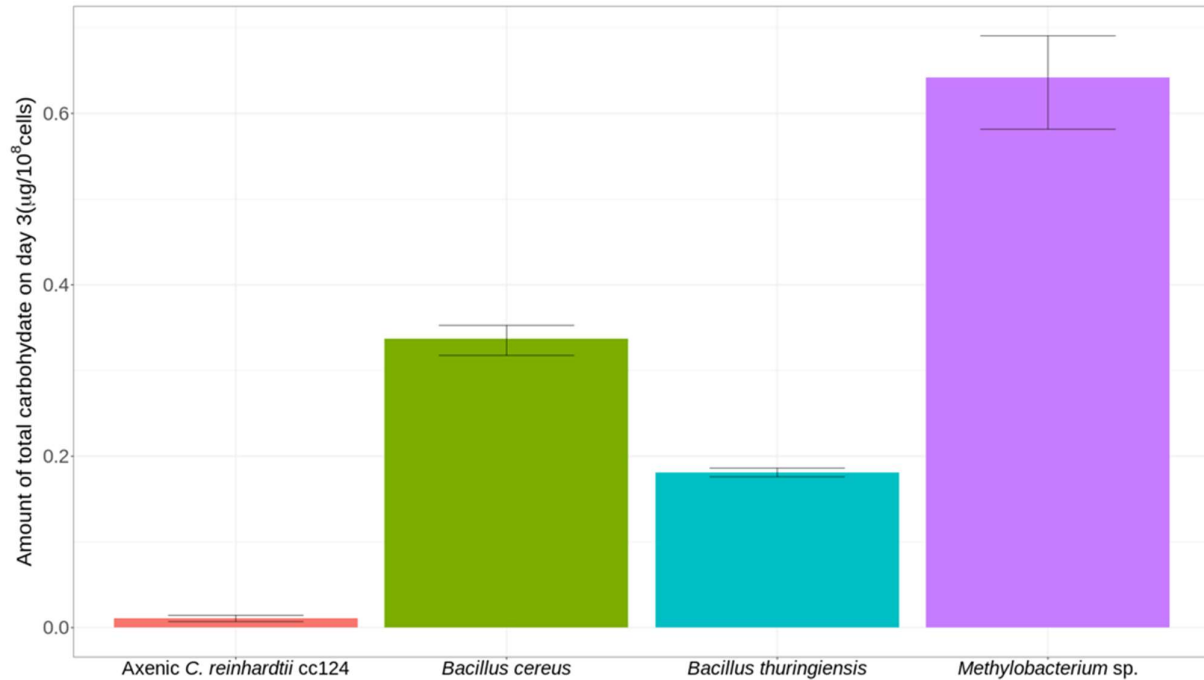
Figure 9A: Total accumulated lipids by *C. reinhardtii* on day 3 post-inoculation
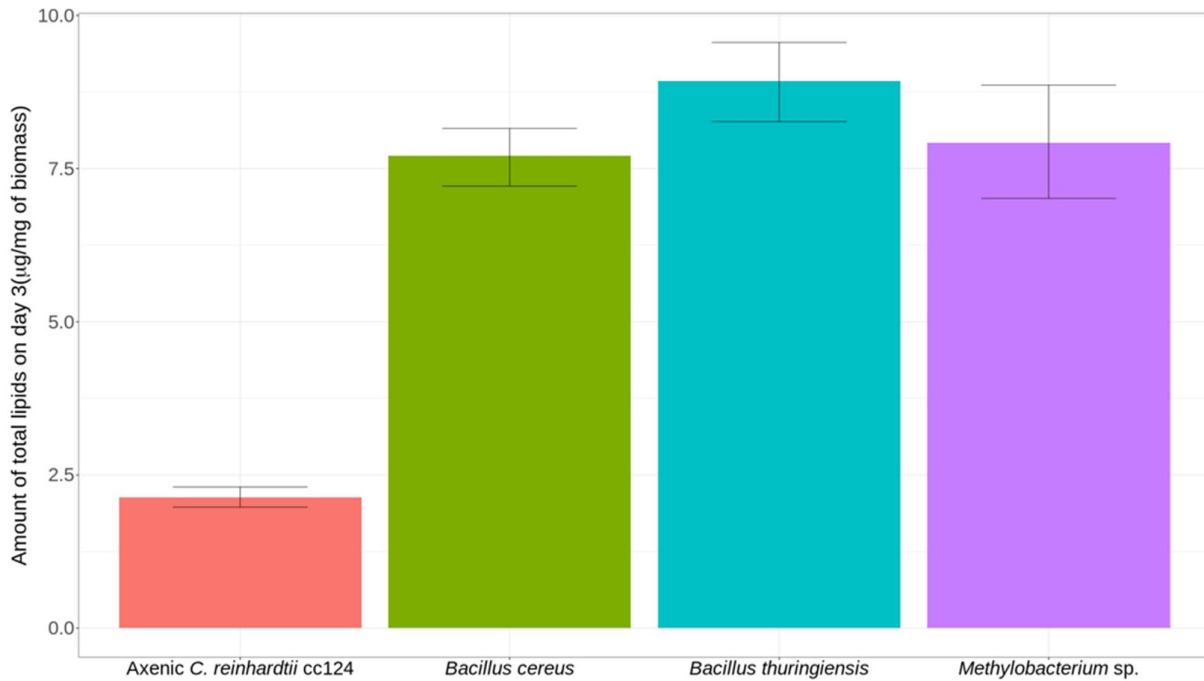
Figure 9B: Visualization of neutral lipids using BODIPY dye on day 3 post-inoculation. A) Axenic condition, B) Co-cultivation with *Methylobacterium* sp., C) Co-cultivation with *Bacillus thuringiensis*, D) Co-cultivation with *Bacillus cereus*. Images on the left are composite images comprising of both fluorescence and optical images. The images on the right are composite images

under chlorophyll autofluorescence and BODIPY specific fluorescence. Red color corresponds to chlorophyll auto-fluorescence and green color corresponds to BODIPY labeled lipid vesicles.
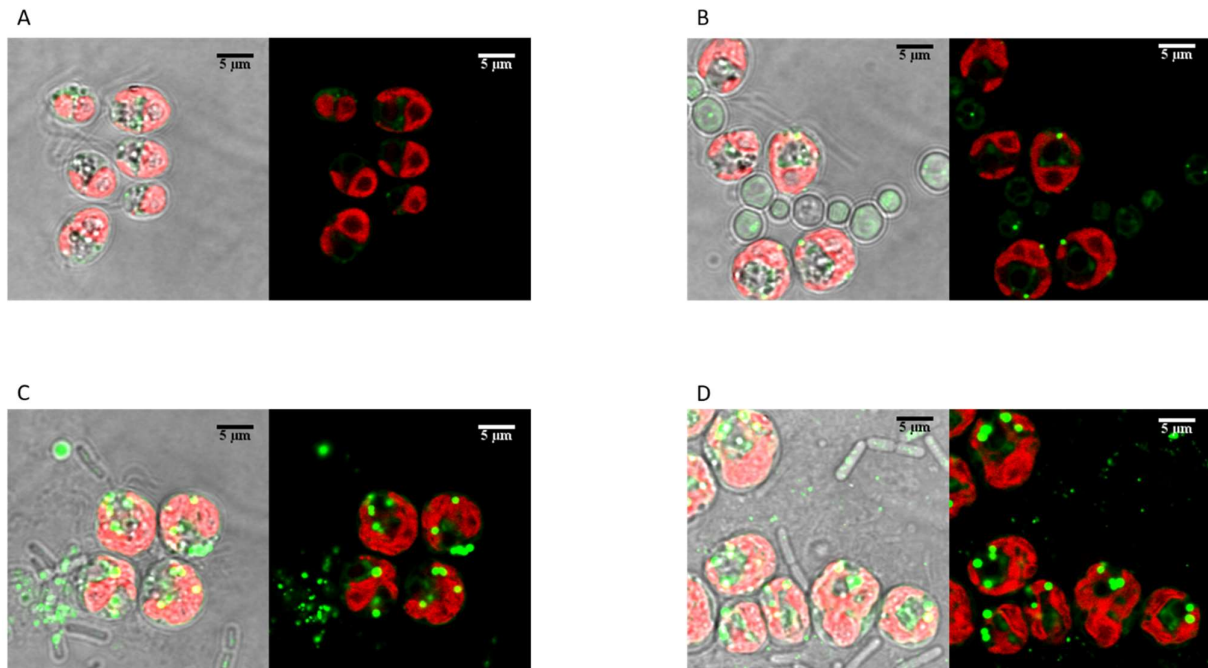
4.1.4 Transcriptome analysis of *C. reinhardtii* under axenic and bacterial co-cultures.

Transcriptome analyses were carried out to reveal pathways enriched for biohydrogen production with 3 bacterial partners and axenic conditions on Day 2 of cultivation. 48 hours post inoculation is typically when the accumulated hydrogen production starts increasing rapidly, and thus was selected as the ideal time point to identify active pathways. Three bacterial strains were selected based on cell count data, hydrogen production, and carbohydrate measurement data. These were *Methylobacterium* sp. (isolated from biostimulant sample), *Bacillus cereus* (isolated from Yellowstone national park), and *Bacillus thuringiensis* (retrieved from frozen stock).

Table 4 shows the metrics for reads pairs generated and used in the analysis. Overall ~93% of read pairs (%) found matches against the reference *C. reinhardtii* v5.6 transcriptome. Figure 10 shows a PCA plot to visualize the similarity between replicates and across samples. All replicates clustered together, and samples from bacterial-associated conditions clustered away from axenic condition indicating that expressed genes were more similar under bacterial association compared to axenic cultivation. Also, samples from both the *Bacillus* co-cultivations clustered closer together compared to samples from *Methylobacterium* sp., indicating that similar genes were expressed. Despite being obtained from different sources, this result shows that members of *Bacillus* genus interact with *C. reinhardtii* similarly.

We were then interested in identifying how genes associated with hydrogen production were expressed across all three bacterial-associated conditions. Differential expression analysis revealed an almost complete rewiring of the metabolic pathways with more than 6000 genes (~37% of all genes) being significantly differentially (adjusted p-value=0.01, and $\log_2$ fold change of 1) regulated under bacterial cultivation compared to axenic condition (Figure 11A,B,C). Such a large-scale change indicates that *C. reinhardtii* is metabolically and physiologically different under bacterial cultivation. Some glimpses of these large-scale changes were observed just in previous experiments with greatly promoted cell growth, hydrogen production, and carbohydrate accumulation compared to axenic cultivation. The low functional annotation rate prevalent across *C. reinhardtii* genome specifically and algal genomes, in general, makes a thorough examination of each gene difficult. Thus, we compared expression profiles to previous experiments involving hydrogen production under sulfur deprivation condition [Toepel et al., 2013, Nguyen et al., 2008]. We also searched for orthologous matches against the proteome of *Lobomonas rostrata* [Helliwell et al., 2017]. *L. rostrata* is a unicellular green alga that requires an exogenous supply of vitamin B_{12}. A total of 37 genes were identified through a similarity search and found to be differentially regulated in our study. Figure 12 provides a brief overview of all the important genes under differential expression across all conditions.

We also identified genes that were differentially regulated and shared either by all samples under bacterial co-cultivation or by samples only under *Bacillus* co-cultivation (Figure 13). A total of 1379 genes were upregulated in axenic condition and shared by all samples under bacterial co-cultivation, while a total of 2270 genes were downregulated in axenic condition and shared by all samples under bacterial co-cultivation. Genes downregulated in axenic conditions were alternatively genes that were upregulated in bacterial-associated conditions. GO enrichment studies were performed on these gene lists to identify important groups differentially expressed either under bacterial co-cultivation or under only co-cultivation with the two *Bacillus* species. The most interesting GO enriched terms were identified in genes downregulated in axenic condition. GO ontology of genes downregulated in axenic condition and shared by all samples under bacterial co-cultivation revealed the presence of terms modulating the salicylic acid pathways, reproductive process and cell division, carbohydrate transport, and vesicle-related genes (Figure 14B). GO ontology of genes downregulated in axenic conditions and shared by samples only under *Bacillus* co-cultivation showed terms related to glycoprotein biosynthesis, transport proteins, and vesicle-related genes (Figure 14D). Finally, GO ontology of genes upregulated in axenic samples showed the enrichment of terms related to amino acid catabolic processes (Figure 14A,C).

Table 4: Read and mapping metrics RNAseq

Co-cultivation condition	Raw read pairs	Trimmed reads pairs	Aligned read pairs	Percentage aligned
Methylobacterium sp.,	21 305 748	15,371,583	14,376,468	93.52
Methylobacterium sp.,	22 203 051	16,041,678	14,753,052	91.96
Methylobacterium sp.,	17 479 085	13,443,718	12,564,094	93.45
Axenic	16 854 901	11,989,770	11,265,031	93.95
Axenic	19 905 683	14,603,083	13,719,666	93.95
Axenic	17 479 085	11,975,099	11,285,215	94.23
Bacillus thuringiensis	17 242 372	12,365,289	11,542,988	93.349
Bacillus thuringiensis	20 331 097	14,556,319	13,584,247	93.32
Bacillus thuringiensis	18 938 118	13,868,381	13,021,734	93.89
Bacillus cereus	20 615 188	15,063,374	14,053,673	93.29
Bacillus cereus	17 311 792	12,216,567	11,361,498	93.00
Bacillus cereus	19 241 785	14,081,217	13,115,941	93.14

Figure 10: PCA plot showing distance between different transcriptome samples. Samples under bacterial association cluster away from samples under axenic condition. Samples cultivated with *Bacillus* species cluster closer compared to samples cultivated with *Methylobacterium* sp.
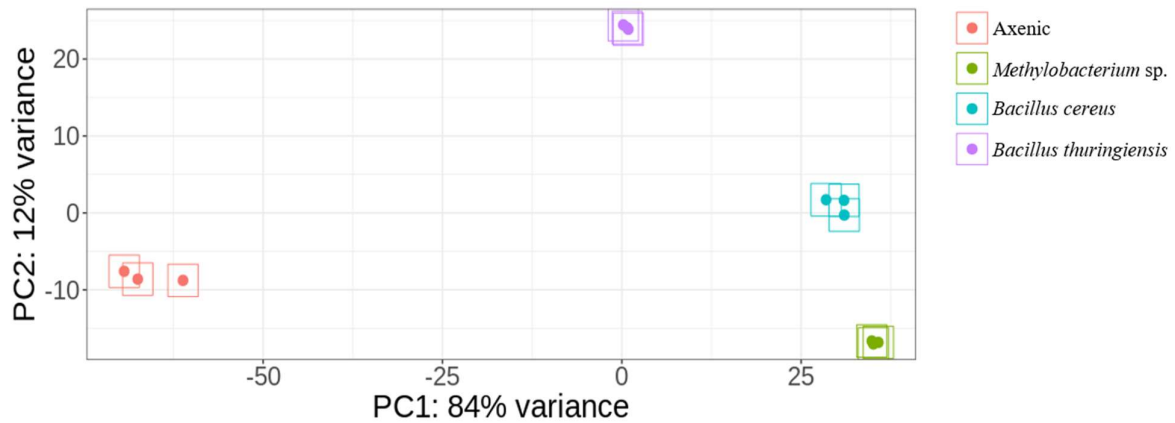
Figure 11A: Volcano plot showing differentially expressed genes between Axenic and *Methylobacterium* sp. samples. A total of 6100 genes out of 16377 genes were differentially regulated at a p-value of 0.01 and a log$_2$ fold change of 1. 2659 genes were upregulated or had higher abundance under axenic condition and 3441 genes were downregulated or had lower abundance under axenic condition.

DEG: 6100 ; UP: 2659 Down: 3441
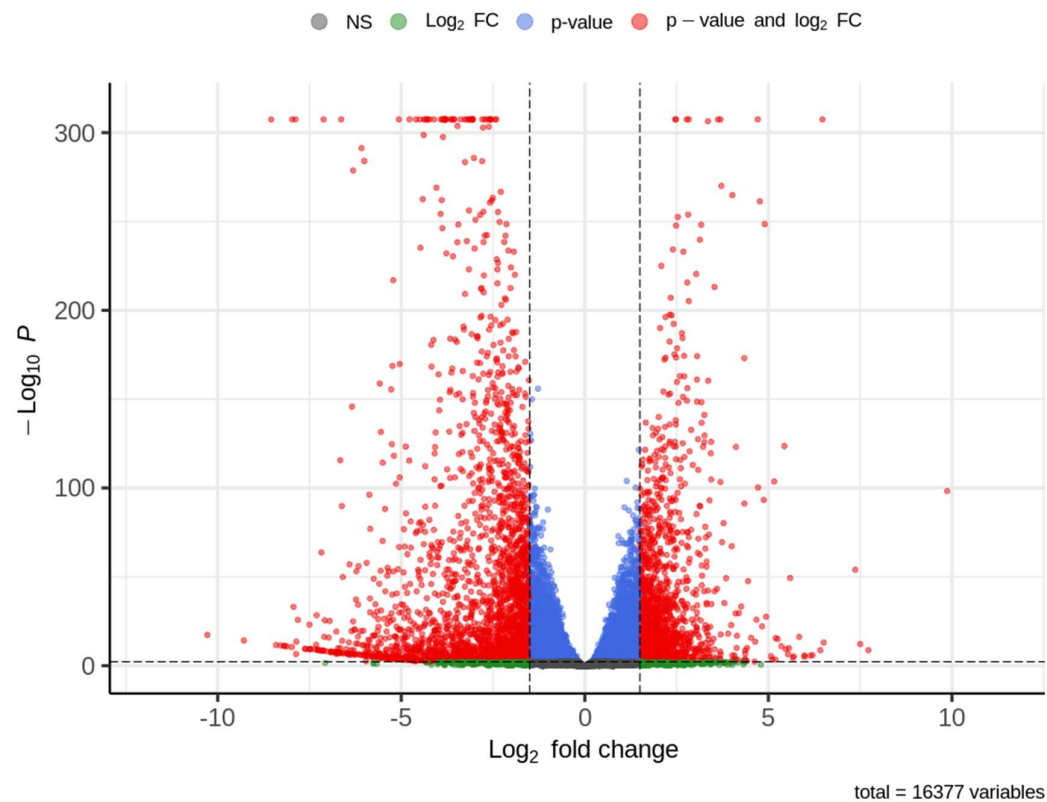
Figure 11B: Volcano plot showing differentially expressed genes between Axenic and *Bacillus thuringiensis* samples. A total of 6871 genes out of 16377 genes were differentially regulated at a p-value of 0.01 and a log$_2$ fold change of 1. 2962 genes were upregulated or had higher abundance under axenic condition and 3909 genes were downregulated or had lower abundance under axenic condition.

DEG: 6871 ; UP: 2962 Down: 3909
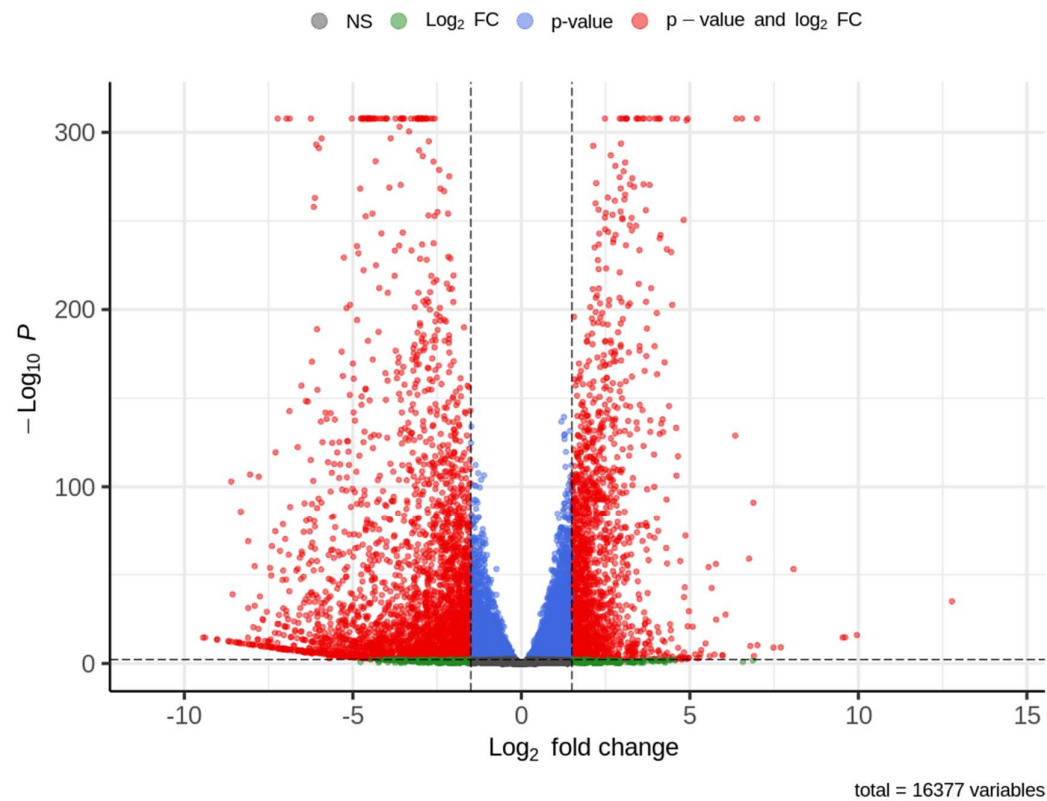
Figure 11C: Volcano plot showing differentially expressed genes between Axenic and *Bacillus thuringiensis* samples. A total of 6745 genes out of 16377 genes were differentially regulated at a p-value of 0.01 and a log₂ fold change of 1. 2781 genes were upregulated or had higher abundance under axenic condition and 3964 genes were downregulated or had lower abundance under axenic condition.
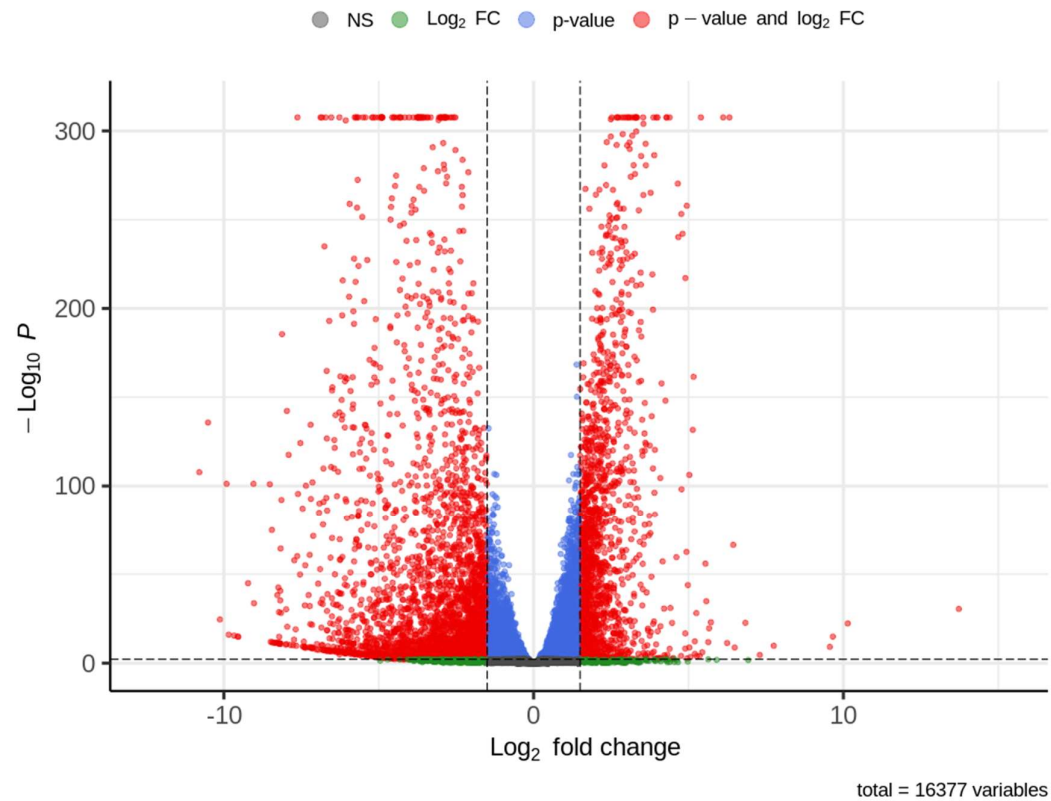
Figure 12: Overview of important differentially regulated genes. The genes are colored by different gene groups. Positive values are colored in red and represent higher gene abundance (upregulation) and negative values are colored in blue and represent lower gene abundance (downregulation).
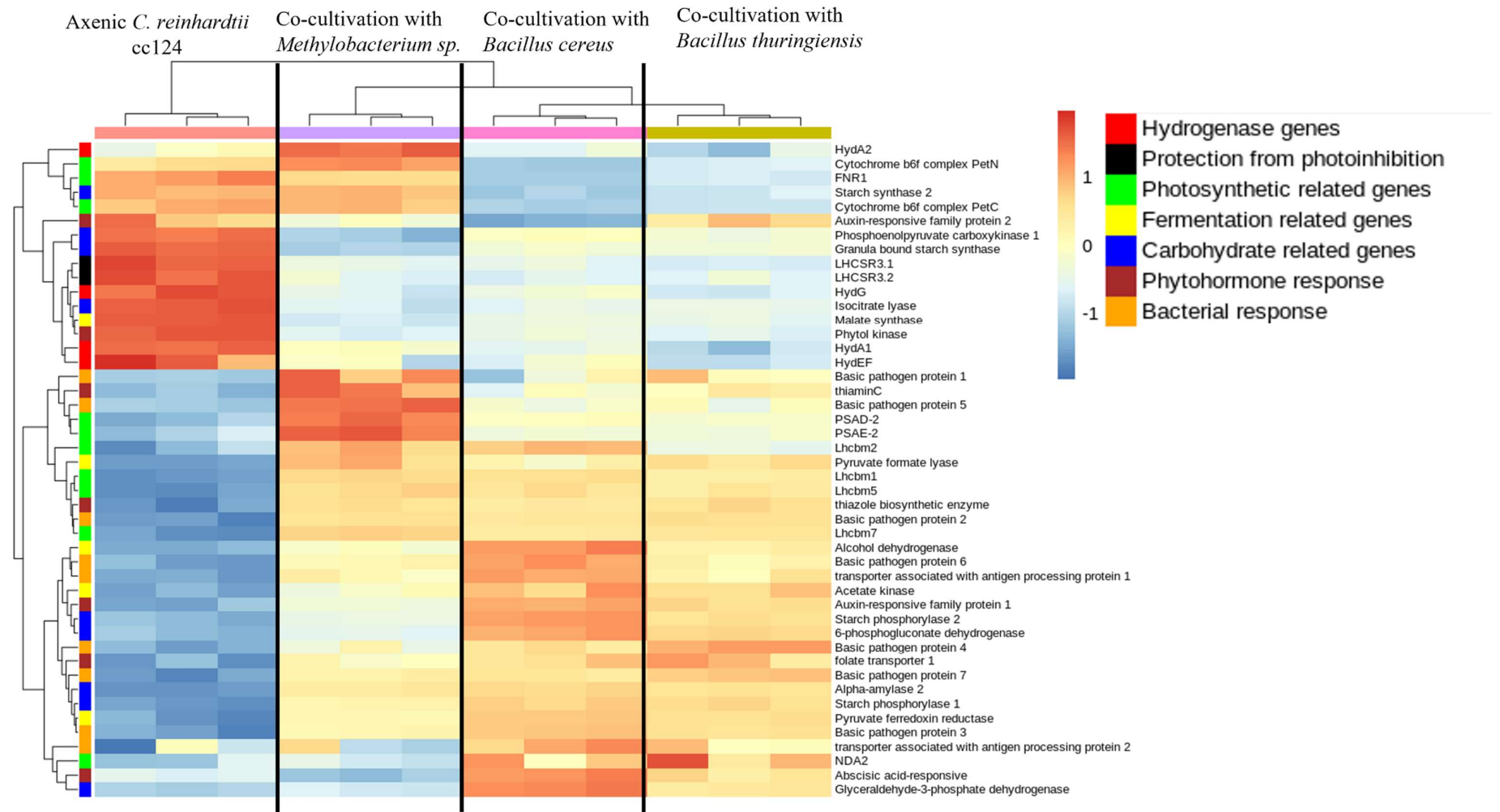
Figure 13: Venn diagram of all genes differentially expressed between all 3 conditions. **A)** Venn diagram represents upregulated genes in axenic condition and shared by all samples under bacterial association. **B)** Venn diagram represents downregulated genes in axenic condition and shared by all samples under bacterial association.
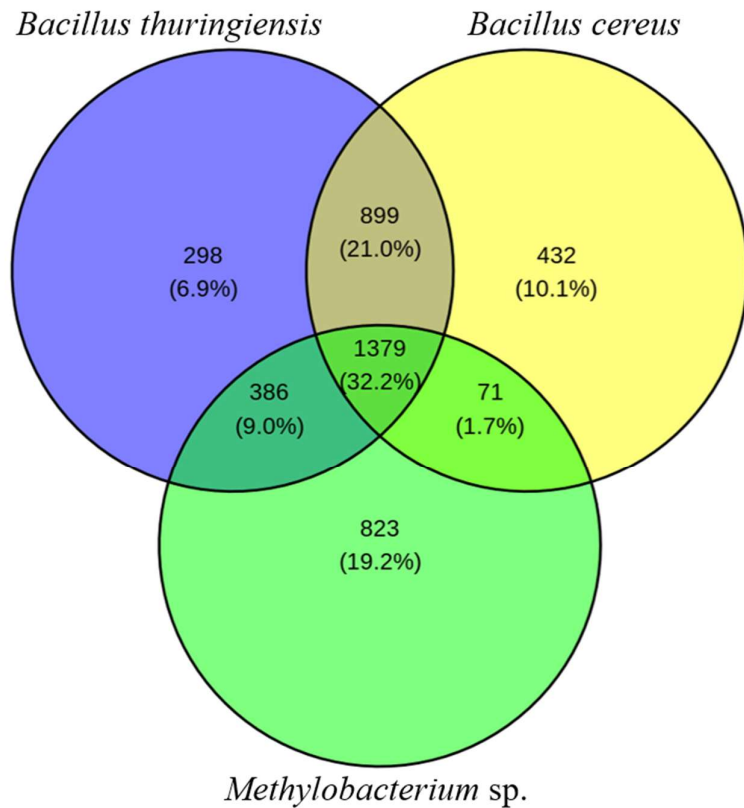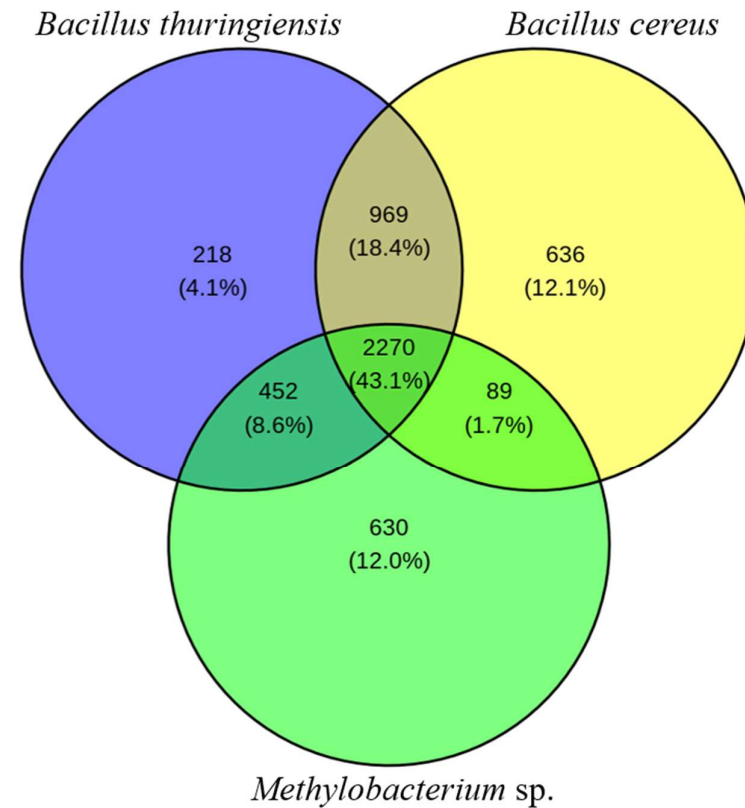
Figure 14A: GO enrichment of upregulated genes in axenic samples and shared by all samples under bacterial co-cultivation.
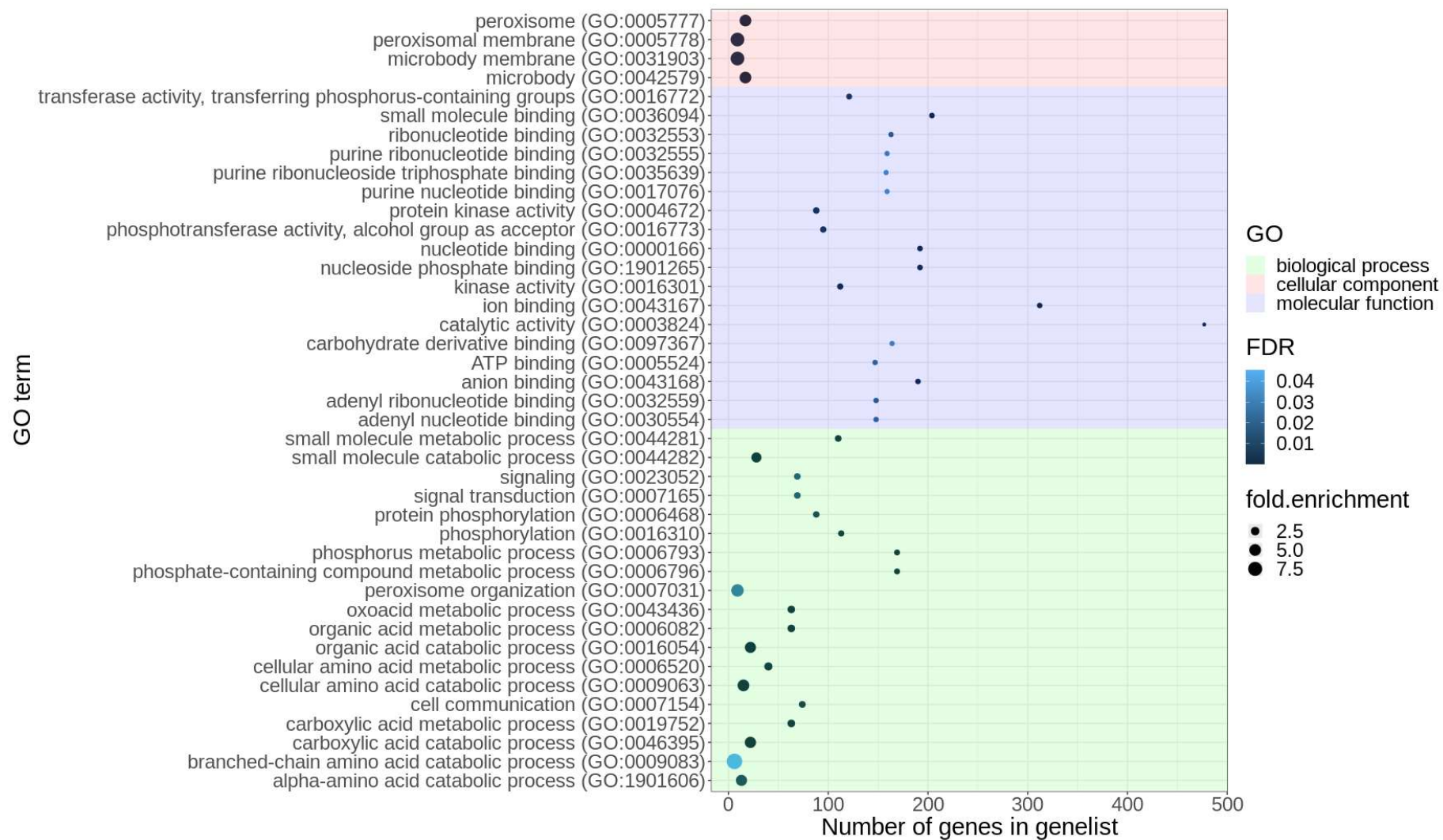
Figure 14B: GO enrichment of downregulated genes in axenic samples and shared by all samples under bacterial co-cultivation.
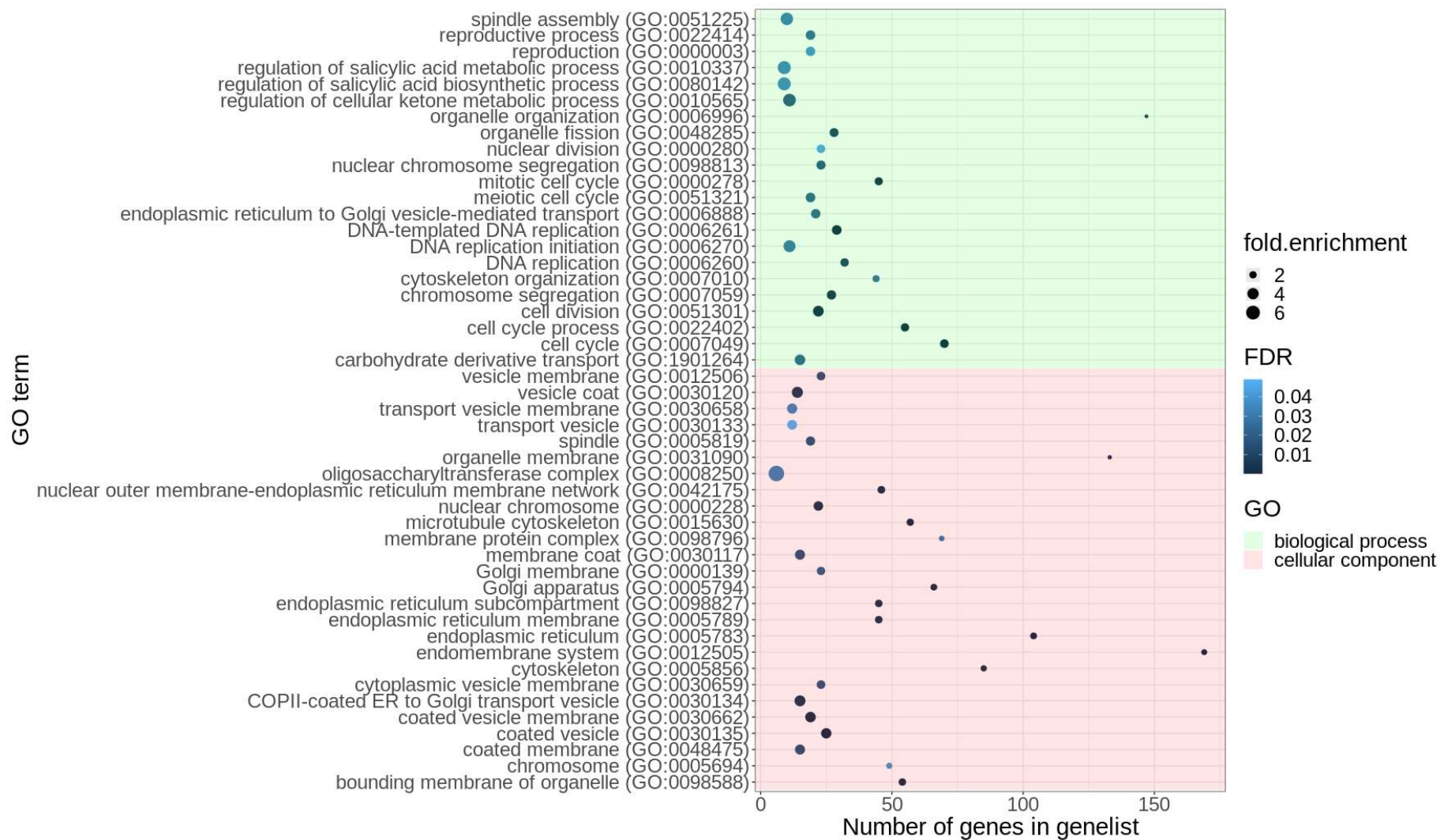
Figure 14C: GO enrichment of upregulated genes in axenic samples and shared by samples under *Bacillus* co-cultivation.
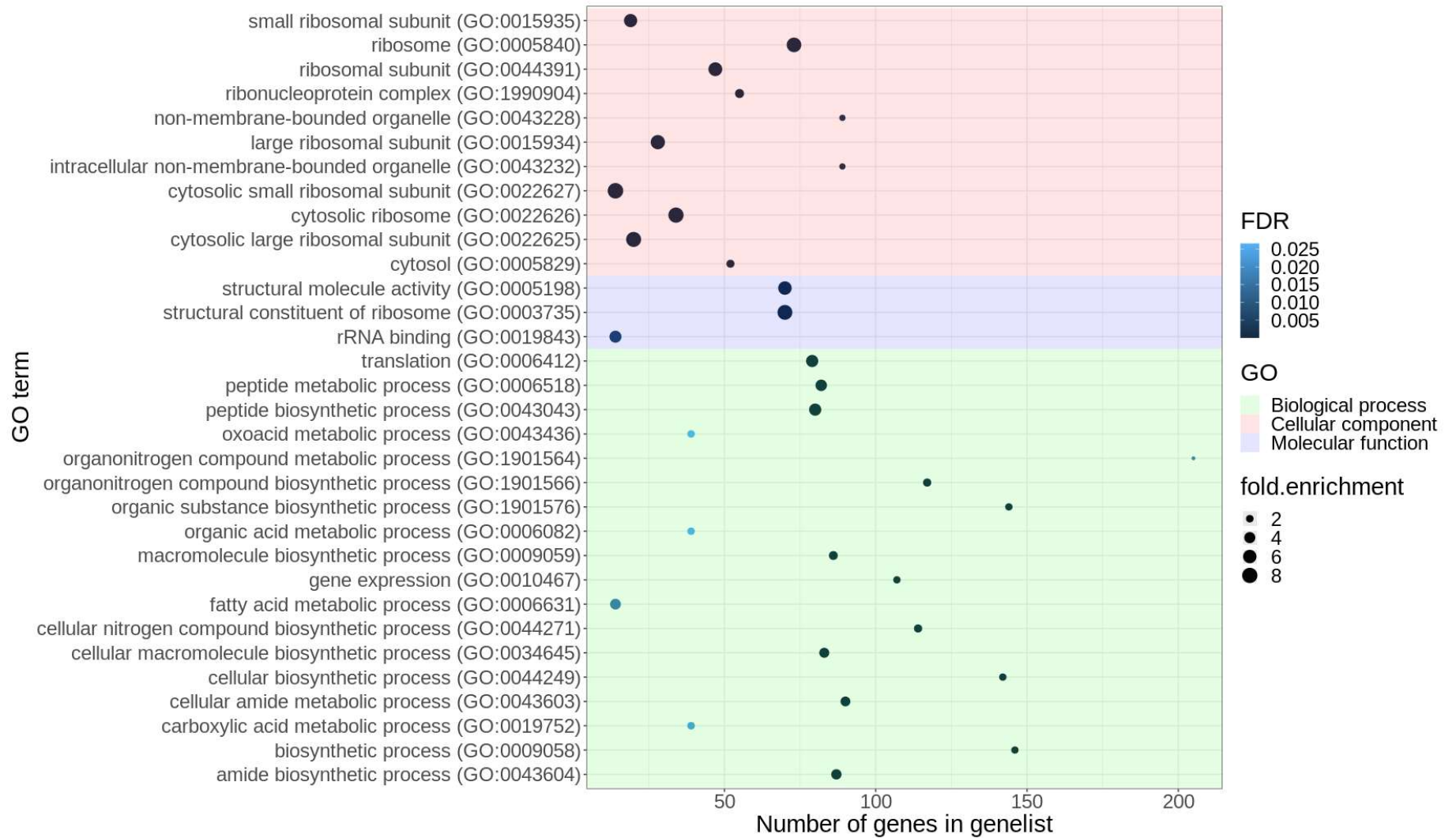
Figure 14D: GO enrichment of downregulated genes in axenic samples and shared by samples under *Bacillus* co-cultivation.
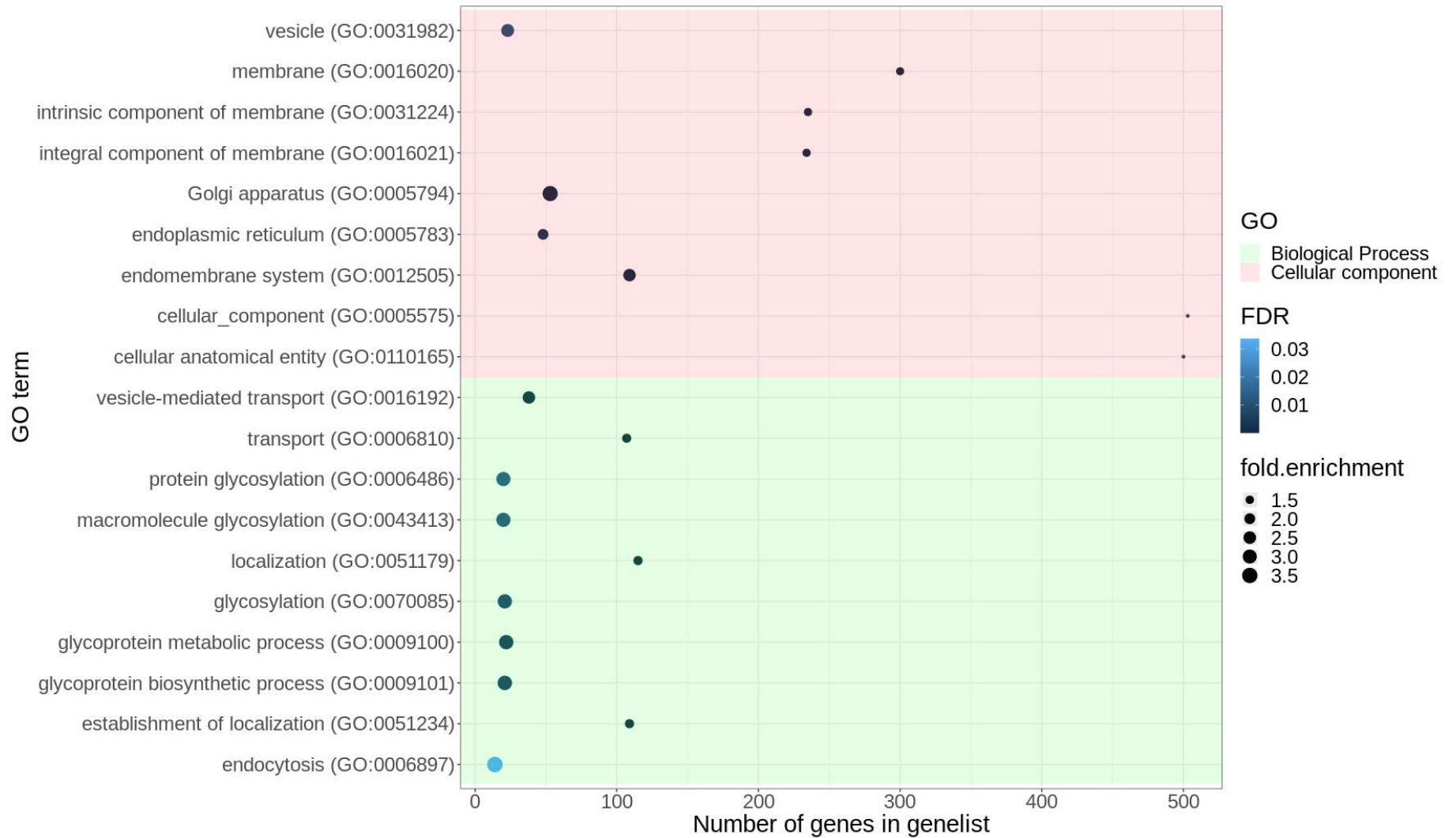
4.2 Part B – Algal-Bacterial Consortia in Combined Biohydrogen Generation and Wastewater Treatment

Bacteria natively present in wastewater effluents have a significant impact on how well photosynthetic green algae recover nutrients. The algal microbiome is a crucial part of the algae holobiont and plays a key role in modulating algal growth and functions in nature. Our suggested method employs a dark fermentation effluent as the substrate for photoheterotrophic cultivation of green algae. Our results demonstrated the existence of a mutualistic interaction between the microbial and *Micractinium* algae population that was treatment dependent and improved the efficiency of biodegradation and algal biohydrogen production. Metagenome investigation on the innovative hybrid biodegradation system offered evidence regarding the pivotal role played by green algae in the removal of phosphorus and nitrogen.

This novel strategy could result in an efficient system that simultaneously reduces organic waste and produces renewable energy. Industrial raw wastewater (RIW) originating from a beer brewing factory was used as our initial substrate for dark fermentation treatment. The dark fermentation effluent (EFF) was then used as culture media for the photoheterotrophic propagation of *Micractinium*. Algal growth and total biomass, biodegradation efficiency, biohydrogen production, and the microbial community structure were monitored and correlated.

Figure 15: Schematic figure of all the treatments used in the study
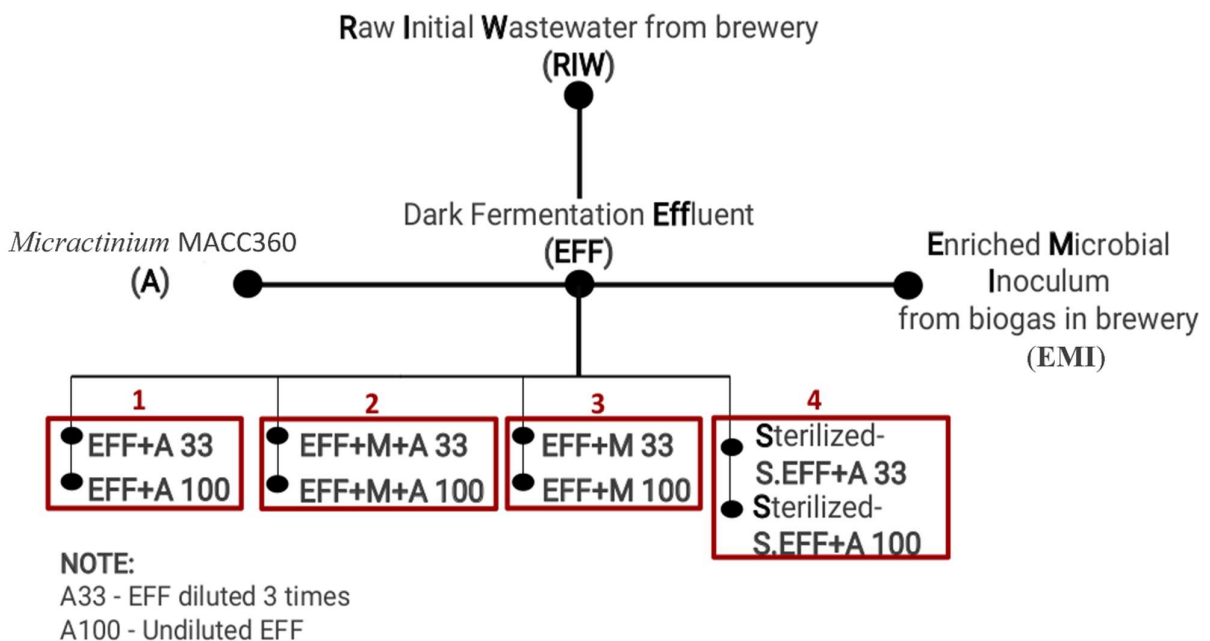
4.2.1 Photo-Fermentative Biomass and Biohydrogen Production

It was crucial to determine whether *Micractinium* could grow and produce a significant amount of biohydrogen when cultivated on dark fermentation effluents. An algae-specific cell counting assay was used to monitor the growth and survival of green algae in the effluent (Figure 16).

The findings demonstrated that green algae could grow in the dark fermentation effluent regardless of filter sterilization treatment (see Table 5 and Figure 15 for sample specifications). *Micractinium* had a steady growth rate in the effluent and demonstrated photosynthetic growth despite the addition of additional enriched microbial inoculum (Figure 16). However, compared to the initial, undiluted effluent, greater algal biomass accumulated in the diluted dark fermentation effluent.

Hydrogen production was monitored during the photoheterotrophic algae cultivation, the headspace was sampled and measured daily during the experiments. (Figure 17). Under the tested experimental conditions, significant variations in daily biohydrogen production rates were observed. The experimental conditions employing green algae in the filter-sterilized effluent generally resulted in moderate biohydrogen yields with a maximum of 52 ml H_2 L^{-1} d^{-1} when grown in the non-diluted effluent (S-EFF+A 100). During the 72-hour experimental period, no appreciable H_2 consumption was found and minimal H_2 production was observed in the dilute, filter-sterilized dark fermentation effluent (S-EFF+A 33).

The addition of enriched microbial inoculum together with the green algae (EFF+M+A 100 and EFF+M+A 33) led to a considerable increase in biohydrogen production. The highest maximum yield (154 ml H_2 L^{-1} d^{-1}) was observed when non-diluted dark fermentation effluent as a culture media (EFF+M+A 100). The dark fermentation effluent with enriched microbial inoculum but without the addition of *Micractinium* inoculum (EFF+M 100 and EFF+M 33) resulted in lower levels of biohydrogen with a maximum of 88 ml H_2 L^{-1} d^{-1} when non-diluted effluent was used as culture media (EFF+M 100). The effluents supplemented with *Micractinium* but lacking additional microbial inoculum (EFF+A 33 and 100) showed comparable biohydrogen generation to that observed in the sterilized effluents with added algae (maximum of 56 ml H_2 L^{-1} d^{-1} on the non-diluted effluent EFF+A 100). However, the observed strong H_2 consumption in these samples (EFF+A 33 and 100) as revealed by the comparison of the daily and the accumulated hydrogen amounts made an important difference (Figure 17).

Table 5: Experimental conditions and sample specifications in the photoheterotrophic degradation phase.

Sample names	Experimental conditions	Effluent concentration
RIW	Raw initial wastewater	-
EMI	Enriched microbial inoculum	-
EFF	Dark fermentation effluent	100%
EFF+A 33	Dark fermentation effluent without enriched microbial inoculum and with 10% *Micractinium* inoculum	33%
EFF+A 100		100%
S-EFF+A 33	Filter-sterilized dark fermentation effluent with 10% *Micractinium* inoculum	33%
S-EFF+A 100		100%
EFF+M+A 33	Dark fermentation effluent with added 5% microbial and 10% *Micractinium* inoculum	33%
EFF+M+A 100		100%
EFF+M 33	Dark fermentation effluent with added 5% microbial inoculum without green algae	33%
EFF+M 100		100%

Figure 16. Variation in algal cell numbers was measured by counting colony-forming units. All diluted samples have a higher number of colony-forming units compared to the non-diluted samples. This variation can be attributed to the lower light penetration in the non-diluted samples.
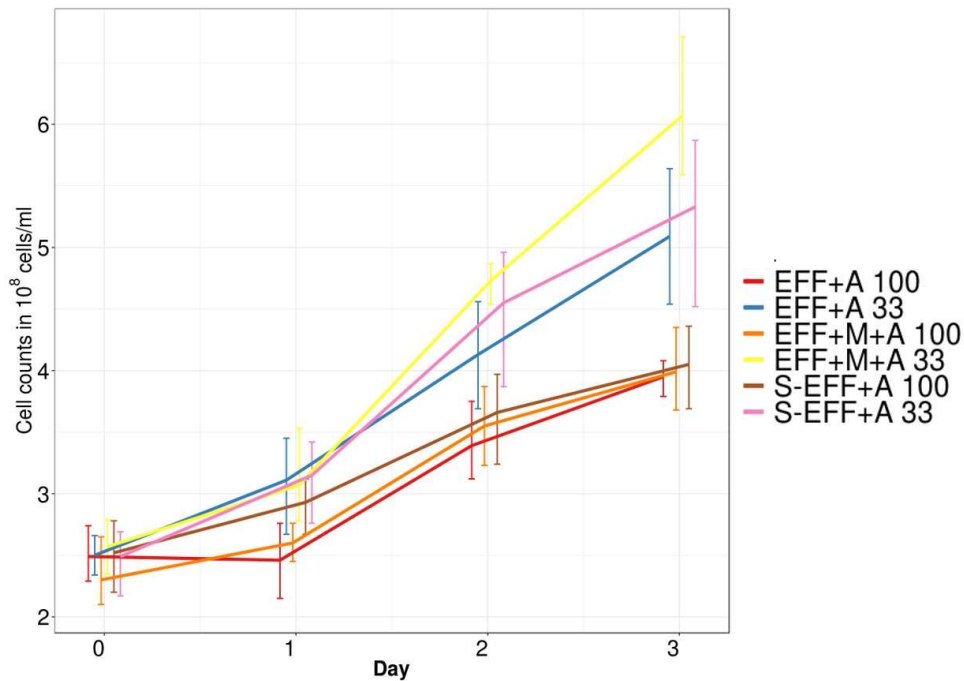
Figure 17: Daily (Panel A) and cumulative biohydrogen production (Panel B) in the photoheterotrophic stage. Photoheterotrophic biohydrogen production experiments were performed using different experimental conditions according to Table 1. Each of these different experimental conditions was investigated using diluted and non-diluted dark fermentation effluent.
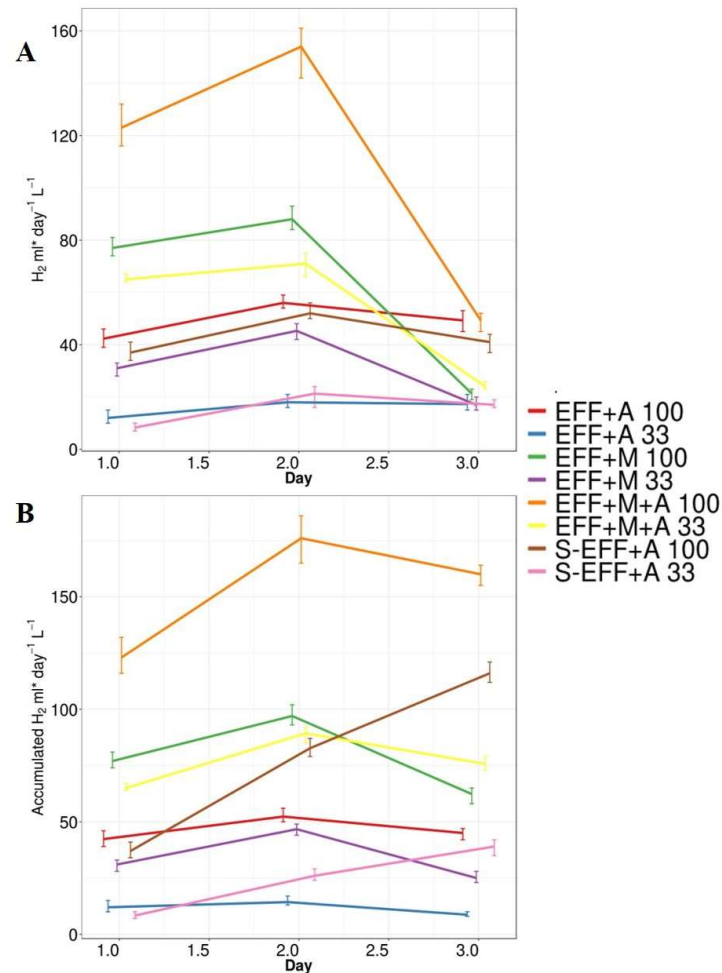
4.2.2 Substrate Utilization (Total N, P, and BOD)

BOD measurements, as well as total nitrogen (N) and total phosphorous (P) investigations, were carried out to examine the effluent treatment potential of the additional green algae in the photoheterotrophic system.

Green algae significantly contributed to total N, P, and BOD consumption under all conditions tested, regardless of the presence of enriched microbial inoculum (Figure 18). Under all experimental conditions, green algae displayed comparable N and P metabolizing efficiency as well as BOD reduction using either diluted or undiluted dark fermentation effluent as substrate (Figure 18). The absence of green algae resulted in significantly decreased biodegradation efficiency, demonstrating that algae play a fundamental role in N and P accumulation during the photoheterotrophic stage.

Interestingly, the addition of enriched microbial inoculum resulted in similar biodegradation across all conditions, indicating that the microbial community was unable to exert further biodegradation. Photosynthetic eukaryotic algae, on the other hand, proved to be exceedingly efficient, metabolizing ~75% of the remaining total N, P, and BOD under illumination. *Micractinium* green algae showed survival, photosynthetic growth, and metabolic activity (N and P utilization) both in the sterilized effluent and in the effluent harboring its natural microbial community (Figure 18).

Figure 18: Substrate degradation rates as a function of total N (Panel A), total P (Panel B), and BOD values (Panel C). Measurements were done at the start and the end (72 h) of the photoheterotrophic degradation experiments. The photoheterotrophic degradation measurements were performed on diluted and non-diluted dark fermentation effluents (33% and 100% concentrations, respectively).
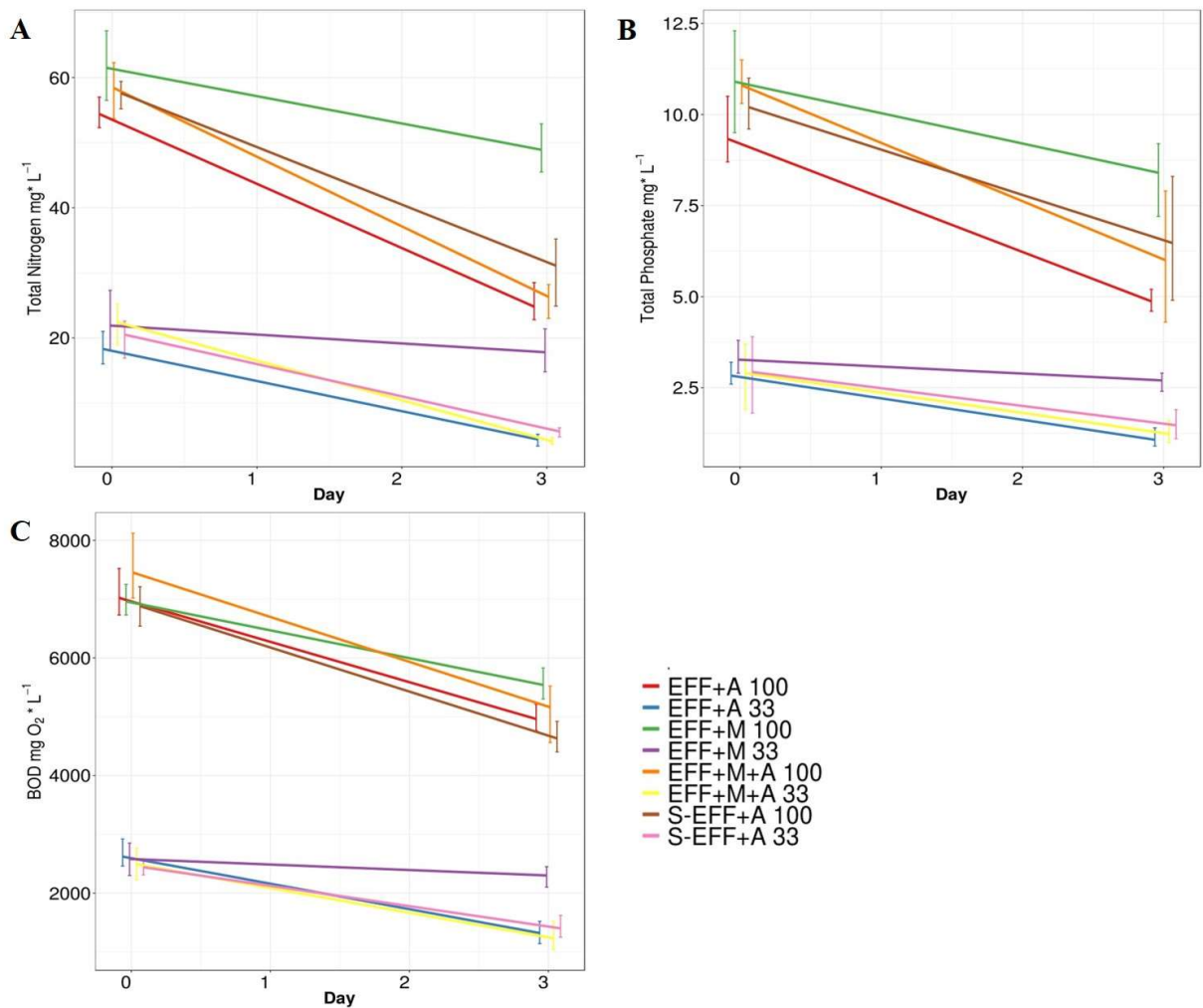
4.2.3 Taxonomic Profiling

MG-RAST was used for taxonomic and functional classification of reads. MG-RAST classified at least 50% of the reads on average for all samples except the enriched microbial inoculum sample

(35%) (Table 6) and the sterilized samples (~15%). Read count table for all samples was downloaded from MG-RAST and filtered to remove classifications with fewer than 5 reads assigned to them. This prevented false positive classifications. Since axenic *Micractinium* culture was used as algae inoculum, and the effluent, as well as the EMI, did not contain any algae (shown by their identified composition), the observed minor presence of other algae hits could be attributed to a lack of reference *Micractinium* genome in the database and similarity of genes shared by green algal species. As a result, all classifications assigned to *Actinastrum*, *Parachlorella*, *Chlamydomonas*, *Chlorella*, *Volvox*, *Prototheca*, and *Helicosporidium* were manually reassigned to *Chlorella*. Alpha diversity was measured by both MG-RAST and Fisher's alpha in R (Table 6, Supplementary figure 3). The enriched microbial inoculum (EMI) samples had the highest alpha diversity, whereas the filter-sterilized samples and RIW had the lowest. Further, a discrepancy was observed in alpha diversity metrics between MG-RAST values and Fisher's alpha. This is because low-count assignments were filtered out when calculating Fisher's alpha in R. Finally, non-diluted wastewater samples had higher diversity than diluted effluent samples. This is most likely due to the fact that when samples were diluted, species with low abundance were lost. Rarefaction curves reflected the alpha diversity values for all samples (Supplementary figure 4). Raw initial wastewater (RIW) and filter sterilized samples showed low species detection while EMI showed high species diversity. It's likely that a small subset of microorganisms with a high abundance in the RIW sample is one reason why there were not many species detected in the RIW sample.

The read count tables were also proportion normalized after filtering out low abundance genera. This allowed us to calculate the distance matrix required for additional analyses. The RIW sample had lower diversity compared to all other samples, and members of the *Lactobacillus* and *Saccharomyces* genus were present in high abundance (Figure 19A). However, the microbiome community profile changed after dark fermentation (EFF). The abundance of *Prevotella, Clostridium, Bacteroides, Anaerolinea, Candidatus Cloacimonas*, and *Megasphera* genus increased while concomitantly *Saccharomyces* and *Lactobacillus* decreased in abundance. The profiles of all photoheterotrophic fermentation samples were comparable with increases in *Prevotella, Veillonella*, *Dialister* genus and a significant decrease in the abundance of *Lactobacillus*. Higher relative abundance of *Acidaminococcus* sp. was detected in the non-diluted wastewater effluent. However, a higher abundance of *Escherichia* sp. was detected in the diluted wastewater effluent. Filter-sterilized samples were not completely sterile, *Prevotella*, and *Lactobacillus* genus were detected in low abundance in both samples along with a few other bacterial genera (Figure 19A).

Table 6: Sequencing data and alpha diversity metrics

Label	Condition	No. of reads sequenced	Avg. length of read	MG-RAST matches	Nonpareil coverage	Alpha diversity from MG-RAST	Fischer alpha in R
RIW	Raw initial wastewater	235940	232 ± 86	141686	71.62	13	31.02
EFF	Dark fermentation effluent	218249	229 ± 81	119154	61.81	36	55.67
EMI	Enriched microbial inoculum	256494	227 ± 83	90912	24.92	129	67.25
EFF+A 33	Dark fermentation effluent without enriched microbial inoculum and with 10% *Micractinium* inoculum	243123	228 ± 80	132832	64.73	58	48.35
EFF+A 100		228264	227 ± 83	121539	64.19	84	51.40
EFF+M+A 33	Dark fermentation effluent with added 5% microbial and 10% *Micractinium* inoculum	210178	232 ± 79	114258	67.41	60	47.08
EFF+M+A 100		234163	228 ± 79	124465	63.54	79	47.19
EFF+M 33	Dark fermentation effluent with added 5% microbial inoculum without green algae	228069	231 ± 80	128660	69.16	63	47.84
EFF+M 100		274021	226 ± 82	147690	70.39	73	48.14
S-EFF+A 33	Filter-sterilized dark fermentation effluent with 10% *Micractinium* inoculum	234332	219 ± 82	33679	64.92	44	17.50
S-EFF+A 100		190933	221 ± 83	33376	62.39	36	10.11

Figure 19A: Taxonomic profiles for all samples at the genus level. Enriched microbial inoculum (EMI) has a different taxonomic profile compared to both the raw initial wastewater (RIW) and dark fermented wastewater (EFF). However, during photo-fermentation, all the samples have a very similar profile and abundance. Higher *Micractinium* (taxonomically shown as *Chlorella*) abundance is seen in diluted samples compared to undiluted samples. This correlates well with cell count assays. The top 15 genera are shown below.

Figure 19B: Distribution of functional profiles. The functions were identified using SEED classification. The enriched microbial inoculum (EMI) showed a similar functional profile compared to that of the dark fermentation effluent (EFF) despite their highly different taxonomic profiles.
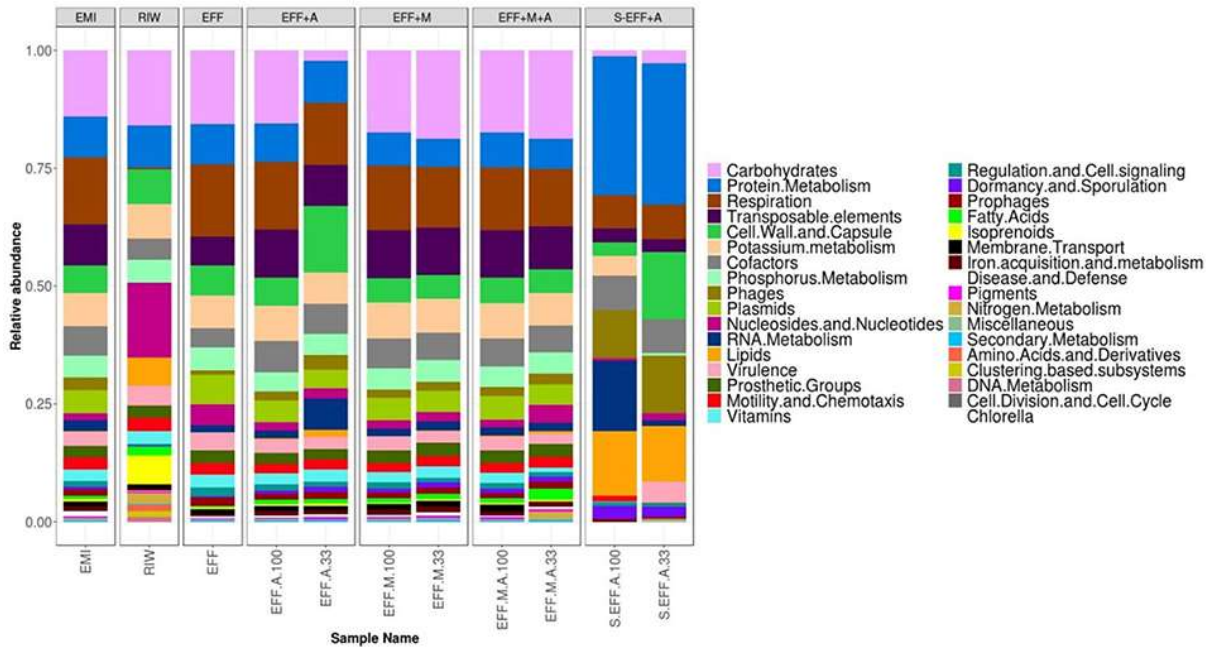
4.2.4 Sample Clustering

A bray-curtis distance matrix was calculated using proportion normalized read counts from taxonomic and functional abundance tables. This distance matrix was used for sample clustering (Figure 20A,B). When using taxonomic abundance tables, samples are primarily clustered by wastewater concentration and then by the presence of enriched microbial inoculum. This meant that some rare microorganisms were responsible for sample clustering, and the overall microbiome composition changed relatively little during the photoheterotrophic stage. The PCA plot constructed using the same distance matrix revealed that the samples with enriched microbial inoculum were considerably different from the other samples (Figure 21A). This is understandable as the microbial inoculum came from a different treatment. Further, there is a great degree of variation between all photoheterotrophic samples and the initial raw wastewater sample (Figure 21B). The effluent concentration drove the clustering of all samples during the photoheterotrophic treatment stage. Adonis-test on the distance matrix of only the photoheterotrophic samples with the presence or absence of either the microbial or the algal inoculum allowed us to determine which inoculum had a stronger role in shaping the microbial community structure. The addition of microbial inoculum considerably altered the community structure while the algal inoculum had only a slight impact (Table 7).

A different relationship was identified when we clustered samples using a bray-curtis distance matrix from functional abundance tables (Figure 20B). We still see samples clustering together by effluent

concentration. However, now both the EMI and EFF samples cluster along with the undiluted samples. This indicates that while taxonomic profiles changed post heat and photoheterotrophic treatment, the functional profiles remained similar.

Figure 20A: Clustering of samples using bray-curtis distance matrix from taxonomic abundance. Samples clustered primarily by dilution rate. Diluted samples clustered together, away from non-diluted samples. Further clustering is seen depending on the presence or absence of enriched microbial inoculum (EMI). Samples that received additional microbial inoculum had a similar taxonomic profile compared to samples that received only algae inoculum.
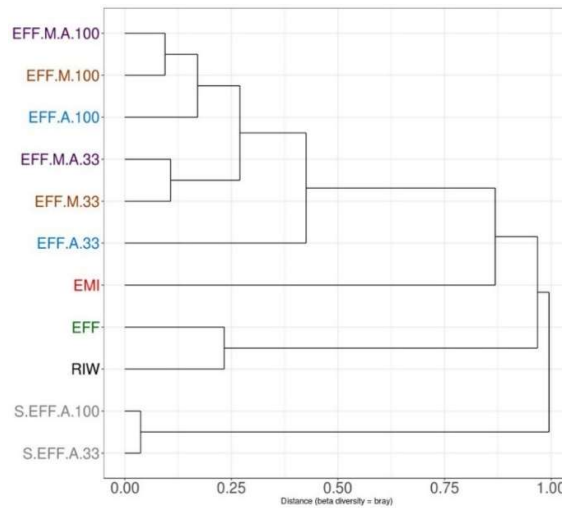
Figure 20B: Clustering of samples using bray-curtis distance matrix from functional abundance. A similar relationship is seen compared to the taxonomic profile where all diluted samples clustered together. The major difference here the EMI sample clustering with the EFF sample indicating the similarity of functional profile despite the dissimilar taxonomic profile.
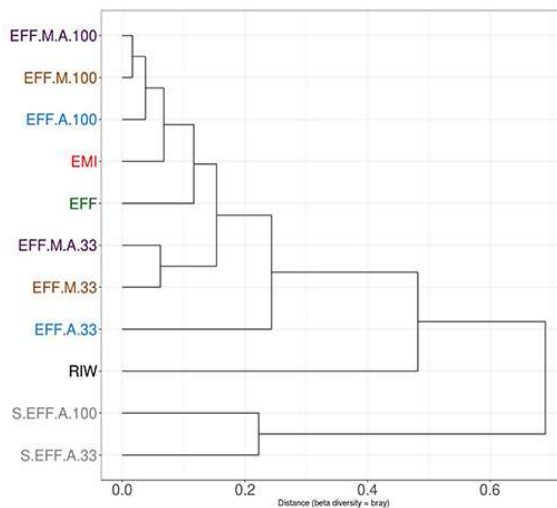
Figure 21A: PCA graphs when all samples are present. Sample clustering was driven by enriched microbial inoculum. Since this sample contained highly diverse microbiota, it clustered away from all other samples. All photoheterotrophic samples clustered together indicating that the photoheterotrophic treatment had similar effects on all samples regardless of the presence or absence of EMI or algal inoculum.
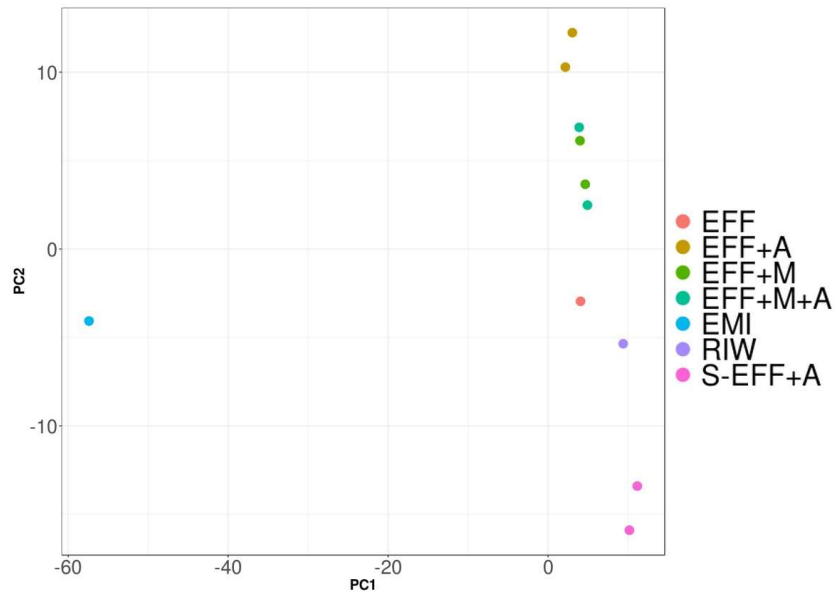
Figure 21B: PCA graphs when excluding enriched microbial inoculum sample. There was low variation in taxonomic profile before and after dark fermentation. All photoheterotrophic samples had similar microbial community profiles.
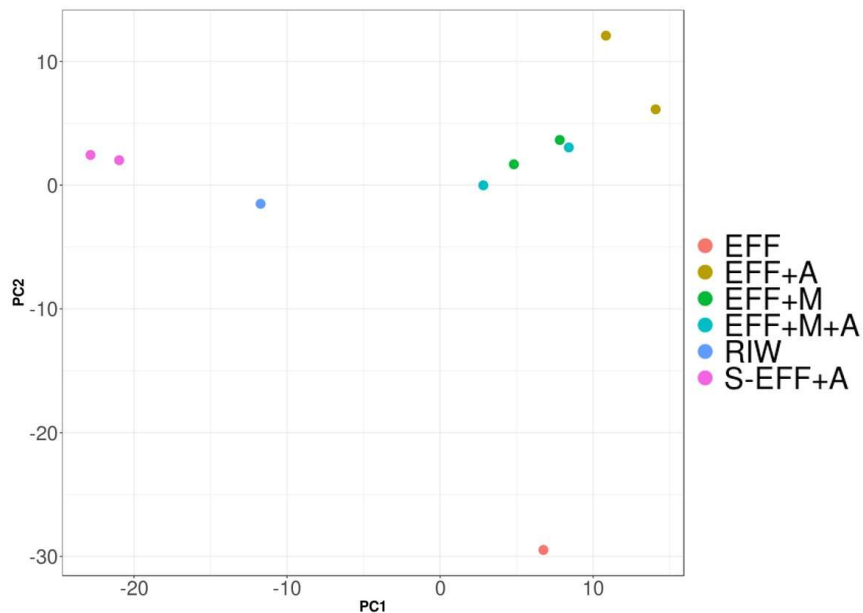
Table 7: Adonis model to test the effects of algal inoculum and microbial inoculum on overall microbial community structure. R^2 value indicates the percentage of variation explained by the term. The addition of the microbial inoculum explains 65% of the changes observed in the microbial community structure while addition of algal inoculum explains only less than 10% of that.

Model	R^2	p-value
Distance matrix of microbiome ~ Microbial_inoculum (EMI)	0.65452	0.06667
Distance matrix of microbiome ~Algal inoculum	0.09718	0.6667
Distance matrix of microbiome ~ Algal + Microbial_inocula	Algal inoculum 0.09734	0.35556
	Microbial inoculum (EMI) 0.61417	0.04444

4.2.5 Metagenome Assembly and Binning

Megahit was used to assemble the reads into a total of 50,165 contigs. These contigs were then binned together in MetaWrap using three different programs. Using the CheckM database, the resulting bins were tested for contamination and completion (Table 8). A total of four distinct bins were assembled, three of them showed a high level of completeness (>70%). These three bins belonged to *Lactobacillus, Prevotella*, and *Veillonella* genus and were uploaded to RAST to get a complete annotation. Gene and protein predictions for these bins were carried out using Prokka. The predicted proteins were then submitted to KEGG to determine the completion of specific co-factor pathways (Table 9). The thiamine biosynthesis pathway was fully encoded in the *Veillonella* genome, and the biotin and cobalamine biosynthesis pathways were almost fully encoded. The pathway for thiamine production was also almost entirely encoded in the *Prevotella* genome. In the *Lactobacillus* genome, no biosynthetic pathways for these specific cofactors could be detected.

Table 8: Basic metrics for the generated bacterial bins. Completion and contamination were identified by using CheckM tool. Bin2 was a poor, highly contaminated, extremely fragmented genome and was dropped from further analysis.

Bin	Completeness	contamination	GC percentage	lineage	N50	size	binner
bin.4	87.18	2.926	37.8	*Lactobacillus*	3652	1.753.136	binA
bin.1	84.82	1.946	40	*Veillonella*	5283	1.648.721	binABC
bin.5	75.8	4.493	37.1	*Prevotella*	2252	2.380.615	binBC
bin.2	16.66	1.379	37.9	Bacteria	1424	1.215.638	binABC

Table 9: Presence of cofactor and vitamin metabolism pathways for all bacterial genomes as identified using KEGG database and BlastKoala.

	Cofactor and vitamin metabolism in the *Veillonella* bin	
M00127	Thiamine biosynthesis, AIR	Complete
M00119	Pantothenate biosynthesis, valine/L-aspartate	1 block missing
M00120	Coenzyme A biosynthesis, pantothenate	2 blocks missing
M00123	Biotin biosynthesis, pimeloyl-ACP/CoA	1 block missing
M00573	Biotin biosynthesis, BioI pathway, long-chain-acyl-ACP	2 blocks missing
M00577	Biotin biosynthesis, BioW pathway, pimelate	1 block missing
M00126	Tetrahydrofolate biosynthesis, GTP	complete
M00841	Tetrahydrofolate biosynthesis, mediated by PTPS, GTP	2 blocks missing
M00842	Tetrahydrobiopterin biosynthesis, GTP	1 block missing
M00843	L-threo-Tetrahydrobiopterin biosynthesis, GTP	1 block missing
M00140	C1-unit interconversion, prokaryotes [PATH:map00670 map01100] (3	complete
M00141	C1-unit interconversion, eukaryotes [PATH:map00670 map01100] (1	1 block missing
M00121	Heme biosynthesis, glutamate	1 block missing
M00846	Siroheme biosynthesis, glutamate	1 block missing
M00122	Cobalamin biosynthesis, cobinamide	1 block missing
M00116	Menaquinone biosynthesis, chorismate	2 blocks missing
	Cofactor and vitamin metabolism in the *Prevotella* bin	
M00127	Thiamine biosynthesis	1 block missing
M00115	NAD biosynthesis, aspartate	2 blocks missing
M00119	Pantothenate biosynthesis, valine/L-aspartate	2 blocks
M00120	Coenzyme A biosynthesis, pantothenate	1 block missing
M00140	C1-unit interconversion, prokaryotes	2 blocks missing
M00116	Menaquinone biosynthesis, chorismate	2 blocks missing
	Cofactor and vitamin metabolism in the *Lactobacillus* bin	
M00125	Riboflavin biosynthesis, GTP	2 blocks missing
M00120	Coenzyme A biosynthesis, pantothenate	2 blocks missing
M00572	Pimeloyl-ACP biosynthesis, BioC-BioH pathway, malonyl-ACP	2 blocks
M00140	C1-unit interconversion, prokaryotes	complete
M00141	C1-unit interconversion, eukaryotes	1 block missing

5 DISCUSSION

5.1 Part A – High-throughput co-culture assays to investigate algal-bacterial interactions

5.1.1 Algal biohydrogen and biomass production under co-cultivation

The first objective of our work was to investigate whether bacteria from the same genus may coexist with green algae, while simultaneously enhancing algal biomass and biohydrogen production. We found no evidence of bacterial members improving algal biomass in a phylogenetic manner. Instead, we see bacterial presence is essential to improving algal growth of *C. reinhardtii* in synthetic wastewater media. Our results empirically demonstrate that bacterial members of the *Bacillus* genus significantly improve biohydrogen production and bacterial members of family *Methylobacteriaceae* show reduced or low biohydrogen production. Other experiments in the lab have confirmed that these bacterial members can not produce hydrogen when cultivated alone in synthetic wastewater media.

Our second general objective was to explore the nature of the enhancement of biohydrogen production. If bacterial members that improved biohydrogen production in *C. reinhardtii* also improved biohydrogen production when co-cultivated with other algal species, then it hints toward a general mechanism of enhancement. On the other hand, if bacterial species that improved biohydrogen in *C. reinhardtii* do not show a similar enhancement in other algal species, then it hints toward a species-specific mechanism. Our results indicated that *Bacillus* species isolated from different sources all showed a high biohydrogen production across 3 different species of green algae. The amount of biohydrogen produced was also comparable to accumulated biohydrogen in previous studies carried out in TAP media, with 10-fold lower algal cell concentration, in the case of *Micractinium* and 100-fold lower algal cell concentration in the case of *C. reinhardtii* (Table 10). Finally, it is important to mention that none of these pairwise co-culture studies have come close to the highest amount of biohydrogen produced in our lab. A previous study using wastewater native microbes in carbohydrate-rich brewery effluent was able to produce upwards of 150 ml L^{-1} culture of hydrogen (Shetty et al., 2019). Future experiments will focus on optimizing algal and bacterial cell concentrations to improve biohydrogen production.

Table 10: Comparison of accumulated hydrogen with previous experiments in our lab.

Total accumulated biohydrogen	Length of hydrogen accumulation	Experimental setup	Reference
88.98 ml L^{-1}	24 hours	Medium: TAP, Algae strain: *Micractinium* MACC 360, Bacterial partner: *E. coli* Δ*hypF* (JW5433), liquid volume: 20 ml, light intensity: 50 μmol m^{-2} s^{-1}, cellular concentration: $3.97 * 10^8$ algae cells ml^{-1}	Lakatos et al., 2017
18.7 ± 1 ml L^{-1}	24 hours	Medium: TAP, algae strain: *Chlamydomonas reinhardtii* cc124, bacterial partner: *E. coli* Δ *hypF* (JW5433), gas-to-liquid volume: 25/15 ml, light intensity: 50 μmol m^{-2} s^{-1}, algae cellular concentration: $1.03 * 10^8$ algae cells ml^{-1}	
6.8 ± 0.3 ml L^{-1}	24 hours	Medium: TAP, algae strain: *Chlamydomonas* sp. 549, bacterial partner: *E. coli* Δ *hypF* (JW5433), gas-to-liquid volume: 20/20 ml, light intensity: 50 μmol m^{-2} s^{-1}, algae cellular concentration: $0.38 * 10^8$ algae cells ml^{-1}	Lakatos et al., 2014
5.8 ml L^{-1}	24 hours	Medium: TAP, algae strain: *Chlamydomonas reinhardtii* cc124, bacterial partner: *E. coli* Δ *hypF* (JW5433), gas-to-liquid volume: 5/35 ml, light intensity: 50 μmol m^{-2} s^{-1}, algae cellular concentration: $1.03 * 10^8$ algae cells ml^{-1}	
14.2 ± 0.324 ml L^{-1}	72 hours	Medium: SWW, algae strain: *Chlamydomonas reinhardtii* cc124, bacterial partner: *Bacillus cereus* , gas-to-liquid volume: 20/20 ml, light intensity: 50 μmol m^{-2} s^{-1}, algae cellular concentration: $0.78*10^6$ algae cells ml^{-1}	This work
13.0 ± 0.724 ml L^{-1}	72 hours	Medium: SWW, algae strain: *Chlamydomonas reinhardtii* cc124, bacterial partner*: Bacillus megaterium* , gas-to-liquid volume: 20/20 ml, light intensity: 50 μmol m^{-2} s^{-1}, algae cellular concentration: $1.16*10^6$ algae cells ml^{-1}	
12.8 ± 1.44 ml L^{-1}	72 hours	Medium: SWW, algae strain: *Chlamydomonas reinhardtii* cc124, bacterial partner: *Bacillus thuringiensis*, gas-to-liquid volume: 20/20 ml, light intensity: 50 μmol m^{-2} s^{-1}, algae cellular concentration: $2.06*10^6$ algae cells ml^{-1}	
42.5 ± 1.2ml L^{-1}	72 hours	Medium: SWW, algae strain: *Micractinium* MACC-360, bacterial partner: *Bacillus cereus*, gas-to-liquid volume: 20/20 ml, light intensity: 50 μmol m^{-2} s^{-1}, algae cellular concentration: $22*10^6$ algae cells ml^{-1}	
35.8 ± 1.6 ml L^{-1}	72 hours	Medium: SWW, algae strain: *Micractinium* MACC-360, bacterial partner: *Bacillus megaterium*, gas-to-liquid volume: 20/20 ml, light intensity: 50 μmol m^{-2} s^{-1}, algae cellular concentration: $17*10^6$ algae cells ml^{-1}	
36.9 ± 1.54ml L^{-1}	72 hours	Medium: SWW, algae strain: *Micractinium* MACC-360, bacterial partner: *Bacillus thuringiensis*, gas-to-liquid volume: 20/20 ml, light intensity: 50 μmol m^{-2} s^{-1}, algae cellular concentration: $19*10^6$ algae cells ml^{-1}	
46.6 ± 0.4 ml L^{-1}	72 hours	Medium: SWW, algae strain: *Parachlorella* MACC-38, bacterial partner: *Bacillus cereus*, gas-to-liquid volume: 20/20 ml, light intensity: 50 μmol m^{-2} s^{-1}, algae cellular concentration: $8.52*10^6$ algae cells ml^{-1}	
35.4 ± 4ml L^{-1}	72 hours	Medium: SWW, algae strain: *Parachlorella* MACC-38, bacterial partner: *Bacillus megaterium*, gas-to-liquid volume: 20/20 ml, light intensity: 50 μmol m^{-2} s^{-1}, algae cellular concentration: $9.27*10^6$ algae cells ml^{-1}	
50.9 ± 2.4ml L^{-1}	72 hours	Medium: SWW, algae strain: *Parachlorella* MACC-38, bacterial partner: *Bacillus thuringiensis*, gas-to-liquid volume: 20/20 ml, light intensity: 50 μmol m^{-2} s^{-1}, algae cellular concentration: $8.19*10^6$ algae cells ml^{-1}	

5.1.2 Physiological changes imposed by bacterial co-cultivation

Our third major objective was a comprehensive study of the changes in algal biomolecule concentration under bacterial co-cultivation. Bacterial association consistently led to an improvement in all algal cellular properties, including cell counts, Chlorophyll a/b ratio, total carbohydrates, and total lipids. Interestingly, we saw higher total carbohydrate accumulation in green algae co-cultivated with *Methylobacterium* sp. compared to *Bacillus* species. This could indicate a stronger fermentative metabolism under *Bacillus* co-cultivation compared to *Methylobacterium* co-cultivation. We examined the gene abundance of important genes, including those involved in fermentation pathways, to see if this was indeed the case.

Confocal microscopy with algal cells stained with BODIPY dye confirmed estimated total lipid measurements. Large lipid bodies were identified only under *Bacillus* co-cultivation, with smaller lipid bodies identified under *Methylobacterium* sp. co-cultivation. No lipid bodies were detected in axenic samples. These results have tremendous implications for algal studies looking to improve lipid production. Apart from using lipid accumulating strains, studies can focus on using bacterial co-cultivations to improve lipid production while concomitantly protecting algal cultures from unwanted bacterial contaminations in an industrial setting. Plant rhizosphere studies have empirically demonstrated that healthy microbiomes have the capacity to prevent and protect the plant against invading microbial pathogens (Li et al., 2021). Disease suppressive soils, rich in certain bacteria are essential in preventing the emergence of the disease as has been demonstrated in the case of tomato plants susceptible to *Ralstonia solanacearum*, bacterial wilting disease (Kwak et al., 2018). We have very few studies adopting a similar approach to protect algal cultivations from invading contaminations. Further, we also do not know if applied algal microbiomes themselves could be a problem as the bacterial community increases in abundance. These are among the many questions that need to be explored to leverage the exceptional potential that algal-bacterial co-cultivations offer.

5.1.3 Transcriptome analysis

Finally, we were interested in a deeper understanding of the transcriptomic responses that occur under axenic and bacterial co-cultivation. Bacterial co-cultivation leads to a complete reorganization of algal gene expression patterns and the best way to explore the plethora of changes is through a though examination of all the important pathways.

5.1.3a Photosynthetic genes

Most of the genes related to photosynthesis were reduced in abundance following sulfur deprivation. Sulfur deprivation leads to irreversible inactivation of PSII, starting with a gradual decline in PSII

activity and leading to a complete inactivation once the environment is anaerobic [Antal et al., 2001]. While this is the most efficient way to produce biohydrogen, it also leads to eventual algal cell death. In our experiments, both the *Bacillus*-associated condition also led to reduced abundance of transcripts related to PSI subunits, with a few exceptions (Table 11). A few genes related to PSI components had slightly higher read abundance under *Bacillus* cultivation compared to axenic. Apart from these few genes, most of the other genes were slightly upregulated under axenic cultivation. Conflictingly, most of the transcripts related to photosynthesis were upregulated under *Methylobacterium* co-cultivation compared to axenic.

Rubisco activase (RCA) and rubisco methyltransferase are highly upregulated (log_2 fold change>1) in axenic condition compared to all three bacterial-associated conditions. These genes are associated with carbon capture mechanisms and play a vital role in improving cell growth under low CO_2 conditions. These genes are also downregulated shortly after sulfur deprivation. It is currently unclear how bacterial association leads to a downregulation of photosynthetic transcripts, similar to what is observed under sulfur deprivation. We also observed a steep upregulation under bacterial co-cultivation of most of the light-harvesting complex proteins; specifically, LHCBM1, LHCBM7, and LHCBM9. This directly contradicts results from the sulfur deprivation study, where most of these genes were reduced in abundance except for LHCBM9 (*Cre06.g284200*). LHCBM9 increased in abundance post-sulfur deprivation [Nguyen et al., 2008]. Nguyen et al., suggested that LHCBM9 induction was correlated with both sulfur deprivation and a microaerobic environment. Considering that all our algal-bacterial co-cultures had a low abundance of oxygen in the headspace, just the microaerobic environment could be a factor in the induction of LHCBM9.

Two other genes; *Cre08.g367500* and *Cre08.g367400* were greatly downregulated under bacterial association with only a few read pairs mapping back to these genes. These almost identical genes differ only in their promoter region and encode LHCSR3 protein [Perozeni et al., 2020]. LHCSR3 is a protein involved in non-photochemical quenching and prevents oxygen-dependent photoinhibition of PSII [Roach et al., 2020]. The low abundance of this protein under bacterial cultivation is another indication that axenic cultivation can lead to photoinhibition and lower efficiency and has important implications for using specific bacterial co-cultivation for commercial production of green algae.

Table 11: List of photosynthetic genes along with their log$_2$ fold-change and p-values. Positive values represent higher gene abundance under axenic condition (upregulation) and negative values represent lower gene abundance under axenic condition (downregulation).

Gene name	*Methylobacterium* sp. samples		*Bacillus thuringiensis* samples		*Bacillus cereus* samples		Gene description
	Log$_2$ fold change	Adjusted p-value	Log$_2$ fold change	Adjusted p-value	Log$_2$ fold change	Adjusted p-value	
Cre12.g548950	-7.97263	0	-7.2278	0	-6.83374	0	Lhcbm7
Cre01.g066917	-3.87602	0	-3.27443	0	-3.74932	0	Lhcbm1
Cre06.g284200	-3.34291	0.004673	-1.15211	0.388568	-2.03362	0.098081	Lhcbm9
Cre16.g687900	-2.15976	1.64E-240	-0.39961	2.21E-09	-0.38607	7.82E-09	PS I light-harvesting complex
Cre08.g365900	-2.04385	6.90E-08	-3.78258	1.88E-27	-2.16965	2.67E-09	Chlorophyll A/B binding protein 1
Cre08.g372450	-1.77456	1.06E-84	-0.24402	0.010383	-0.46452	6.00E-07	PS II subunit Q
Cre17.g724300	-1.73156	1.05E-88	-0.11443	0.227677	0.144407	0.122985	PS I subunit K
Cre10.g420350	-1.7078	9.32E-80	-0.49583	7.40E-08	-0.48038	1.94E-07	PSAE-2
Cre03.g156900	-1.63886	4.36E-113	-1.45433	3.52E-90	-1.55095	1.08E-102	Lhcbm5
Cre09.g412100	-1.60787	1.02E-124	-0.30628	1.06E-05	-0.47245	6.46E-12	PS I subunit F
Cre06.g283050	-1.572	7.09E-82	0.578311	3.86E-12	1.107045	5.70E-41	PS I light-harvesting complex
Cre05.g238332	-1.5492	1.24E-108	-0.63905	1.58E-19	-0.73446	2.05E-25	PSAD-2
Cre07.g330250	-1.47664	1.61E-79	-0.11278	0.185303	0.170848	0.040177	PS I subunit H-1
Cre12.g486300	-1.26551	2.17E-77	-0.53991	3.93E-15	-0.48645	1.62E-12	PS I subunit l
Cre11.g467573	-1.23092	9.77E-77	0.294957	1.54E-05	0.689631	9.89E-25	PS I light-harvesting complex
Cre11.g467573	-1.23092	9.77E-77	0.294957	1.54E-05	0.689631	9.89E-25	PS I light-harvesting complex
Cre12.g508750	-1.19215	9.53E-73	-0.35536	1.34E-07	-0.28284	3.13E-05	PS I light-harvesting complex
Cre10.g425900	-1.1675	2.07E-42	0.494191	1.34E-08	0.912396	3.39E-26	PS I light-harvesting complex
Cre03.g148750	-1.14538	6.33E-07	-1.24832	1.51E-08	-1.49758	5.31E-12	Chlorophyllase 1
Cre07.g334550	-1.09875	3.61E-50	0.06715	0.417141	0.47888	1.75E-10	PS I subunit P
Cre06.g278213	-0.94565	1.12E-29	0.231699	0.007699	0.489899	8.31E-09	PS I light-harvesting complex
Cre09.g396213	-0.92224	1.57E-35	0.529722	1.46E-12	0.327388	1.55E-05	PS II oxygen-evolving complex 1
Cre12.g560950	-0.88883	7.59E-28	0.559018	9.73E-12	0.747736	5.66E-20	PS I subunit G
Cre05.g243800	-0.86979	1.23E-32	0.011311	0.906099	0.410724	3.80E-08	PS II family protein
Cre07.g344950	-0.85209	3.88E-34	0.586002	9.23E-17	0.733803	1.56E-25	PS I light-harvesting complex

Cre02.g120150	-0.74808	1.34E-19	0.008512	0.93763	0.315313	0.000183	RUBISCO small chain 2
Cre12.g548400	-0.74663	5.88E-24	-0.29596	8.57E-05	-0.74493	5.44E-24	Lhcbm2
Cre02.g082750	-0.70853	9.15E-18	1.297362	2.59E-56	1.254453	8.58E-53	PS II subunit X
Cre02.g082500	-0.66107	2.29E-15	0.852887	9.45E-25	1.180836	3.34E-46	PS I reaction center PSI-N
Cre16.g650100	-0.61391	2.34E-16	1.201057	6.98E-59	1.640812	2.12E-108	Cytochrome b6f complex PetN
Cre06.g261000	-0.52203	4.48E-11	1.75545	2.68E-112	1.816149	3.50E-120	PS II subunit R
Cre03.g182551	-0.39307	2.94E-05	0.838887	7.90E-20	1.200618	3.05E-39	Electron transporter; plastocyanin 1
Cre11.g467689	0.064003	0.487582	1.642308	7.39E-95	1.878471	1.24E-123	Cytochrome b6f complex PetC
Cre16.g661350	0.132496	0.174581	1.365234	4.70E-48	1.428691	1.96E-52	RUBISCO large subunit methyltransferase
Cre06.g278245	0.347195	0.361712	-0.75901	0.011483	-1.59324	1.47E-08	Pheophorbide a oxygenase
Cre06.g283950	0.376035	3.17E-05	0.28913	0.001273	-0.23049	0.010564	Lhcbm4
Cre10.g423500	0.37962	1.25E-07	1.190444	3.02E-63	1.138421	1.78E-58	Haeme oxygenase 3
Cre02.g120100	0.468555	2.32E-09	1.660721	3.11E-103	2.043852	2.62E-155	RUBISCO small chain 1A
Cre04.g229300	1.012548	4.10E-70	1.320899	6.27E-119	1.504326	7.42E-154	RUBISCO activase
Cre03.g186450	1.616079	1.24E-10	0.931278	1.75E-05	0.750452	0.000463	RUBISCO methyltransferase
Cre08.g368700	1.642057	4.41E-40	2.04903	1.25E-63	2.317846	2.49E-78	RUBISCO methyltransferase
Cre08.g367500	5.254653	3.50E-15	5.080741	8.3E-21	5.665242	1.14E-19	LHCSR3.1
Cre08.g367400	6.506758	2.99E-13	9.534798	8.32E-15	5.724984	5.36E-23	LHCSR3.1

5.1.3b Carbohydrate metabolism genes

Most starch metabolism genes are strongly upregulated in studies where *C. reinhardtii* is subjected to sulfur deprivation [Toepel et al., 2013, Nguyen et al., 2008]. All enzymes active in the glycolytic pathway were identified with maximum expression coinciding with peak hydrogen production. Apart from these, starch synthase genes (*Cre03.g185250, Cre17.g721500*), phosphorylase (*Cre07.g336950, Cre12.g552200*) and starch degradation gene (alpha-amylase - *Cre08.g362450*), all showed improved expression.

In our study, some of these enzymes followed similar patterns observed when *C. reinhardtii* were subjected to sulfur deprivation and were downregulated in axenic compared to bacterial co-cultivation with a few exceptions, like the starch synthase genes and a few genes from the glycolytic pathway (Table 12) (phosphoglycerate kinase, glucose-6-phosphate isomerase, pyruvate dehydrogenase kinase, phosphoenolpyruvate carboxykinase 1).

Interestingly, the gene encoding isocitrate lyase is extremely upregulated in axenic compared to bacterial co-cultivation. isocitrate lyase is the key enzyme involved in the TCA cycle shunt by bypassing the oxidative steps in the TCA cycle. Plancke et al., showed that lack of Isocitrate lyase lead to a dramatic increase in both; total cellular fatty acid level and relative amount of neutral lipids in TAP media [Plancke et al., 2013]. Finally, 6-phosphogluconate dehydrogenase, an enzyme involved in the pentose phosphate pathways was significantly upregulated in both *Bacillus* co-cultivation and slightly upregulated in *Methylobacterium* sp. co-cultivation. All these have important implications for hydrogen production as starch degradation directly contributes to improved biohydrogen production through the indirect biophotolysis and dark fermentation pathway.

Table 12: List of carbohydrate metabolism genes along with their log$_2$ fold-change and p-values. Positive values represent higher gene abundance under axenic condition (upregulation) and negative values represent lower gene abundance under axenic condition (downregulation).

Gene name	*Methylobacterium* sp. samples		*Bacillus thuringiensis* samples		*Bacillus cereus* samples		Gene description
	Log$_2$ fold change	Adjusted p-value	Log$_2$ fold change	Adjusted p-value	Log$_2$ fold change	Adjusted p-value	
Cre12.g553250	-3.53963	4.10E-105	-4.54985	2.87E-181	-4.62779	5.21E-188	Phosphofructokinase 5
Cre08.g362450	-2.6705	8.04E-173	-2.83669	1.52E-201	-3.03907	3.91E-233	Alpha-amylase 2
Cre12.g552200	-2.25033	4.91E-163	-2.75675	1.04E-251	-2.90058	1.50E-279	Starch phosphorylase
Cre07.g336950	-1.28482	2.26E-32	-2.7137	1.23E-159	-3.54569	1.54E-277	Starch phosphorylase
Cre01.g029300	-1.06098	2.23E-31	-0.28835	0.002269	-0.04845	0.657581	Triosephosphate isomerase 1
Cre12.g526800	-0.72397	5.09E-11	-1.96427	6.33E-86	-2.3708	5.56E-127	6-phosphogluconate dehydrogen-ase
Cre12.g485150	-0.36047	4.24E-06	-1.69331	2.29E-118	-2.70952	0	Glyceraldehyde-3-phosphate dehy-drogenase
Cre12.g533550	-0.35769	1.39E-07	-0.05874	0.42946	0.164797	0.017811	Pyruvate kinase 1
Cre03.g185250	0.028855	0.758887	1.764911	7.78E-119	2.112004	4.52E-168	Starch synthase 2
Cre05.g241750	0.31946	0.000945	1.179874	1.93E-35	1.026589	7.11E-28	Pyruvate dehydrogenase kinase
Cre10.g444700	0.343968	1.30E-08	-0.57509	1.89E-23	-0.82273	5.29E-47	Starch branching enzyme 2.2
Cre11.g467770	0.352885	5.60E-07	0.602385	3.44E-18	0.280095	7.13E-05	Phosphoglycerate kinase
Cre03.g144847	0.530075	7.26E-08	-0.19682	0.042339	-0.42749	4.70E-06	Pyruvate kinase 3
Cre11.g476650	0.610072	0.001104	-0.18917	0.282753	-0.50269	0.002073	Starch debranching enzyme
Cre03.g175400	1.167076	1.94E-68	0.830848	1.35E-36	0.684767	2.15E-25	Glucose-6-phosphate isomerase
Cre06.g282800	2.138119	3.88E-153	1.904654	1.44E-122	1.980041	2.05E-132	Isocitrate lyase
Cre02.g141400	2.368365	6.57E-196	1.556764	1.80E-86	1.304415	3.40E-61	Phosphoenolpyruvate carboxyki-nase 1
Cre17.g721500	3.69357	0	2.574922	2.17E-242	2.550798	1.20E-238	Granula bound starch synthase

5.1.3c Fermentation-related genes

There was strong evidence that dark fermentative pathways increased under bacterial cultivation. Enzymes such as pyruvate formate lyase (PFL) and pyruvate ferredoxin reductase (PFR), both of which are directly involved in breaking down pyruvate with concomitant release of biohydrogen had greatly increased expression under bacterial co-cultivation (Table 13). Other genes encoding enzymes like alcohol dehydrogenase, and acetate kinase were both highly upregulated under *Bacillus* co-cultivation and moderately upregulated under *Methylobacterium* sp. cultivation. Both these enzymes are among the main source of reducing equivalents for cells under anaerobic stress [Toepel et al., 2013, Whitney et al., 2010]. Finally, the gene encoding malate synthase was downregulated under bacterial association. Malate synthase is involved in the glyoxalate cycle and together with Isocitrate lyase, is required to bypass the oxidative steps of the TCA cycle. TCA cycle generated NADH/FADH2 are major electron sources required for hydrogen production [Yang et al., 2014], reduced expression of these genes could be another reason how bacterial co-cultivation leads to improved algal hydrogen production. Currently, it is unknown how bacterial association can bring about the same metabolic changes.

Another important enzyme, NDA2 (*Cre19.g750547*) was significantly upregulated only under co-cultivation with both *Bacillus* species. NDA2 is a type II NADH dehydrogenase involved in transferring electrons generated during the breakdown of complex carbohydrates such as starch. Increased hydrogen production was also observed when *C. reinhardtii* overexpressed NDA2 [Baltz et al., 2014].

Mutant *C. reinhardtii* lacking isocitrate lyase also showed a sharp decrease in malate synthase, leading to lipid accumulation [Plancke et al., 2013]. Another factor contributing to the lower expression of malate synthase may be the ability of bacterial co-cultivation to directly lower the expression of isocitrate lyase.

These results taken together with the carbohydrate measurement results seem to indicate carbohydrate breakdown is upregulated under *Bacillus* co-cultivation, leading to increased hydrogen production. Comparatively lower expression reveals this pathway is less active under co-cultivation with *Methylobacterium* sp. *C. reinhardtii* co-cultivated with both *Bacillus* species had lower accumulated carbohydrates compared to co-cultivation with *Methylobacterium* sp., providing more evidence to this theory.

Table 13: List of fermentation genes along with their log$_2$ fold-change and p-values. Positive values represent higher gene abundance under axenic condition (upregulation) and negative values represent lower gene abundance under axenic condition (downregulation).

Gene name	*Methylobacterium* sp. samples		*Bacillus thuringiensis* samples		*Bacillus cereus* samples		Gene description
	Log$_2$ fold change	Adjusted p-value	Log$_2$ fold change	Adjusted p-value	Log$_2$ fold change	Adjusted p-value	
Cre01.g044800	-0.70681	4.86E-32	-0.62592	1.63E-25	-0.49259	2.78E-16	Pyruvate formate lyase
Cre02.g095137	-5.84391	2.20E-76	-7.29286	1.01E-118	-7.9654	1.68E-141	Pyruvate ferredoxin reductase
Cre03.g144807	2.77603	0	2.477686	0	2.363236	3.62E-292	Malate synthase
Cre09.g396700	-1.2007	1.43E-05	-1.88766	1.09E-13	-2.0893	9.69E-17	Acetate kinase
Cre17.g746997	-1.22202	3.17E-45	-1.58482	9.12E-77	-2.43924	7.97E-182	Alcohol dehydrogenase
Cre19.g750547	-0.05042	0.606351	-0.36043	1.18E-05	-0.29963	0.000302	NADH dehydrogenase (NDA2)

5.1.3d Hydrogen-related genes

A very interesting observation was identified with most of the hydrogenase genes being slightly upregulated under axenic conditions (Log$_2$ fold change< 1) (Table 14). This is interesting, considering that no hydrogen production is observed under axenic condition. These results seem to indicate that the microaerobic environment created by bacterial co-cultivation is essential in maintaining the activity of hydrogenase enzyme. We also observed that *hydA2* was slightly upregulated in samples co-cultivated with *Methylobacterium* sp. *Hyda2* is an isoform of the hydrogenase gene and displays a lower affinity to ferredoxin and a catalytic preference for hydrogen consumption [Engelbrecht et al., 2021]. Higher expression of *hyda2* in *Methylobacterium* sp. co-cultivated samples can potentially lead to lower hydrogen yields.

Table 14: List of hydrogenase-related genes along with their log$_2$ fold-change and p-values. Positive values represent higher gene abundance under axenic condition (upregulation) and negative values represent lower gene abundance under axenic condition (downregulation).

Gene name	*Methylobacterium* sp. samples		*Bacillus thuringiensis* samples		*Bacillus cereus* samples		Gene description
	Log$_2$ fold change	Adjusted p-value	Log$_2$ fold change	Adjusted p-value	Log$_2$ fold change	Adjusted p-value	
Cre03.g199800	0.571648	2.00E-20	0.92601	6.37E-52	0.734057	3.42E-33	hyda1
Cre06.g296700	0.942394	4.81E-51	0.995129	1.93E-57	0.790008	8.62E-37	hydg
Cre06.g296750	0.585171	1.37E-09	0.73975	9.11E-15	0.560542	5.05E-09	hydef
Cre09.g396600	-0.63328	2.83E-12	0.298107	0.001374	0.144413	0.134797	hyda2

5.1.3e Genes related to bacterial interaction

To explore the presence of genes differentially regulated to bacterial presence we studied the expression pattern of mitogen-activated protein kinases (MAPK) and heat shock proteins identified in a previous study [Helliwell et al., 2017].

MAPK cascades play integral roles in transduction of external stimuli by phosphorylation of downstream signaling targets such as other kinases, cytoskeleton proteins, and transcription factors in eukaryotes. For the most part, the exact roles of MAPKs in *Chlamydomonas* are presently unknown. However, contemporary studies have revealed the extensive role they play in nitrogen metabolism [Gomez-Osuna et al., 2020], lipid biosynthesis [Yang et al., 2018] under salt stress, and regulating flagellar length [Wang et al., 2019]. In plants, MAPK cascades play crucial roles in modulating immune responses and can influence production of various phytohormones including Salicylic acid, Jasmonic acid, Auxin, and Gibberellins. Our results indicate that MAP2k, MAPK4, and MKP2 are differentially regulated among *Bacillus* co-cultivation compared to both axenic and *Methylobacterium* sp. cultivation. These could be important genes that are differentially upregulated

under *Bacillus* interaction. However, what their precise roles are is yet to be determined. Apart from genes encoding MAPK proteins, we also saw differential regulation of several heat shock proteins. Helliwell et al., also these identified proteins to be differentially upregulated when *Lobomonas rostrata* was cultivated with *Mesorhizobium loti*. However, in our study, all but one heat shock protein was drastically upregulated only in axenic condition (Table 15). Finally, we also see a reorganization in some membrane protein (*Cre17.g700750*) and flagellar associated proteins (*Cre03.g164250, Cre06.g269950, Cre12.g528000*). The membrane protein is extremely interesting as the expression is extremely downregulated in under *Bacillus* co-cultivation and moderately downregulated under *Methylobacterium* sp. co-cultivation.

While we have very little understanding of the exact function of these genes under bacterial association, it is extremely interesting to note that these genes are similarly expressed for bacterial members of the same genus, indicating that *C. reinhardtii* could either identify and respond to the bacteria themselves or the environment imposed by bacterial co-cultivation.

Table 15: List of genes related to bacterial interaction along with their Log$_2$ fold-change and p-values. Positive values represent higher gene abundance under axenic condition (upregulation) and negative values represent lower gene abundance under axenic condition (downregulation).

Gene name	*Methylobacterium* sp. samples		*Bacillus thuringiensis* samples		*Bacillus cereus* samples		Gene description
	Log$_2$ fold change	Adjusted p-value	Log$_2$ fold change	Adjusted p-value	Log$_2$ fold change	Adjusted p-value	
Cre01.g055457	-2.65881	0.063376	-8.37402	4.69E-12	-9.67002	1.11E-15	MAP2k
Cre17.g745447	-0.5749	0.021621	-3.01405	4.94E-52	-3.564	1.08E-73	MAPK4
Cre06.g267250	-0.64032	0.000111	-2.35757	7.40E-55	-2.5681	3.34E-65	MKP2
Cre13.g582650	-1.06094	2.21E-09	-1.6442	2.43E-23	-0.81932	2.47E-06	MAPK1
Cre06.g269950	-0.32538	6.48E-05	-1.47616	7.74E-84	-1.55902	1.15E-93	Flagellar associated protein
Cre09.g393200	-0.70526	9.41E-13	-1.44834	1.19E-52	-1.06976	4.77E-29	Heat shock protein 70C
Cre03.g164250	-0.97388	4.09E-19	-1.39414	2.83E-40	-0.50303	4.53E-06	Flagellar associated protein
Cre02.g080650	-1.03183	3.86E-33	-1.14496	4.44E-41	-1.19099	2.10E-44	Heat shock protein 90B
Cre12.g517000	-0.24209	0.129458	-0.86005	6.21E-10	-1.08324	2.71E-15	MAPKKK7
Cre09.g395150	-0.62858	4.12E-06	-0.8568	3.66E-11	-1.74675	1.05E-44	MKP3
Cre08.g385050	0.576851	4.14E-09	-0.44896	1.14E-06	-0.49191	8.74E-08	MAPK2
Cre13.g607300	-0.32885	0.086581	-0.43636	0.01341	-0.56506	0.001072	MAPK5
Cre15.g635700	0.584218	1.47E-09	-0.40349	1.14E-05	-0.96712	2.74E-27	MAPKKK12
Cre03.g194100	0.230276	0.016647	-0.25958	0.004229	-0.35509	7.26E-05	MAPKKK3
Cre12.g508900	-1.71912	1.01E-09	-0.20263	0.520568	-0.31104	0.310462	MAPK6
Cre06.g284650	-0.286	0.005295	-0.11181	0.285024	-0.18945	0.058857	MKP6
Cre16.g661100	-0.31621	0.002395	-0.10917	0.312773	0.490803	1.89E-06	MAPK7
Cre06.g249150	-0.2536	0.03555	-0.06072	0.638033	0.004398	0.981696	MAPKK1
Cre07.g316600	0.59482	0.01261	0.19871	0.387402	0.22761	0.318551	MKP5
Cre07.g317300	-0.21562	0.092236	0.228256	0.067343	0.110219	0.398767	MAPKKKK1
Cre12.g509000	0.400675	0.014449	0.421472	0.007055	0.511506	0.00102	MAPK3
Cre01.g010000	0.444883	4.83E-05	0.494128	1.81E-06	0.294477	0.004486	MAPK8
Cre03.g154250	0.665444	2.40E-11	0.531938	4.95E-08	0.538381	3.32E-08	MAPKKK6

Cre12.g528000	-0.66261	1.67E-32	0.647538	6.16E-31	0.753943	1.85E-41	FAP303
Cre06.g250100	0.327858	4.25E-08	0.892998	1.87E-52	0.994125	1.23E-64	Heat shock protein 70B
Cre02.g090850	0.627033	3.09E-09	1.074967	3.41E-25	0.834292	4.84E-16	ClpB chaperone
Cre09.g395100	0.209236	0.028463	1.214556	8.60E-40	1.257621	1.23E-42	MKP4
Cre09.g416950	0.975306	1.24E-12	1.223217	2.28E-20	1.34879	3.26E-24	MKP1
Cre14.g630750	1.50817	1.19E-43	1.241553	7.51E-35	0.887288	2.47E-19	MAPKKK10
Cre09.g393850	0.821196	3.89E-09	1.367696	1.77E-23	0.535955	3.90E-05	MAPKKK2
Cre12.g545950	1.926039	9.17E-13	1.545605	4.03E-11	0.857385	0.000104	MAPKKK9
Cre08.g372100	0.749496	8.26E-16	1.561255	1.52E-64	1.209526	2.25E-39	Heat shock 70kDa protein
Cre06.g278162	-1.37084	1.35E-76	1.657248	2.25E-105	2.683205	2.50E-257	Pherophorin
Cre08.g373300	1.633131	2.06E-60	2.104046	6.61E-102	1.736388	7.35E-75	MAPKKK1
Cre16.g689650	1.280836	1.76E-70	2.137398	3.49E-191	1.786869	4.61E-137	Autophagy protein
Cre07.g325741	0.254278	0.0287	3.416359	1.97E-135	4.128171	5.88E-157	sodium-dependent phosphate transporter
Cre17.g700750	2.122209	1.83E-109	6.37918	0	6.320891	0	Inner membrane protein

5.1.4 Gene ontology enrichment analysis

GO ontology enrichment was carried out on differentially expressed genes shared by all samples under bacterial co-cultivation and on differentially expressed genes shared only by samples under *Bacillus* co-cultivation. A total of 1379 genes were upregulated in axenic samples and shared by all samples under bacterial co-cultivation (Figure 14A), while a total of 899 genes were upregulated in axenic samples and shared by samples under *Bacillus* co-cultivation (Figure 14C). GO enrichment on these two lists allowed us to identify which algal genes were expressed when algae were growing in sterile conditions. Most of the enrichment terms were related to amino acid catabolic process. One big reason for this could be *C. reinhardtii* shows poor uptake of urea and urea is a major Nitrogen source in SWW media. Thus, shifting their metabolism to breaking down and scavenging proteins and amino acids within themselves to sustain growth and development.

On the other hand, a total of 2270 genes were downregulated in axenic samples and shared by all samples under bacterial co-cultivation, while a total of 969 genes were downregulated in axenic samples and shared by samples under *Bacillus* co-cultivation. Genes that are downregulated in axenic samples can alternatively be described as being upregulated under bacterial association. The GO enrichment of the 2270 genes upregulated shared by all samples under bacterial association identified enrichment of genes related to Salicylic acid biosynthetic and metabolic process (Figure 14B). This is an extremely important observation because plants use Salicylic acid as both an immune signal and a carbon source for microbial growth [Lebeis et al., 2015, Eichmann 2020]. Salicylic acid is used by the plant host as a defense hormone to modulate which microbes are allowed to colonize their roots and which microbes are eliminated. Microbes that can colonize the plant roots can use Salicylic acid as a carbon source. This is the first-ever description of green algae producing and upregulating Salicylic acid biosynthesis in response to bacterial cultivation. This also implies that green algae, like plants, might be able to sculpt and modulate their associated microbiomes. Apart from Salicylic acid biosynthesis, we also observed enrichment of GO terms related to reproduction and cell division, transport proteins, transport vesicles, and vesicle membranes. The enrichment of GO terms related to reproduction and cell division is understandable, considering we see a large improvement in algal biomass under bacterial co-cultivation. The vesicle-related GO terms could correspond to the increased lipid vesicles observed under bacterial co-cultivation. Finally, enrichment of transport proteins could be related to increased secretion of carbohydrates and signaling molecules responding to bacterial presence.

GO term enrichment of 969 genes upregulated and shared between both *Bacillus* co-cultivation revealed the presence of glycoprotein biosynthesis and metabolic process (Figure 14D). Glycoproteins are a superfamily of cell wall proteins. They come in many forms and play essential roles in plant-bacteria interaction; including defense of plant cells from pathogens [Chaliha et al.,

2018] to promoting symbiotic bacteria to bind to the surface of the plant roots [Xie et al., 2012]. The exact mechanism of plant glycoprotein interaction with bacteria remains elusive. In our study, we see that both species of *Bacillus* are closely bound to the algal cell surface. The question if glycoproteins play a role in this bond still remains to be answered. However, the GO enrichment for these proteins only under *Bacillus* co-cultivation is an exciting new observation and further evidence that algal response to bacterial presence might be similar to those observed in plant-bacteria interactions.

5.2 Part B – Algal-Bacterial Consortia in Combined Biohydrogen Generation and Wastewater Treatment

There are a number of difficulties that arise while operating biodegradation systems in constantly changing microenvironments. These issues must be resolved to create and execute commercially viable solutions for effective biological wastewater treatment and energy production. Several green algae-based photoheterotrophic strategies were used in this study. The major objective of our research was to assess the potential of dark fermentation effluent as a source of photoheterotrophic algae biomass and concurrent biohydrogen evolution. Throughout the photo-fermentation stage of the hybrid (dark and photo-fermentation) biodegradation process, algal growth characteristics, biodegradation effectiveness, and changes in the effluent microbial population were recorded. The dark fermentation effluent allowed algae to flourish. However, there were differences in the growth of the algae, with the diluted effluent showing somewhat more biomass and a greater growth rate than the non-diluted dark fermentation effluent. The increased accessibility of light in the diluted effluent is most likely the cause of this variation. Importantly, *Micractinium* showed higher rates of biodegradation and generated greater volume of biohydrogen in undiluted effluents.

The small increase in algal cell number seen in the presence of enriched microbial inoculum (EMI) was not significant and had no discernible impact on the growth of the algae during photo-fermentation. Here, an important conclusion was the fact that EMI addition did not inhibit algal growth. During photo-fermentation, EMI had a favorable impact on both the daily and cumulative production of H_2, and greater H_2 evolution was seen in the samples containing EMI. The production of H_2 was demonstrated to be cumulative, with contributions from the EMI and *Micractinium* (Figure 17). Data indicated a higher contribution of EMI to the total H_2 production compared to the algal contribution ~60–65% of the total H_2 was produced by the EMI while 35–40% could be assigned to *Micractinium*. The results also indicated that the pretreatment step selectively inhibited methanogenic archaea in EMI. Since hydrogen is efficiently utilized by hydrogenotrophic archaea, restriction of methanogenesis is integral to render H_2 into an end-product in the metabolic flow [Venkata Mohan, 2008]. Pretreatment can also select for hydrogen-producing bacteria and led to a larger hydrogen yield [Xiao and Liu, 2009; Kim et al., 2013; Phowan and Danvirutai, 2014]. Pretreatment temperatures ranged from 65 to 121°C administered over a duration of 10 min to 24 h [Selembo et al., 2009; Xiao and Liu, 2009; Sivagurunathan et al., 2014]. Heat treatments showed varying degrees of efficiency with more intense treatments also leading to a higher loss in bacterial abundance. A previous study in our lab showed that heat treatment for 1 h at 70°C was sufficient to inhibit hydrogen-consuming microbes in wastewater [Boboescu et al., 2013].

A similar amount of daily H_2 was produced in EFF-A and S-EFF-A samples, while a significantly higher amount of H_2 was accumulated in the S-EFF-A samples, indicating that the filter sterilization

successfully reduced H_2 consuming bacteria (even if the sterilization was not complete as can be seen in Figure 4), while strong H_2 uptake was observed in the dark fermentation effluent samples containing green algae (EFF-A). It is important to note that increasing H_2 evolution was observed on the first and the second days of the experiments in all samples, while strongly decreased daily H_2 production was detected on the third day regardless of the sample conditions. Thus, both green algae and hydrogen-evolving bacteria found suitable substrate conditions (presumably accessible electrons) in the first 48 h of the photo-fermentation. The photosynthetic oxygen produced by the green algae did not inhibit the hydrogenase enzymes (neither algal Fe-hydrogenases nor bacterial Fe- and NiFe-hydrogenases), the active respiration of the bacterial community (even in the S-EFF-A samples) scavenged oxygen as it was shown in earlier studies [Lakatos et al., 2014, 2017].

Changes in total nitrogen, total phosphorous, and BOD reflected the efficiency of biodegradation during the photo-fermentation phase and demonstrated the crucial role played by green algae in the process. The presence of green algae was indispensable for efficient N and P consumption as well as BOD decrease in the photo-fermentation stage. The role of the enriched microbial inoculum in photoheterotrophic stage appeared to be marginal in further element uptake and degradation of organic molecules. EMI has around 10–20% biodegradation efficiency on the dark fermentation effluent compared to that of the green algae being around 35–50%. This finding is intriguing because it suggests that the nutrient composition of the dark fermentation effluent is presumably more accessible to the photosynthetic green algae than to the bacterial communities developed during anaerobic dark fermentation. Thus, the metabolic functions performed by dark fermentation communities already involved in biodegradation during the first dark fermentation phase can be complemented by *Micractinium* metabolism.

Culture-independent methods of microbial community analysis can be carried out by either sequencing the 16S rRNA gene or metagenome sequencing. While 16S rRNA gene sequencing is cost-effective and can be used in identifying taxa, whole metagenome shotgun sequencing increases the accuracy of species-level microbial community characterization and can be used to predict functional potential of the microbiota. When looking at the taxonomic profiles, large differences can be observed between the EMI sample and all other samples. The EMI sample was obtained from a brewery and was heat treated to remove methanogenic *Archaea* that readily consume H_2. The fundamental cause of the significant change in the taxonomic profile of EMI from all other samples is heat treatment. In addition, the abundance of the *Lactobacillus* and *Saccharomyces* genus was much lower in all the photoheterotrophic samples compared to RIW and EFF samples. The reason for this decrease is not fully understood, if we saw this decrease only in samples with additional enriched microbial inoculum (EFF+M), it could be attributed to negative interactions between the organisms. But this relative decline in abundance is significant for biohydrogen generation since *Lactobacillus*

can reduce H_2 outputs by redirecting H_2 potential to the creation of lactate. [Higgins et al., 2018]. Following photoheterotrophic treatment, the abundance of *Prevotella* and *Veillonella* genus increased across all samples. The presence of *Prevotella* bacteria is common in H_2 reactors [Castelló et al., 2011], and the members of this genus have the potential to co-aggregate with other microbes to form granules [Li et al., 2006].

The bacterial community was impacted to a greater degree by the addition of enriched microbial inoculum compared to the addition of algal inoculum. *Micractinium* did not have a strong effect on shaping the community, instead, the various interactions taking place between different bacterial species might have made the changes. The low impact of *Micractinium* on changing the microbiome structure could very well be due to the short duration of the photoheterotrophic stage, which was only 3 days. Further research is needed to elucidate the complex metabolic interactions among the main identified bacterial groups and the photosynthetic green algae.

The SEED-based functional classification provided an overview of the functional potential of all samples (Figure 19B). It's interesting to see that RIW and EFF clustered apart from EMI when samples were grouped based on their taxonomic characteristics (Figure 20A). However, EMI and EFF grouped together when samples were clustered based on their functional characteristics (Figure 20B). This indicated that the relatively small taxonomic changes brought about by dark fermentation of the RIW sample enriched members to perform broad-scale functions similar to those being carried out in EMI. Further, carbohydrate metabolism was performed primarily by the bacterial members of the community as this function was found in low abundance in filter-sterilized samples and in diluted EFF+A samples. While protein and lipid metabolism genes were mostly identified in high abundance in filter-sterilized samples alone.

We were also interested in exploring the biosynthetic potential of various important secondary metabolites. Hence, all the bacterial samples were compared against the KEGG database. Interestingly, both the *Veillonella* and *Prevotella* bins had complete pathways for thiamine biosynthesis. The *Veillonella* bin genome also had partially complete pathways for biotin and cobalamin biosynthesis. These cofactors are particularly important for algal growth. Previous studies involving 306 algal species showed that more than 51% required cobalamin, 22% required thiamine, and 6% required biotin [Croft et al., 2006]. Thus, despite the low abundance of the *Veillonella* bin, it might be performing extremely integral functions for the growth of *Micractinium*.

Algal microbiome studies represent a nascent field, with just a handful of studies exploring the algal phycosphere [Krohn-Molt et al., 2017], and fewer still exploring the interactions between the algal host and its bacterial partner [Gonzalez and Bashan, 2000; Croft et al., 2006; Higgins et al., 2018]. A deeper knowledge of these interactions and the advantages and disadvantages brought about to the host algal species can provide us with insights into how to enhance growth and development without

the usage of bacterial species. Our research suggested that the dual approach of wastewater treatment and concurrent biohydrogen evolution using a two-stage photoheterotrophic and dark fermentation has a promising future.

6. CONCLUSION

6.1 Part A – High-throughput co-culture assays to investigate algal-bacterial interactions

Algal cultivation in agricultural and municipal effluents is an attractive goal for algal studies. This is because these wastewater effluents are typically rich in nutrients required to support algal growth and development, while also exploring the possibility to convert the recovered algal biomass into medium or low-value products. There also have been several studies exploring the use of food-waste effluents as cultivation media. However, to arrive at this destination we need a meticulous understanding of how cultivated algal species will interact with both the native microbiome and invading microbial contaminants. This is a requirement even for the industrial cultivation of green algae.

However, most algal studies are carried out in TAP or a similar growth media to prevent noise from contaminating microbial species. Studies of algal growth in TAP media have been invaluable in generating data and helping us understand their molecular workings during growth and development. TAP media is also useful for biohydrogen studies as the acetate in the media is essential to improve biohydrogen production. However, exogenous addition of carbon would not be a sustainable way to generate biohydrogen and it also limits our understanding to just these environments.

In the present study, we made use of synthetic wastewater media to simulate municipal wastewater effluents and co-cultivated *C. reinhardtii* with twenty-eight different bacterial members, representing three different phyla and isolated from different environments. The initial growth and biohydrogen studies identified the importance of *Bacillus* species in improving biohydrogen production. In fact, under this condition comparable amounts of accumulated biohydrogen were obtained compared to previous studies in our lab using TAP media (Table 10). A cross-species study utilizing two other species of green algae: *Micractinium* and *Parachlorella* showed that *Bacillus* species could also improve biohydrogen production with these two green algae. Taken together these studies offer an additional avenue to improve biohydrogen production. Previous studies using genetically engineered green algae have shown to generate more than 500 ml L^{-1} culture [Steinbeck et al., 2015, Kruse et al., 2005]. Future studies might find success in generating higher accumulated biohydrogen if mutants with truncated antenna size or deleted Proton gradient related like protein [Steinbeck et al., 2015] are co-cultivated with bacterial members.

Finally, results from these studies have far-reaching consequences in other algal bioenergy fields. In this study, we have also demonstrated that *Bacillus* co-cultivation directly improves accumulated lipids and lipid production. An extension of this study towards improving lipid production for biofuel is yet another attractive avenue. Finally, this is the first study exploring the impact of bacterial co-cultivation on the algal host. We see not only a complete reorganization of the algal transcriptome, but also evidence that green algae, like plants, are capable of using salicylic acid along with upregulating cell wall genes like glycoproteins to respond to bacterial presence.

6.2 Part B – Algal-Bacterial Consortia in Combined Biohydrogen Generation and Wastewater Treatment

A novel hybrid biohydrogen-producing system was investigated in the present study using a two-stage biodegradation approach (microbial dark fermentation followed by photoheterotrophic treatment using *Micractinium* green algae). We have focused on the second photo-fermentative stage of this biodegradation process. A series of outputs ranging from nitrogen and phosphorous removal through biological oxygen demand to the composition of the biodegradation communities were carefully monitored during the photo-fermentation experiments. Special attention was paid to the correlations between the rearrangements of the involved algal-bacterial communities and the performance of the biodegradation system. Finally, it was also observed that both algal and bacterial members were essential for the high biohydrogen production observed in this study.

In this project, we have not only used whole metagenome shotgun sequencing to characterize the microbial community during different stages of wastewater treatment but also applied this approach to track how the major functions changed across the different stages. We have used the contigs to bin the genomes of the most abundant species in the biodegradation system. The whole genome bins provide a better understanding of microbial functions specifically enriched, therefore being significant in the photoheterotrophic stage of our wastewater treatment pipeline.

7. SUMMARY

For the past few decades, green algae have been exploited as agents to enhance the bioremediation of wastewater effluents with high nutrient levels. Under specific circumstances, green algae belonging to the taxon Chlorophyta have also demonstrated to be effective biohydrogen producers. Hydrogenase, an enzyme that can only function in anaerobic environments, catalyzes the synthesis of biohydrogen.

Several strategies have been explored to maintain high hydrogenase activity. These include nutrient deprivation to inactivate oxygen-evolving PSII, genetic transformation of different parts of the photosynthetic electron chain, and commonly available oxygen absorbers.

Algal-bacterial co-cultures have recently been the subject of several investigations aimed at biohydrogen generation. Co-cultures provide several advantages over monocultures, primarily in an ecological context. In natural ecosystems, algae live in association with a multitude of different organisms collectively termed the microbiome. The associated microbiome is generally found surrounding or attached to the algal host in a region called the phycosphere. Algal hosts release dissolved organic matter or signaling molecules to promote certain bacterial communities in the phycosphere. The bacterial partners, in turn, improve the growth of algal hosts by providing additional major essential nutrients (N, P), vitamins, phytohormones, and siderophores. Bacterial respiration can also mitigate problems arising from the high dissolved oxygen concentrations and prevent algal photo-oxidative culture death. Consumption of O_2 by bacterial respiration raises photosynthetic efficiency by allowing Rubisco to preferentially bind CO_2 rather than O_2.

In this project, we investigated the utility of bacterial partners in maintaining a microoxic environment, enabling algae to thrive in high-nutrient wastewater, and treating wastewater while producing copious amounts of biohydrogen.

Our results indicated that algal biohydrogen production is directly impacted during co-cultivation with specific bacterial members. We also identified that co-cultivation with all, but one bacterium led to an improvement in *C. reinhardtii* cc124 growth. *Bacillus* species isolated from different environments can reproducibly improve biohydrogen production across two other species of green algae: *Micractinium* MACC-360 and *Parachlorella* MACC-38. Co-cultivation of *C. reinhardtii* with different *Bacillus* species also improved algal lipid accumulation and biohydrogen production, while co-cultivation with *Methylobacterium* sp. led to greater carbohydrate accumulation and very low hydrogen production.

We also carried out transcriptome studies to look at gene expression of *C. reinhardtii* under axenic cultivation and co-cultivation with *Bacillus cereus*, *Bacillus thuringiensis,* and *Methylobacterium* sp. There was an increased expression of NDA2 only in algae co-cultivated with both *Bacillus* species.

NDA2 is a type II NADH dehydrogenase involved in the transfer of electrons from the breakdown of carbohydrates to ferredoxin. We also observed the *hyda2* transcript being upregulated only in algae co-cultivated with *Methylobacterium* sp. The *hyda2* isoform of exhibits a greater predilection for consuming hydrogen. This could be another reason for low hydrogen production. On the other hand, *C. reinhardtii* co-cultivated with *Bacillus* had upregulated genes involved in fermentation. Enzymes such as pyruvate formate lyase (PFL) and pyruvate ferredoxin reductase (PFR), both of which are directly involved in breaking down pyruvate with concomitant release of biohydrogen had greatly increased expression under bacterial co-cultivation. Improved biohydrogen generation may result from the upregulation of genes involved in fermentation processes. We also identified a low expression of stress-related light-harvesting complexes under bacterial co-cultivation. These results coupled with the phenotypic observation of high lipid and carbohydrate accumulation provide a compelling argument for the need to investigate and cultivate algae with bacterial partners.

Our studies with brewery wastewater effluents revealed that *Micractinium* MACC-360 could photo-heterotrophically grow while bioremediating the effluents. The concentration of wastewater played a major role in nutrient uptake. Algae grown in undiluted wastewater effluent had a high rate of nutrient uptake, despite accumulating lower biomass. Furthermore, we found that the presence of algae is necessary for effective nutrient uptake and that heat pre-treatment is a key step in maintaining high biohydrogen production. Samples with heat-treated microbial inoculum along with algae produced the highest amount of biohydrogen, while samples without heat-treated microbial inoculum produced the lowest amount of biohydrogen. Finally, we also identified that filter sterilization did not lead to the removal of all bacteria from the effluent.

Heat treatment and photofermentation both exhibited significant effects on the microbial community, according to metagenomic analyses. Heat treatment changed the microbiome community structure. Bacteria from the *Lactobacillus* genus reduced in abundance while bacteria from *Clostridium* increased in abundance. On the other hand, the three-day photofermentation led to a significant increase in bacteria from the genus *Prevotella*, *Clostridium,* and *Veillonella*. Complete pathways for the biosynthesis of vitamins were found in the whole genome assembled bins of *Prevotella* and *Veillonella*, which may help increase the algal growth rate. Finally, we discovered that although bacterial taxonomy varies across samples, the corresponding function does not. The study shows that it is feasible to produce biohydrogen in addition to contaminant removal using current algal-based remediation technologies.

8. ÖSSZEGZÉS

Az elmúlt néhány évtizedben elkezdtek mikroalgákat is használni magas tápanyagtartalmú szennyvizek bioremediációjának fokozására. A *Chlorophyta* taxonba tartozó eukarióta zöldalgák bizonyos körülmények között hatékony biohidrogén-termelőnek is mutatkoztak. A hidrogenázok olyan enzimek, amelyek lehetővé teszik a biohidrogén szintézisét, azonban csak anaerob környezetben képesek működni.

Számos módszert vizsgáltak már a magas és folyamatos hidrogéntermelő hidrogenáz-aktivitás fenntartására zöldalgákban. Ezek közé tartozik a tápanyagmegvonás (elsősorban a kén megvonása) az oxigént fejlesztő PSII inaktiválása érdekében, a fotoszintetikus elektrontranszportlánc különböző részeinek genetikai módosítása, illetve általánosan fellelhető oxigénkötő ágensek használata.

A közelmúltban számos, a biohidrogén előállítására irányuló vizsgálat tárgyát képezték az alga-baktérium vegyes kultúrák. A vegyes kultúrák, elsősorban ökológiai szempontból, számos előnnyel rendelkeznek az alga monokultúrákkal szemben. A természetes ökoszisztémákban a mikroalgák számos különböző mikroorganizmussal élnek együtt, amelyeket együttesen fikoszférának nevezünk. Az algák oldott szerves anyagokat vagy jelátviteli folyamatokban résztvevő molekulákat bocsátanak ki, ezzel támogatva bizonyos baktériumközösségeket a fikoszférában. A baktérium partnerek pedig további fő esszenciális tápanyagok (N, P), vitaminok, fitohormonok és sziderofórok termelésével biztosítják az algagazdák fokozott növekedését. A bakteriális légzés a magas oldott oxigénkoncentrációból eredő problémákat is enyhítheti, és megakadályozhatja az alga kultúrák fotooxidatív károsodását. A bakteriális respiráció emellett növeli a fotoszintetikus hatékonyságot azáltal, hogy fokozza a Rubisco enzim affinitását a CO_2 megkötésére az oxigénnel szemben.

A dolgozatban bemutatott munkában a bakteriális partnerek felhasználhatóságát vizsgáltuk az alga alapú biohidrogén termelésben és ezzel párhuzamosan szennyvízkezelésben.

Eredményeink azt mutatták, hogy a mikroalgák biohidrogén termelését közvetlenül befolyásolja bizonyos baktériumokkal való együttes növesztés. A különböző környezetekből izolált *Bacillus* fajok reprodukálhatóan képesek javítani a biohidrogéntermelést több mikroalga faj esetében. Azt is azonosítottuk, hogy a bármely baktériummal történő együttes nevelés, a *C. reinhardtii* cc124 növekedését fokozta. A *C. reinhardtii* cc124 különböző *Bacillus* fajokkal történő együttes növesztése serkentette a mikroalgák lipidfelhalmozódását és biohidrogén termelését is, míg a *Methylobacterium* sp. együttes növesztése nagyobb szénhidrátfelhalmozódáshoz és nagyon alacsony hidrogéntermeléshez vezetett. Transzkriptom-vizsgálatokat is végeztünk, hogy megvizsgáljuk a *C.*

reinhardtii cc124 génexpresszióját axénikus növesztés, illetve *Bacillus cereus*, *Bacillus thuringiensis* és *Methylobacterium* sp. baktériumokkal történő együttes növesztés esetén. A *Methylobacterium*-mal együtt növesztett *C. reinhardtii* cc124 az FNR1 expresszióját növelte. Az FNR1 elméletileg elektronokat vonhat el a hidrogenáztól, ami alacsony biohidrogén termelést eredményezhet. Azt is megfigyeltük, hogy a *hydA2* gén csak a *Methylobacterium*–mal együtt növesztett mintákban mutatott megnövekedett expressziót. A *hydA2* izoforma nagyobb hajlamot mutat a hidrogén fogyasztására, ez lehet az alacsony hidrogéntermelés másik oka. Másrészt a *Bacillus* baktériumokkal együtt növesztett *C. reinhardtii* cc124 esetében a fotofermentációban és a sötét fermentációban részt vevő gének expressziója mutatott növekedést. A hatékonyabb biohidrogén-termelés, a fermentációs folyamatokban részt vevő gének megnövekedett expressziójával függhet össze. A hidrogéntermelési értékek mellett a megnövekedett lipid- és szénhidrát-akkumuláció is meggyőző érvként szolgál a mikroalgák baktériumpartnerekkel történő növesztése mellett.

Élelmiszeripari szennyvízzel végzett vizsgálataink kimutatták, hogy a *Micractinium* MACC-360 képes fotoheterotróf módon növekedni szennyvízben, miközben aktív bioremediáció zajlik. A szennyvíz koncentrációja nagy szerepet játszik az algák növekedésében és tápanyagfelvételében. Megállapítottuk, hogy a mikroalgák jelenléte szignifikánsan hozzájárult a hatékony tápanyagfelvételhez, és hogy a hővel történő előkezelés kulcsfontosságú lépés a magas biohidrogén-termelés fenntartásához. A hőkezelt mikrobiális inokulumot tartalmazó mikroalga kultúra minták termelték a legnagyobb mennyiségű biohidrogént. A hőkezelés és a fotofermentáció egyaránt jelentős hatást gyakorolt a mikrobiális közösségre a metagenomikai elemzések szerint. A hőkezelés megváltoztatta a mikrobiom közösség összetételét, a *Lactobacillus* nemzetséghez tartozó baktériumok relatív gyakorisága drasztikusan csökkent, míg a *Clostridium* nemzetséghez tartozó baktériumok aránya nőtt. A háromnapos fotofermentáció a *Prevotella*, *Clostridium* és *Veillonella* nemzetségbe tartozó baktériumok számának jelentős növekedéséhez vezetett. A metagenomból felépített *Prevotella* és a *Veillonella* genomokban vitaminok bioszintézisének teljes útvonalait azonosítottuk, jelezve, hogy ezek a baktériumok hozzájárulnak a specifikus alga biomassza növekedéséhez. A kísérleteink meggyőzően igazolták, hogy a szennyvizek tápanyagtartalmának csökkentése mellett párhozamosan biohidrogén előállítása is megvalósítható az általunk fejlesztett zöldalga alapú technológiával.

9. ACKNOWLEDGEMENTS

If you trust in yourself, and believe in your dreams, and follow your star. . .
you'll still get beaten by people who spent their time working hard and learning things and weren't so lazy.

-Terry Prachett

First and foremost, I want to thank my advisor Dr. Gergely Maróti for being an inspiration in more ways than I can describe. His experience, generosity, and support has been invaluable in formulating my research questions and has allowed me to work on a diverse set of projects. I'll always be grateful for your patience, understanding, and unfaltering support and for being a role model for me to adopt. This thesis and my projects in particular would be far from complete without me acknowledging all the support I received from my lab colleagues. Berni, Atesz, Roland, Vaishali, Gabi, Mate, and Margaret; I am thankful for your presence in the lab. The endless discussions that we had and the ceaseless laughter we shared during and out of the lab has been a source of great joy and a bountiful well of memories.

I would also like to Prof. Imre Vas, Head of the Institute of Plant Biology for being an inspiration for all us students and providing a friendly and collaborative environment. Thank you for your guidance and support during all these years.

I would also like to thank members from other labs; Dr. Balazs Balint for his guidance and unceasing support and always answering the hordes of questions I had, Dr. Torda Varga from whom I learnt so much more on phylogenetic analysis, Gábor Patyi for his help and support in the lab and Dr. Roland Tengolics for his advice and lessons on how best to use the GC system in the lab.

I will forever be grateful to all my past teachers and advisors. Dr. Uma Mohan, who first taught me biology in high school, Prof. Sheshshayee Sreeman who took valuable time off to educate and encourage an extremely confused college student, Dr. N Sathyanarayana who taught me the importance of hard work and whose lessons I still try to inculcate in my life till this day, Dr. Deepa Agashe who took me in as a fresh Bachelors student and encouraged me to think critically of questions from an ecological view and Dr. Maren Friesen whose work ethic showed me the importance of excellence. My life would just be a pale shadow without meeting and learning from you all.

I would also like to show my appreciation to Alsatia Lohr, for your continued support and for being a sounding board when things got tough. I would also like to thank the many friends that I have made during my years in Hungary, Sarshad, Eniko, Avra, Balaji, Jason, Walliyulah, Shyam, and many others. Thank you for your presence and support in this journey. I am grateful to be able to lean on each one of you.

I have reserved a special place to talk about my parents; Dr. Bharathraj Shetty and Priti Shetty. Words can't justify or describe the gratitude that I feel for you. Without your sacrifices and encouragement, I would have never reached here. Thank you Pa, for inspiring my curiosity and encouraging me to ask questions; and thank you Ma for giving me the resilience to stand up despite my failures. It was your parenting and support that made me confident in taking up a Ph.D. I would also like to thank my grandfather, Dr. K. S. Naik, whose list of achievements has only been increasing the older he gets. Thank you ajja, for showing me that getting older just means there is more time for improvement. Finally, I would like to dedicate this thesis to my grandmother, Shanta R. Punja. It is said a person is never truly gone until we forget them. It has been so many years since I lost you, but paradoxically your stories and the memories we shared grow stronger every year. Until we meet again.

10. REFERENCES

1. Antal, T. K., T. E. Krendeleva, T. V. Laurinavichene, V. V. Makarova, A. A. Tsygankov, M. Seibert, and A. B. Rubin. 2001. "The Relationship between the Photosystem 2 Activity and Hydrogen Production in Sulfur Deprived Chlamydomonas Reinhardtii Cells." *Doklady. Biochemistry and Biophysics* 381 (1): 371–74. https://doi.org/10.1023/A:1013315310173.

2. Ban, Shidong, Weitie Lin, Fangyan Wu, and Jianfei Luo. 2018. "Algal-Bacterial Cooperation Improves Algal Photolysis-Mediated Hydrogen Production." *Bioresource Technology* 251 (December 2017): 350–57. https://doi.org/10.1016/j.biortech.2017.12.072.

3. Baltz, Anthony, Kieu-Van Dang, Audrey Beyly, Pascaline Auroy, Pierre Richaud, Laurent Cournac, and Gilles Peltier. "Plastidial expression of type II NAD (P) H dehydrogenase increases the reducing state of plastoquinones and hydrogen photoproduction rate by the indirect pathway in Chlamydomonas reinhardtii." *Plant physiology* 165, no. 3 (2014): 1344-1352.

4. Ben-Zvi, Oren, Eyal Dafni, Yael Feldman, and Iftach Yacoby. 2019. "Re-Routing Photosynthetic Energy for Continuous Hydrogen Production in Vivo." *Biotechnology for Biofuels* 12 (1): 1–13. https://doi.org/10.1186/s13068-019-1608-3.

5. Boboescu, Iulian Zoltan, Mariana Ilie, Vasile Daniel Gherman, Ion Mirel, Bernadett Pap, Adina Negrea, Éva Kondorosi, Tibor Bíró, and Gergely Maróti. 2014. "Revealing the Factors Influencing a Fermentative Biohydrogen Production Process Using Industrial Wastewater as Fermentation Substrate," 1–15.

6. Castelló, E, V Perna, J Wenzel, L Borzacconi, and C Etchebehere. 2011. "Microbial Community Composition and Reactor Performance during Hydrogen Production in a UASB Reactor Fed with Raw Cheese Whey Inoculated with Compost." *Water Science and Technology* 64 (11): 2265–73. https://doi.org/10.2166/wst.2011.706.

7. Chader, Samira, Hocine Hacene, and Spiros N. Agathos. 2009. "Study of Hydrogen Production by Three Strains of Chlorella Isolated from the Soil in the Algerian Sahara." *International Journal of Hydrogen Energy* 34 (11): 4941–46. https://doi.org/10.1016/j.ijhydene.2008.10.058.

8. Chaliha, Chayanika, Michael D. Rugen, Robert A. Field, and Eeshan Kalita. 2018. "Glycans as Modulators of Plant Defense against Filamentous Pathogens." *Frontiers in Plant Science* 9 (July): 1–16. https://doi.org/10.3389/fpls.2018.00928.

9. Chen, Hsu Ching, A. Jamila Newton, and Anastasios Melis. 2005. "Role of SulP, a Nuclear-Encoded Chloroplast Sulfate Permease, in Sulfate Transport and H_2 Evolution in Chlamydomonas Reinhardtii." *Photosynthesis Research* 84 (1–3): 289–96. https://doi.org/10.1007/s11120-004-7157-y.

10. Croft, Martin T., Andrew D. Lawrence, Evelyne Raux-Deery, Martin J. Warren, and Alison G. Smith. 2005. "Algae Acquire Vitamin B12 through a Symbiotic Relationship with Bacteria." *Nature* 438 (7064): 90–93. https://doi.org/10.1038/nature04056.

11. Doebbe, Anja, Jens Rupprecht, Julia Beckmann, Jan H. Mussgnug, Armin Hallmann, Ben Hankamer, and Olaf Kruse. 2007. "Functional Integration of the HUP1 Hexose Symporter Gene into the Genome of C. Reinhardtii: Impacts on Biological H_2 Production." *Journal of Biotechnology* 131 (1): 27–33. https://doi.org/10.1016/j.jbiotec.2007.05.017.

12. Engelbrecht, Vera, Kristina Liedtke, Andreas Rutz, Shanika Yadav, Alexander Günzel, and Thomas Happe. "One isoform for one task? The second hydrogenase of Chlamydomonas reinhardtii prefers hydrogen uptake." *International Journal of Hydrogen Energy* 46, no. 10 (2021): 7165-7175.

13. Eichmann, Ruth, Luke Richards, and Patrick Schäfer. 2021. "Hormones as Go-Betweens in Plant Microbiome Assembly." *Plant Journal* 105 (2): 518–41. https://doi.org/10.1111/tpj.15135.

14. Erbes, David L., Dan King, and Martin Gibbs. 1979. " Inactivation of Hydrogenase in Cell-Free Extracts and Whole Cells of Chlamydomonas Reinhardi by Oxygen ." *Plant Physiology* 63 (6): 1138–42. https://doi.org/10.1104/pp.63.6.1138.

15. Forestier, Marc, Paul King, Liping Zhang, Matthew Posewitz, Sarah Schwarzer, Thomas Happe, Maria L. Ghirardi, and Michael Seibert. "Expression of two [Fe]-hydrogenases in Chlamydomonas reinhardtii under anaerobic conditions." *European Journal of Biochemistry* 270, no. 13 (2003): 2750-2758.

16. Gaffron, Hans, and Jack Rubin. "Fermentative and photochemical production of hydrogen in algae." *The Journal of General Physiology* 26, no. 2 (1942): 219-240.

17. Ghirardi, Maria Lucia, Alexandra Dubini, Jianping Yu, and Pin Ching Maness. 2009. "Photobiological Hydrogen-Producing Systems." *Chemical Society Reviews* 38 (1): 52–61. https://doi.org/10.1039/b718939g.

18. Ghrardi, Maria L. 1997. "Oxygen Sensitivity of Algal H_2-Production." *Applied Biochemistry and Biotechnology - Part A Enzyme Engineering and Biotechnology* 63–65 (1): 141–51. https://doi.org/10.1007/bf02920420.

19. Gomez-Osuna, Aitor, Victoria Calatrava, Aurora Galvan, Emilio Fernandez, and Angel Llamas. 2020. "Identification of the Mapk Cascade and Its Relationship with Nitrogen Metabolism in the Green Alga Chlamydomonasreinhardtii." *International Journal of Molecular Sciences* 21 (10). https://doi.org/10.3390/ijms21103417.

20. Gonzalez, Luz E., and Yoav Bashan. 2000. "Increased Growth of the Microalga Chlorella Vulgaris When Coimmobilized and Cocultured in Alginate Beads with the Plant-Growth-Promoting Bacterium Azospirillum Brasilense." *Applied and Environmental Microbiology* 66 (4): 1527–31. https://doi.org/10.1128/AEM.66.4.1527-1531.2000.

21. Han, Wei, Yun Yi Hu, Shi Yi Li, Fei Fei Li, and Jun Hong Tang. 2016. "Biohydrogen Production from Waste Bread in a Continuous Stirred Tank Reactor: A Techno-Economic Analysis." *Bioresource Technology* 221: 318–23. https://doi.org/10.1016/j.biortech.2016.09.055.

22. Happe, Thomas, and J. Dirk Naber. "Isolation, characterization and N-terminal amino acid sequence of hydrogenase from the green alga Chlamydomonas reinhardtii." *European journal of biochemistry* 214, no. 2 (1993): 475-481.

23. He, Meilin, Ling Li, Jianguo Liu, and Litao Zhang. 2015. "Improvement of H_2 Photoproduction in Chlorella Pyrenoidosa in Artificial and Natural Seawater by Addition of Acetic Acid and Control of Nutrients." *Algal Research* 10: 104–9. https://doi.org/10.1016/j.algal.2015.04.018.

24. He, Meilin, Ling Li, Litao Zhang, and Jianguo Liu. 2012. "The Enhancement of Hydrogen Photoproduction in Chlorella Protothecoides Exposed to Nitrogen Limitation and Sulfur Deprivation." *International Journal of Hydrogen Energy* 37 (22): 16903–15. https://doi.org/10.1016/j.ijhydene.2012.08.121.

25. Hein, Mette, M. Folager Pedersen, and Kaj Sand-Jensen. "Size-dependent nitrogen uptake in micro-and macroalgae." *Marine ecology progress series. Oldendorf* 118, no. 1 (1995): 247-253.

26. Helliwell, Katherine E., Jagroop Pandhal, Matthew B. Cooper, Joseph Longworth, Ulrich Johan Kudahl, David A. Russo, Eleanor V. Tomsett, et al. 2018. "Quantitative Proteomics of a B12-Dependent Alga Grown in Coculture with Bacteria Reveals Metabolic Tradeoffs Required for Mutualism." *New Phytologist* 217 (2): 599–612. https://doi.org/10.1111/nph.14832.

27. Hemschemeier, Anja, Swanny Fouchard, Laurent Cournac, Gilles Peltier, and Thomas Happe. 2008. "Hydrogen Production by Chlamydomonas Reinhardtii: An Elaborate Interplay of Electron Sources and Sinks." *Planta* 227 (2): 397–407. https://doi.org/10.1007/s00425-007-0626-8.

28. Higgins, B T, I Gennity, P S Fitzgerald, S J Ceballos, O Fiehn, and J S Vander Gheynst. 2018. "Algal-Bacterial Synergy in Treatment of Winery Wastewater. Npj Clean Water 1 (1): 6."

29. Jackson, D. D., and J. W. Ellms. "On odors and tastes of surface waters with special reference to Anabaena, a microscopical organism found in certain water supplies of Massachusetts." *Rep. Mass. State Board Health* 1896 (1896): 410-420.

30. Kanehisa, Minoru, Yoko Sato, and Kanae Morishima. 2016. "BlastKOALA and GhostKOALA: KEGG Tools for Functional Characterization of Genome and Metagenome Sequences." *Journal of Molecular Biology* 428 (4): 726–31. https://doi.org/10.1016/J.JMB.2015.11.006.

31. Kim, Mijung, Chunguang Liu, Jin Won Noh, Yingnan Yang, Sechang Oh, Kazuya Shimizu, Dong Yeol Lee, and Zhenya Zhang. 2013. "Hydrogen and Methane Production from Untreated Rice Straw and Raw Sewage Sludge under Thermophilic Anaerobic Conditions." *International Journal of Hydrogen Energy* 38 (21): 8648–56. https://doi.org/10.1016/j.ijhydene.2013.04.079.

32. Krishna, Pilla Sankara, Stenbjörn Styring, and Fikret Mamedov. 2019. "Photosystem Ratio Imbalance Promotes Direct Sustainable H_2 Production in: Chlamydomonas Reinhardtii." *Green Chemistry* 21 (17): 4683–90. https://doi.org/10.1039/c9gc01416k.

33. Krohn-Molt, Ines, Malik Alawi, Konrad U. Förstner, Alena Wiegandt, Lia Burkhardt, Daniela Indenbirken, Melanie Thieß, et al. 2017. "Insights into Microalga and Bacteria Interactions of Selected Phycosphere Biofilms Using Metagenomic, Transcriptomic, and Proteomic Approaches." *Frontiers in Microbiology*. https://doi.org/10.3389/fmicb.2017.01941.

34. Kruse, Olaf, Jens Rupprecht, Klaus Peter Bader, Skye Thomas-Hall, Peer Martin Schenk, Giovanni Finazzi, and Ben Hankamer. 2005. "Improved Photobiological H_2 Production in Engineered Green Algal Cells." *Journal of Biological Chemistry* 280 (40): 34170–77. https://doi.org/10.1074/jbc.M503840200.

35. Kwak, Min Jung, Hyun Gi Kong, Kihyuck Choi, Soon Kyeong Kwon, Ju Yeon Song, Jidam Lee, Pyeong An Lee, et al. 2018. "Rhizosphere Microbiome Structure Alters to Enable Wilt Resistance in Tomato." *Nature Biotechnology* 36 (11): 1100–1116. https://doi.org/10.1038/nbt.4232.

36. Lakatos, Gergely, Daniella Balogh, Attila Farkas, Vince Ördög, Péter Tamás Nagy, Tibor Bíró, and Gergely Maróti. 2017. "Factors Influencing Algal Photobiohydrogen Production in Algal-Bacterial Co-Cultures." *Algal Research* 28 (January): 161–71. https://doi.org/10.1016/j.algal.2017.10.024.

37. Lakatos, Gergely, Zsuzsanna Deák, Imre Vass, Tamás Rétfalvi, Szabolcs Rozgonyi, Gábor Rákhely, Vince Ördög, Éva Kondorosi, and Gergely Maróti. 2014. "Bacterial Symbionts Enhance Photo-Fermentative Hydrogen Evolution of Chlamydomonas Algae." *Green Chemistry* 16 (11): 4716–27. https://doi.org/10.1039/c4gc00745j.

38. Lebeis, Sarah L., Sur Herrera Paredes, Derek S. Lundberg, Natalie Breakfield, Jase Gehring, Meredith McDonald, Stephanie Malfatti, et al. 2015. "Salicylic Acid Modulates Colonization of the Root Microbiome by Specific Bacterial Taxa." *Science* 349 (6250): 860–64. https://doi.org/10.1126/science.aaa8764.

39. Li, C, T Zhang, and H H P Fang. 2006. "Fermentative Hydrogen Production in Packed-Bed and Packing-Free Upflow Reactors." *Water Science and Technology* 54 (9): 95–103.

40. Li, Dinghua, Chi Man Liu, Ruibang Luo, Kunihiko Sadakane, and Tak Wah Lam. 2015. "MEGAHIT: An Ultra-Fast Single-Node Solution for Large and Complex Metagenomics Assembly via Succinct de Bruijn Graph." *Bioinformatics*. https://doi.org/10.1093/bioinformatics/btv033.

41. Li, Jingtao, Chenyang Wang, Wenxing Liang, and Sihui Liu. 2021. "Rhizosphere Microbiome: The Emerging Barrier in Plant-Pathogen Interactions." *Frontiers in Microbiology* 12 (October). https://doi.org/10.3389/fmicb.2021.772420.

42. Lin, Hsin Di, Bang Hung Liu, Ting Ting Kuo, Hsieh Chin Tsai, Teng Yung Feng, Chieh Chen Huang, and Lee Feng Chien. 2013. "Knockdown of PsbO Leads to Induction of HydA and Production of Photobiological H_2 in the Green Alga Chlorella Sp. DT." *Bioresource Technology* 143: 154–62. https://doi.org/10.1016/j.biortech.2013.05.101.

43. Lomoth, Reiner, and Sascha Ott. 2009. "Introducing a Dark Reaction to Photochemistry: Photocatalytic Hydrogen from [FeFe] Hydrogenase Active Site Model Complexes." *Dalton Transactions*, no. 45: 9952–59. https://doi.org/10.1039/b911129h.

44. Losos, Jonathan B. 2008. "Phylogenetic Niche Conservatism, Phylogenetic Signal and the Relationship between Phylogenetic Relatedness and Ecological Similarity among Species." *Ecology Letters* 11 (10): 995–1003. https://doi.org/10.1111/j.1461-0248.2008.01229.x.

45. Martiny, Jennifer B.H., Stuart E. Jones, Jay T. Lennon, and Adam C. Martiny. 2015. "Microbiomes in Light of Traits: A Phylogenetic Perspective." *Science* 350 (6261). https://doi.org/10.1126/science.aac9323.

46. Melis, A., L. Zhang, M. Forestier, M. L. Ghirardi, and M. Seibert. 2000. "Sustained Photobiological Hydrogen Gas Production upon Reversible Inactivation of Oxygen Evolution in the Green Alga Chlamydomonas Reinhardtii." *Plant Physiology* 122 (1): 127–35. https://doi.org/10.1104/pp.122.1.127.

47. Merchant, S S, G B Witman, A Terry, A Salamov, L K Fritz-Laylin, L Marechal-Drouard, S E Prochnik, O Vallon, E H Harris, and S J Karpowicz. 2007. "The Chlamydomonas Genome Reveals the Evolution of Key Animal and Plant Functions." *Science* 318 (5848): 245–50.

48. Meuser, Jonathan E., Eric S. Boyd, Gennady Ananyev, Devin Karns, Randor Radakovits, U. M.Narayana Murthy, Maria L. Ghirardi, G. Charles Dismukes, John W. Peters, and Matthew C. Posewitz. 2011. "Evolutionary Significance of an Algal Gene Encoding an [FeFe]-Hydrogenase with F-Domain Homology and Hydrogenase Activity in Chlorella Variabilis NC64A." *Planta* 234 (4): 829–43. https://doi.org/10.1007/s00425-011-1431-y.

49. Meuser, Jonathan E., Sarah D'Adamo, Robert E. Jinkerson, Florence Mus, Wenqiang Yang, Maria L. Ghirardi, Michael Seibert, Arthur R. Grossman, and Matthew C. Posewitz. 2012. "Genetic Disruption of Both Chlamydomonas Reinhardtii [FeFe]-Hydrogenases: Insight into the Role of HYDA2 in H_2 Production." *Biochemical and Biophysical Research Communications* 417 (2): 704–9. https://doi.org/10.1016/j.bbrc.2011.12.002.

50. Meyer, Folker, D. Paarmann, M. D'Souza, R. Olson, E. M. Glass, M. Kubal, T. Paczian, et al. 2008. "The Metagenomics RAST Server - A Public Resource for the Automatic Phylogenetic and Functional Analysis of Metagenomes." *BMC Bioinformatics* 9: 1–8. https://doi.org/10.1186/1471-2105-9-386.

51. Nguyen, Anh Vu, Skye R. Thomas-Hall, Alizée Malnoë, Matthew Timmins, Jan H. Mussgnug, Jens Rupprecht, Olaf Kruse, Ben Hankamer, and Peer M. Schenk. 2008. "Transcriptome for Photobiological Hydrogen Production Induced by Sulfur Deprivation in the Green Alga Chlamydomonas Reinhardtii." *Eukaryotic Cell* 7 (11): 1965–79. https://doi.org/10.1128/EC.00418-07.

52. Nwoba, Emeka G., Bede S. Mickan, and Navid R. Moheimani. 2019. "Chlorella Sp. Growth under Batch and Fed-Batch Conditions with Effluent Recycling When Treating the Effluent of Food Waste Anaerobic Digestate." *Journal of Applied Phycology* 31 (6): 3545–56. https://doi.org/10.1007/s10811-019-01878-7.

53. Oey, Melanie, Ian L. Ross, Evan Stephens, Janina Steinbeck, Juliane Wolf, Khairul Adzfa Radzun, Johannes Kügler, Andrew K. Ringsmuth, Olaf Kruse, and Ben Hankamer. 2013. "RNAi Knock-Down of LHCBM1, 2 and 3 Increases Photosynthetic H_2 Production Efficiency of the Green Alga Chlamydomonas Reinhardtii." *PLoS ONE* 8 (4). https://doi.org/10.1371/journal.pone.0061375.

54. Oksanen, J, F G Blanchet, R Kindt, P Legendre, P R Minchin, R B O'hara, G L Simpson, P Solymos, and M Stevens. 2016. "HH, & Wagner, H.(2013). Vegan: Community Ecology Package. R Package Version 2.0-7."

55. Perozeni, Federico, Giorgia Beghini, Stefano Cazzaniga, and Matteo Ballottari. 2020. "Chlamydomonas Reinhardtii LHCSR1 and LHCSR3 Proteins Involved in Photoprotective Non-Photochemical Quenching Have Different Quenching Efficiency and Different Carotenoid Affinity." *Scientific Reports* 10 (1): 1–10. https://doi.org/10.1038/s41598-020-78985-w.

56. Phowan, Pantipa, and Paiboon Danvirutai. 2014. "Hydrogen Production from Cassava Pulp Hydrolysate by Mixed Seed Cultures: Effects of Initial PH, Substrate and Biomass Concentrations." *Biomass and Bioenergy* 64: 1–10. https://doi.org/10.1016/j.biombioe.2014.03.057.

57. Pinto, T. S., F. X. Malcata, J. D. Arrabaça, J. M. Silva, R. J. Spreitzer, and M. G. Esquível. 2013. "Rubisco Mutants of Chlamydomonas Reinhardtii Enhance Photosynthetic Hydrogen Production." *Applied Microbiology and Biotechnology* 97 (12): 5635–43. https://doi.org/10.1007/s00253-013-4920-z.

58. Plancke, Charlotte, Helene Vigeolas, Ricarda Höhner, Stephane Roberty, Barbara Emonds-Alt, Véronique Larosa, Remi Willamme, et al. 2014. "Lack of Isocitrate Lyase in Chlamydomonas Leads to Changes in Carbon Metabolism and in the Response to Oxidative Stress under Mixotrophic Growth." *Plant Journal* 77 (3): 404–17. https://doi.org/10.1111/tpj.12392.

59. Polle, Juergen E.W., Sarada Devi Kanakagiri, and Anastasios Melis. 2003. "Tla1, a DNA Insertional Transformant of the Green Alga Chlamydomonas Reinhardtii with a Truncated Light-Harvesting Chlorophyll Antenna Size." *Planta* 217 (1): 49–59. https://doi.org/10.1007/s00425-002-0968-1.

60. Posewitz, Matthew C., Paul W. King, Sharon L. Smolinski, Liping Zhang, Michael Seibert, and Maria L. Ghirardi. 2004. "Discovery of Two Novel Radical S-Adenosylmethionine Proteins Required for the Assembly of an Active [Fe] Hydrogenase." *Journal of Biological Chemistry* 279 (24): 25711–20. https://doi.org/10.1074/jbc.M403206200.

61. Prabakar, Desika, Varshini T. Manimudi, Subha Suvetha K, Swetha Sampath, Durga Madhab Mahapatra, Karthik Rajendran, and Arivalagan Pugazhendhi. 2018. "Advanced Biohydrogen Production Using Pretreated Industrial Waste: Outlook and Prospects." *Renewable and Sustainable Energy Reviews* 96 (August 2017): 306–24. https://doi.org/10.1016/j.rser.2018.08.006.

62. Rashid, Naim, Kisay Lee, and Qaisar Mahmood. 2011. "Bio-Hydrogen Production by Chlorella Vulgaris under Diverse Photoperiods." *Bioresource Technology* 102 (2): 2101–4. https://doi.org/10.1016/j.biortech.2010.08.032.

63. Reshef, Leah, Omry Koren, Yossi Loya, Ilana Zilber-Rosenberg, and Eugene Rosenberg. 2006. "The Coral Probiotic Hypothesis." *Environmental Microbiology* 8 (12): 2068–73. https://doi.org/10.1111/j.1462-2920.2006.01148.x.

64. Roach, Thomas, Chae Sun Na, Wolfgang Stöggl, and Anja Krieger-Liszkay. 2021. "The Non-Photochemical Quenching Protein LHCSR3 Prevents Oxygen-Dependent Photoinhibition in Chlamydomonas Reinhardtii." *Journal of Experimental Botany* 71 (9): 2650–60. https://doi.org/10.1093/JXB/ERAA022.

65. Rodriguez-R, Luis M., and Konstantinos T. Konstantinidis. 2014. "Nonpareil: A Redundancy-Based Approach to Assess the Level of Coverage in Metagenomic Datasets." *Bioinformatics* 30 (5): 629–35. https://doi.org/10.1093/bioinformatics/btt584.

66. Rühle, Thilo, Anja Hemschemeier, Anastasios Melis, and Thomas Happe. 2008. "A Novel Screening Protocol for the Isolation of Hydrogen Producing Chlamydomonas Reinhardtii Strains." *BMC Plant Biology* 8: 1–13. https://doi.org/10.1186/1471-2229-8-107.

67. Ruiz-Marin, Alejandro, Yunuen Canedo-López, and Paolah Chávez-Fuentes. 2020. "Biohydrogen Production by Chlorella Vulgaris and Scenedesmus Obliquus Immobilized Cultivated in Artificial Wastewater under Different Light Quality." *AMB Express* 10 (1). https://doi.org/10.1186/s13568-020-01129-w.

68. Seemann, Torsten. 2014. "Prokka: Rapid Prokaryotic Genome Annotation." *Bioinformatics* 30 (14): 2068–69. https://doi.org/10.1093/bioinformatics/btu153.

69. Selembo, Priscilla A., Joe M. Perez, Wallis A. Lloyd, and Bruce E. Logan. 2009. "2009Selembo - Enhanced Hydrogen and 1 3-propanediol Production from Glycerol by Fermentation.Pdf."

70. Shetty, Prateek, Iulian Z. Boboescu, Bernadett Pap, Roland Wirth, Kornél L. Kovács, Tibor Bíró, Zoltán Futó, Richard Allen White, and Gergely Maróti. 2019. "Exploitation of Algal-Bacterial Consortia in Combined Biohydrogen Generation and Wastewater Treatment." *Frontiers in Energy Research* 7 (JUN): 1–13. https://doi.org/10.3389/fenrg.2019.00052.

71. Show, K. Y., D. J. Lee, J. H. Tay, C. Y. Lin, and J. S. Chang. 2012. "Biohydrogen Production: Current Perspectives and the Way Forward." *International Journal of Hydrogen Energy* 37 (20): 15616–31. https://doi.org/10.1016/j.ijhydene.2012.04.109.

72. Shu, Longfei, and Zhangli Hu. 2012. "Characterization and Differential Expression of MicroRNAs Elicited by Sulfur Deprivation in Chlamydomonas Reinhardtii." *BMC Genomics* 13 (1): 108. https://doi.org/10.1186/1471-2164-13-108.

73. Sivagurunathan, Periyasamy, Biswarup Sen, and Chiu Yue Lin. 2014. "Batch Fermentative Hydrogen Production by Enriched Mixed Culture: Combination Strategy and Their Microbial Composition." *Journal of Bioscience and Bioengineering* 117 (2): 222–28. https://doi.org/10.1016/j.jbiosc.2013.07.015.

74. Stapleton, James A., and James R. Swartz. 2010. "Development of an in Vitro Compartmentalization Screen for High-Throughput Directed Evolution of [FeFe] Hydrogenases." *PLoS ONE* 5 (12): 1–8. https://doi.org/10.1371/journal.pone.0015275.

75. Steinbeck, Janina, Denitsa Nikolova, Robert Weingarten, Xenie Johnson, Pierre Richaud, Gilles Peltier, Marita Hermann, Leonardo Magneschi, and Michael Hippler. 2015. "Deletion of Proton Gradient Regulation 5 (PGR5) and PGR5-Like 1 (PGRL1) Proteins Promote Sustainable Light-Driven Hydrogen Production in Chlamydomonas Reinhardtii Due to Increased PSII Activity under Sulfur Deprivation." *Frontiers in Plant Science* 6 (OCTOBER): 1–11. https://doi.org/10.3389/fpls.2015.00892.

76. Stocker, Thomas. 2014. *Climate Change 2013: The Physical Science Basis: Working Group I Contribution to the Fifth Assessment Report of the Intergovernmental Panel on Climate Change*. Cambridge university press.

77. Subramanian, Sowmya, Amanda N. Barry, Shayani Pieris, and Richard T. Sayre. 2013. "Comparative Energetics and Kinetics of Autotrophic Lipid and Starch Metabolism in Chlorophytic Microalgae: Implications for Biomass and Biofuel Production." *Biotechnology for Biofuels*. https://doi.org/10.1186/1754-6834-6-150.

78. Surzycki, Raymond, Laurent Cournac, Gilles Peltier, and Jean David Rochaix. 2007. "Potential for Hydrogen Production with Inducible Chloroplast Gene Expression in Chlamydomonas." *Proceedings of the National Academy of Sciences of the United States of America* 104 (44): 17548–53. https://doi.org/10.1073/pnas.0704205104.

79. Toepel, Jörg, Maike Illmer-Kephalides, Sebastian Jaenicke, Jasmin Straube, Patrick May, Alexander Goesmann, and Olaf Kruse. 2013. "New Insights into Chlamydomonas Reinhardtii Hydrogen Production Processes by Combined Microarray/RNA-Seq Transcriptomics." *Plant Biotechnology Journal* 11 (6): 717–33. https://doi.org/10.1111/pbi.12062.

80. Tolleter, Dimitri, Bart Ghysels, Jean Alric, Dimitris Petroutsos, Irina Tolstygina, Danuta Krawietz, Thomas Happe, et al. 2011. "Control of Hydrogen Photoproduction by the Proton Gradient Generated by Cyclic Electron Flow in Chlamydomonas Reinhardtii." *Plant Cell* 23 (7): 2619–30. https://doi.org/10.1105/tpc.111.086876.

81. Torzillo, Giuseppe, Alberto Scoma, Cecilia Faraloni, Alba Ena, and Udo Johanningmeier. 2009. "Increased Hydrogen Photoproduction by Means of a Sulfur-Deprived Chlamydomonas Reinhardtii D1 Protein Mutant." *International Journal of Hydrogen Energy* 34 (10): 4529–36. https://doi.org/10.1016/j.ijhydene.2008.07.093.

82. Wang, Yingrui, Yahui Ren, and Junmin Pan. 2019. "Regulation of Flagellar Assembly and Length in Chlamydomonas by LF4, a MAPK-Related Kinase." *FASEB Journal* 33 (5): 6431–41. https://doi.org/10.1096/fj.201802375RR.

83. Wang, Yue, Huanling Yang, Xinna Zhang, Fei Han, Wenfeng Tu, and Wenqiang Yang. 2020. "Microalgal Hydrogen Production." *Small Methods* 4 (3): 1–18. https://doi.org/10.1002/smtd.201900514.

84. Wickham, H Ggplot, and C Ggplot Sievert. 2016. "2. Elegant Graphics for Data Analysis." Spinger International Publishing.

85. Wirth, Roland, Gergely Lakatos, Tamás Böjti, Gergely Maróti, Zoltán Bagi, Gábor Rákhely, and Kornél L. Kovács. 2018. "Anaerobic Gaseous Biofuel Production Using Microalgal Biomass – A Review." *Anaerobe* 52 (August): 1–8. https://doi.org/10.1016/J.ANAEROBE.2018.05.008.

86. Wu, Shuangxiu, Lili Xu, Rui Huang, and Quanxi Wang. 2011. "Improved Biohydrogen Production with an Expression of Codon-Optimized HemH and Lba Genes in the Chloroplast of Chlamydomonas Reinhardtii." *Bioresource Technology* 102 (3): 2610–16. https://doi.org/10.1016/j.biortech.2010.09.123.

87. Wu, Shuangxiu, Rui Huang, Lili Xu, Guangyu Yan, and Quanxi Wang. 2010. "Improved Hydrogen Production with Expression of HemH and Lba Genes in Chloroplast of Chlamydomonas Reinhardtii." *Journal of Biotechnology* 146 (3): 120–25. https://doi.org/10.1016/j.jbiotec.2010.01.023.

88. Wu, Shuangxiu, Xiaoxu Li, Jun Yu, and Quanxi Wang. 2012. "Increased Hydrogen Production in Co-Culture of Chlamydomonas Reinhardtii and Bradyrhizobium Japonicum." *Bioresource Technology* 123: 184–88. https://doi.org/10.1016/j.biortech.2012.07.055.

89. Xiao, Benyi, and Junxin Liu. 2009. "Biological Hydrogen Production from Sterilized Sewage Sludge by Anaerobic Self-Fermentation." *Journal of Hazardous Materials* 168 (1): 163–67. https://doi.org/10.1016/j.jhazmat.2009.02.008.

90. Xie, Fang, Alan Williams, Anne Edwards, and J. Allan Downie. 2012. "A Plant Arabinogalactan-like Glycoprotein Promotes a Novel Type of Polar Surface Attachment by Rhizobium Leguminosarum." *Molecular Plant-Microbe Interactions* 25 (2): 250–58. https://doi.org/10.1094/MPMI-08-11-0211.

91. Xu, Fu Qiao, Wei Min Ma, and Xin Guang Zhu. 2011. "Introducing Pyruvate Oxidase into the Chloroplast of Chlamydomonas Reinhardtii Increases Oxygen Consumption and Promotes Hydrogen Production." *International Journal of Hydrogen Energy* 36 (17): 10648–54. https://doi.org/10.1016/j.ijhydene.2011.05.130.

92. Yang, Ahreum, William I. Suh, Nam Kyu Kang, Bongsoo Lee, and Yong Keun Chang. 2018. "MAPK/ERK and JNK Pathways Regulate Lipid Synthesis and Cell Growth of Chlamydomonas Reinhardtii under Osmotic Stress, Respectively." *Scientific Reports* 8 (1): 1–12. https://doi.org/10.1038/s41598-018-32216-5.

93. Yang, Dawei, Yanting Zhang, Dinesh Kumar Barupal, Xiaolei Fan, Reid Gustafson, Rongbo Guo, and Oliver Fiehn. 2014. "Metabolomics of Photobiological Hydrogen Production Induced by CCCP in Chlamydomonas Reinhardtii." *International Journal of Hydrogen Energy* 39 (1): 150–58. https://doi.org/10.1016/j.ijhydene.2013.09.116.

94. Zhang, Litao, Meilin He, and Jianguo Liu. 2014. "The Enhancement Mechanism of Hydrogen Photoproduction in Chlorella Protothecoides under Nitrogen Limitation and Sulfur Deprivation." *International Journal of Hydrogen Energy* 39 (17): 8969–76. https://doi.org/10.1016/j.ijhydene.2014.04.045.
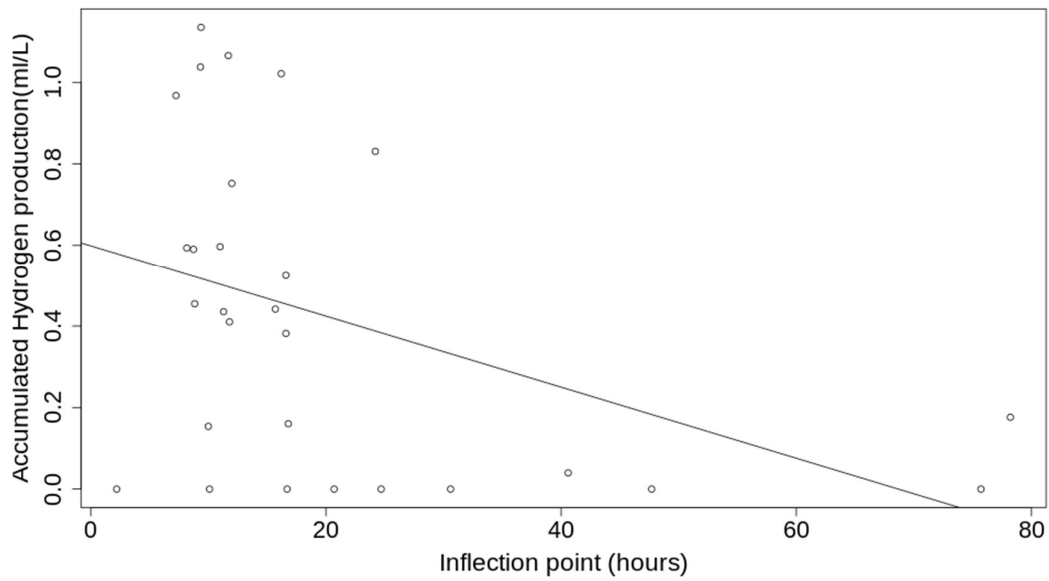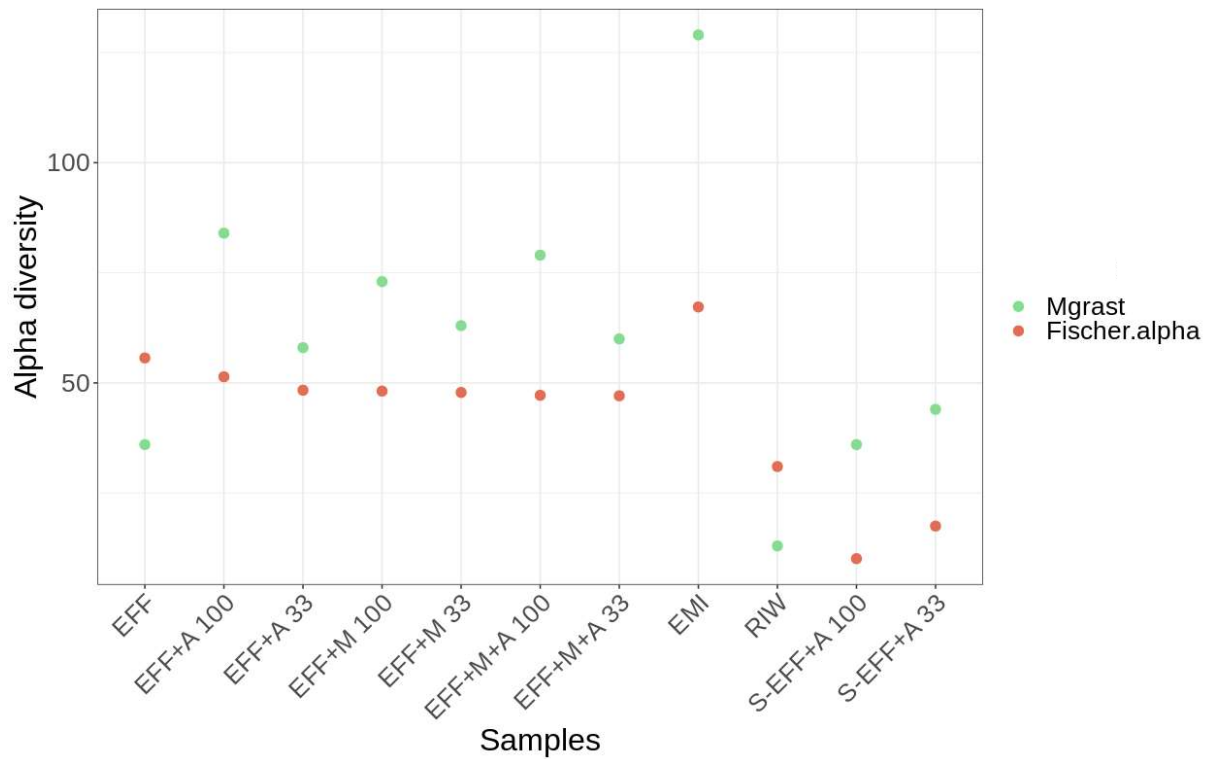
11. APPENDIX

Supplementary figures

Supplementary Figure 1: Alternative representation of accumulated biohydrogen across 28 bacterial species.
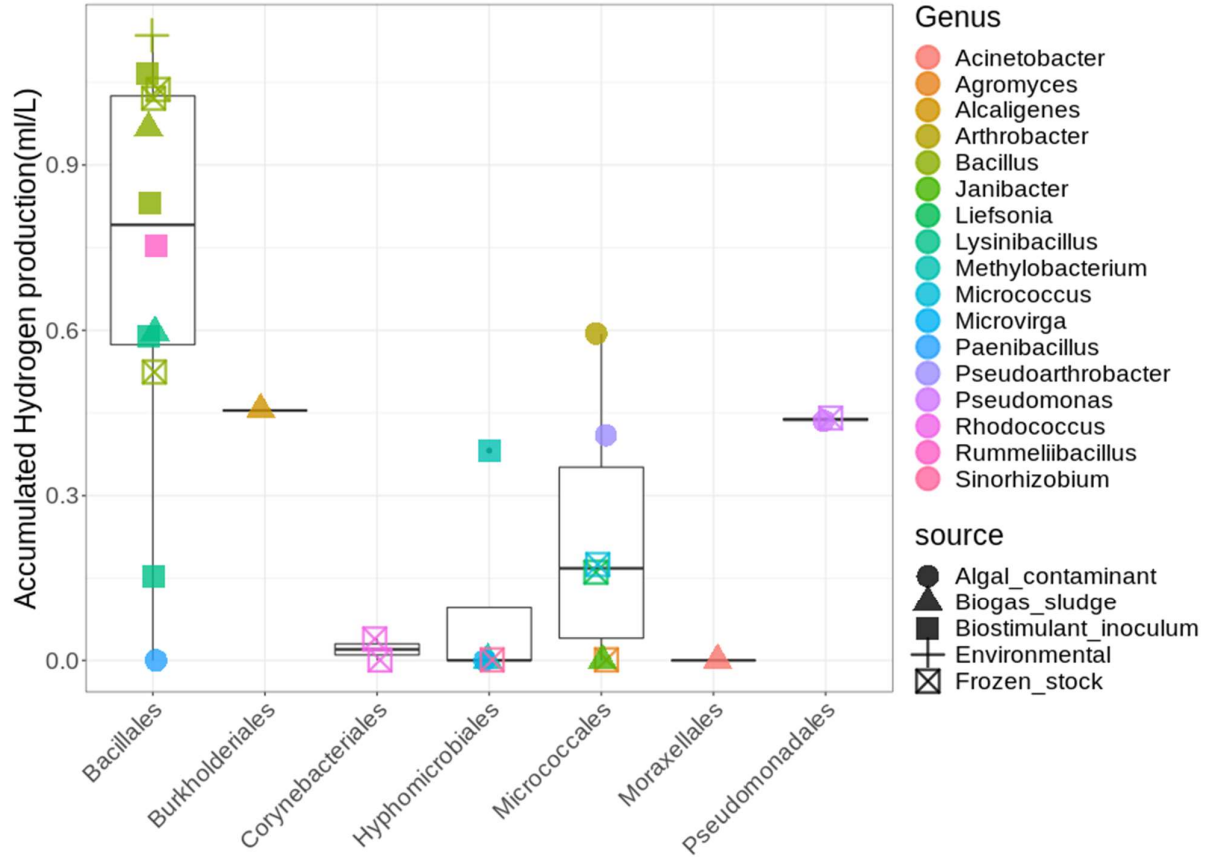
Supplementary Figure 2: Weak relationship was identified between accumulated biohydrogen and Bacterial inflection point.

Supplementary figure 3: Alpha diversity values calculated from MG-RAST and R analysis.

Supplementary figure 4: Rarefaction curves for all samples. RIW and both the filtered sterilized samples had much lower number of species detected, while EMI had the highest.